UNIVERSIDADE FEDERAL DE SANTA CATARINA

CAMPUS FLORIANÓPOLIS

POSTGRADUATE PROGRAM OF MECHANICAL ENGINEERING

Alinne Geronimo

Constraint analysis of the human knee structures in different ranges of flexion-extension and its representation by Theory of Mechanisms

Florianópolis

2022

Alinne Geronimo

Constraint analysis of the human knee structures in different ranges of flexion-extension and its representation by Theory of Mechanisms

Master's thesis submitted to Postgraduate Program of Mechanical Engineering at Universidade Federal de Santa Catarina for the degree of Master in Mechanical Engineering.
Advisor: Prof. Rodrigo de Souza Vieira, Dr. Eng.
Co-advisor: Prof. Estevan Hideki Murai, Dr. Eng.

Florianópolis

2022

Alinne Geronimo

Constraint analysis of the human knee structures in different ranges of flexion-extension and its representation by Theory of Mechanisms

The present work in masters level was evaluated and approved by an examining board composed by the following members:

Prof. Henrique Simas, Dr. Eng.
Universidade Federal de Santa Catarina

Prof. Julio Cesar Frantz, Dr. Eng.
Centro Universitário de Brusque

Prof. Leonardo Mejia Rincon, Dr. Eng.
Universidade Federal de Santa Catarina

We certify that this is the **original and final version** of the conclusion work which was deemed adequate for obtaining the title of Master in Mechanical Engineering.

<hr>

Coordination of Postgraduate Program

<hr>

Prof. Rodrigo de Souza Vieira, Dr. Eng.
Advisor

<hr>

Prof. Estevan Hideki Murai, Dr. Eng.
Co-advisor

Florianópolis, 2022.

For all of those who carry a spark of curiosity that shines upon science.

ACKNOWLEDGEMENTS

RESUMO

Articulações do corpo humano possuem uma biomecânica que pode ser muito complexa, como é o caso do joelho. O movimento de flexão do joelho humano une rotação com translação em um espaço de trabalho tridimensional, sendo restringido e suportado por suas estruturas internas, apresentando um grande desafio ao tentar replicar seu movimento interno durante uma simples caminhada. Esta dissertação tem por objetivo discutir sobre as estruturas do joelho humano, sua biomecânica e possíveis equivalências em projeto de mecanismos. Tendo por objetivo revisar os modelos de mecanismos já propostos na literatura e revisar estudos clínicos. Identificar as restrições ativas impostas pelas estruturas do joelho humano em cada movimento equivalente a um grau de liberdade. Através da análise dos estudos clínicos é proposta uma nova abordagem para o desenvolvimento de mecanismos equivalentes ao joelho humano, replicando as restrições impostas pelos ligamentos e utilizando dados experimentais de inserção ligamentar na construção dos mecanismos propostos. O desenvolvimento do modelo teve por objetivo geral, contribuir para o desenvolvimento de próteses e contribuir no estudo de distribuição de forças dentro do joelho humano. Para tal, foi aplicada uma análise de trajetória e posteriormente, uma análise estática, replicando um estudo experimental e comparando os resultados. O modelo proposto mostrou potencial para o desenvolvimento de mecanismos planares com trajetória similar ao joelho humano, e trouxe discussão sobre a representação mecânica dos ligamentos para uma análise estática, propondo algumas considerações. A presente dissertação também trouxe uma introdução para a discussão sobre o uso de mecanismos reconfiguráveis em aplicações biomecânicas.

Palavras-chave: mecanismos, restrições, joelho humano, reconfiguráveis, próteses.

RESUMO EXPANDIDO

INTRODUÇÃO

O estudo da biomecânica a sua aplicação no desenvolvimento de próteses e órteses sofre continuos avanços no decorrer dos anos. O joelho humano, por exemplo, é o foco de diferentes estudos que analisam seu movimento, a distribuição das forças internas e a variação de seu comportamento durante a sua trajetória. Na maioria das vezes, estes estudos tem por objetivo contribuir em procedimentos cirúrgicos, aprimorar ou desenvolver próteses internas ou externas e auxiliar no desenvolvimento de órteses. Partindo da análise da trajetória, diferentes mecanismos foram propostos e estudados para melhor representar o movimento do joelho. Mecanismos policentricos como o quatro-barras e o cinco-barras, conseguem entregar uma trajetória mais próxima do joelho humano, se analisado o movimento planar de flexão-extensão, sendo muito utilizados no desenvolvimento de próteses externas. Pesquisas recentes utilizaram mecanismos espaciais para replicar o movimento do joelho humano. Estes estudos tinham por objetivo, além de replicar o movimento do joelho, analisar as forças internas e contribuir para procedimentos cirurgicos. Há dois modos de representar o joelho humano por Teoria de Mecanismos, analisando o joelho passivo, o qual possui 1 grau de liberdade e sua trajetória é resultado de sua estrutura anatomica. Ou analisando o joelho ativo, que possui 6 graus de liberdade e sofre influência de forças internas como a ativação muscular e externas durante o movimento. A análise do joelho passivo permite o estudo das diferentes restrições presentes na estrutura do joelho, e o fato de apresentar apenas 1 grau de liberdade simplifica o estudo por Teoria de Mecanismos. O joelho humano é formado por quatro ossos e inúmeras estruturas moles, como ligamentos e meniscos. O estado de tensão de cada uma das estruturas do joelho pode variar de acordo com o ângulo de flexão-extensão ao qual ele está submetido. Analisando o joelho como um mecanismo, a variação de tensões das estruturas moles impacta diretamente em sua cadeia cinemática e na distribuição de forças. Neste sentido, é proposto um estudo das restrições presentes no joelho humano durante o movimento de flexão-extensão, analisando as diferentes cadeias cinemáticas presentes durante o movimento e visando contribuir no desenvolvimento de mecanismos mais similares ao joelho humano.

OBJETIVOS

Esta dissertação tem por objetivo identificar as restrições impostas pelas estruturas do joelho humano durante o movimento de flexão-extensão, analisando o comportamento de cada ligamento e propondo mecanismos equivalentes para cada faixa de flexão-extensão analisada, utilizando os quatro ligamentos principais. Também é proposto a análise da trajetória dos mecanismos desenvolvidos e posterior análise estática, comparando as forças internas calculadas do Ligamento Anterior Cruzado com estudos experimentais.

METODOLOGIA

Para analisar as restrições impostas por cada ligamento no joelho humano, este trabalho utiliza como base testes clínicos utilizado na medicina, comparando os resultados obtidos através da Teoria de Mecanismos. Estes testes indicam quais estruturas devem estar tensionadas durante um movimento específico do joelho, estes movimentos foram traduzidos para graus de liberdade equivalentes, possibilitando a análise das restrições impostas por cada estrutura durante cada teste clínico. Para analisar cada mecanismo desenvolvido, o Método de Reshetov foi utilizado, este método utiliza uma tabela para distribuir as liber-

dades de cada junta do mecanismo, identificando o grau de liberdade e as restrições de cada mecanismo. Para análise de trajetória, foi utilizada a análise de posição por cinemática direta das juntas, este método é algébrico e resulta no posicionamento das juntas a partir de uma entrada, que na presente dissertação foi o ângulo de flexão-extensão analisado. A Teoria dos Helicóides e o Método de Davies foram utilizados durante a análise estática dos mecanismos desenvolvidos. O Método de Davies adaptou a primeira e segunda Lei de Kircchoff para análise de mecanismos, utilizando a Teoria dos Grafos e a Teoria de Helicoides, sendo uma ferramenta excelente para a análise de mecanismos complexos.

RESULTADOS E DISCUSSÕES

Um ligamento não possui um comportamento linear, resultado da estrutura de suas fibras e composição não monofásica. Os mecanismos propostos, apresentaram uma perspectiva diferente para o joelho humano, propondo e analisando diversas cadeias cinemáticas presentes durante o movimento de flexão-extensão, comparando o joelho humano com um mecanismo reconfigurável, uma abordagem que traz inovação e um novo olhar para o desenvolvimento da reprentação do joelho por Teoria de Mecanismos. Sobre a análise de trajetória, os mecanismos desenvolvidos estão dentro do espaço de trabalho planar e apresentaram trajetória próxima ao do joelho humano no plano de flexão-extensão. É possivel observar que para algumas faixas de flexão a trajetória foi mais próxima de dados experimentais do que para outras, isto é resultado do movimendo espacial do joelho humano, aumentando a divergencia com o modelo proposto, ou do posicionamento das juntas. Sobre a análise estática, por apresentar muitas restrições redundantes, os mecanismos propostos não apresentaram solução viável em uma abordágem tridimensional, assim foi necessária a análise planar. O resultado das forças internas do ACL foi comparado com dados experimentais, é possivel observar que entre 15°e 30°o mecanismo converge com os dados experimentais, já para os ângulos 0°, 60°e 90°, a convergência depende da intensidade da força externa aplicada. As divergências encontradas no resultado da análise estática eram esperadas, visto que a análise estática traz um reflexo da trajetória do mecanismo.

CONSIDERAÇÕES FINAIS

A presente dissertação revisou a anatomia do joelho humano e dos diferentes estudos envolvendo Teoria de Mecanismos. Também foi proposta uma nova abordagem, desenvolvendo uma equivalência de restrições mecânicas a partir do estudo de testes clínicos. Esta dissertação traz à discussão o comportamento de cada estrutura do joelho humano, visualizando o joelho como um mecanismos reconfiguravel e estudando a cadeia cinemática equivalente de cada faixa de flexão-extensão de forma individual. Durante a análise, cada estrutura interna do joelho é avaliada individualmente, resultando no grau de liberdade equivalente e na direção das restrições impostas. Este estudo traduziu os testes clínicos para equivalencias mecânicas, facilitando o desenvolvimendo dos mecanismos. A partir dos mecanismos desenvolvidos é possível analisar o grau de liberdade de cada mecanismo, aplicar a análise de posição resultando na trajetória e em seguida, aplicar o Método de Davies para obter a análise estática. O resultado obtido para a análise estática se mostrou muito positivo para o plano z-y, divergindo no eixo x por se tratar de mecanismos planares. A análise estática convergiu com os resultados experimentais para algumas faixas de flexão e divergiu para outras, dependendo da intensidade da força externa aplicada. Este resultado pode ser resultado dos mecanismos propostos serem espaciais, mas também abre para discussão a validade da equivalência mecânica proposta para cada estrutura, visto que há

diferentes modos de interpretação por mecanismo das restrições impostas pelas estruturas moles do joelho, deixando como discussão quais pares cinemáticos ou quais tipos de junta seriam as mais indicadas para cada estrutura, apresentando um grau de convergencia maior. Mesmo sem a convergência total da análise estática, esta dissertação apresentou uma proposta inovadora, analisando as diferentes cadeias cinemáticas contidas no joelho humano de acordo com o grau de flexão-extensão. Este trabalho contribui positivamente no desenvolvimento de próteses e órteses, entregando um estudo detalhado das restrições contidas no joelho humano. Esta dissertação é o primeiro passo, trazendo para discussão o uso de mecanismos reconfiguráveis em aplicações biomecânicas.

Palavras-chave: mecanismos, restrições, joelho humano, reconfiguráveis, próteses.

ABSTRACT

Joints of the human body have a biomechanics that can be very complex, as is the case of the knee. The human knee flexion-extension movement unites rotation with translation in a three-dimensional workspace, being constraint and supported by its internal structures, presenting a great challenge when one intends to replicate the internal movement of the knee in, what may be call, a simple walk. This thesis aims to discuss the structures of the human knee, its biomechanics and possible equivalences in mechanisms design. The present work aims to review the models of mechanisms already proposed in the literature and review clinical studies, identifying the active constraints imposed by the structures of the human knee in equivalent degrees of freedom. Through the analysis of clinical studies is proposed a new approach to the development of mechanisms equivalent to the human knee, replicating the constraints imposed by the main ligaments and using experimental data of ligament insertion areas. The development of the model aims to contribute in the development of prostheses and contribute to the study of force distribution within the human knee. Therefore, a trajectory analysis was made and then a static analysis, replicating an experimental study and comparing the results to the experimental data. The proposed model showed potential for the development of planar mechanisms with a similar trajectory to the human knee, and brought to discussion the mechanical representation of the ligaments for a static analysis, proposing some considerations. This thesis also brought an introduction to the discussion about the use of reconfigurable mechanisms in biomechanical applications.

keywords: mechanisms, constraints, human knee, reconfigurable, prostheses.

LIST OF FIGURES

LIST OF TABLES

LIST OF SYMBOLS

$\$$ Screw

$\$^M$ Twist

$\$^A$ Wrench

$\$_0$ Position vector

$\$_{0_j}$ Position vector of a joint

λ Workspace

ν Mechanism loop

ψ^M Twist magnitude of velocity

ψ^A Wrench magnitude of load

θ Flexion angle

θ_j Position angle of a revolute joint

B_M Circuit matrix

C_N Redundant constraints

di_j Initial position of the joints

d_j Displacement of the joint

e Edge

$\vec{F}_R$ Resultant force

G_A Action Graph

G_c Coupling Graph

G_M Movement Graph

h Twist pitch

H_l Link length

I_C Incidency matrix

j Joint

l Link

L_j Final length or position of a joint

M Mobility

P Point

Q_A Cutset matrix

R Rotation

$\hat{\text{S}}^{\text{A}}$ Wrench geometrical element

$\hat{\text{S}}^{\text{M}}$ Twist geometrical element

T Translation

$\vec{\text{T}}_{\text{P}}$ Couple moment

v Vertex

Vp Linear velocity

w Angular velocity

LIST OF ACRONYMS

3D	Three-dimensional
ACL	Anterior Cruciate Ligament
dMCL	Deep Medial Collateral Ligament
DoF	Degree of Freedom
FEA	Finite Element Analysis
LCL	Lateral Collateral Ligament
MCL	Medial Collateral Ligament
MFL	Meniscofemoral Ligaments
OPL	Oblique popliteal ligament
PCL	Posterior Cruciate Ligament
PLC	Popliteofibular Ligament Complex
TKR	Total Knee Replacement

CONTENTS

1 INTRODUCTION

The kinematics of the human knee has been the subject of different studies aiming to develop prosthesis, orthosis or to determine forces in a specific point, contributing to surgical procedures, as ligaments reconstruction.

At first, the human knee was represented as a single revolute joint, but this consideration did not delivered an accurate trajectory, since the human knee kinematics is composed by movements of rotation and translation.

Then, some approaches used a four-bar or even five-bar mechanism to represent the human knee joint, as polycentric mechanisms, they can deliver a trajectory closer to the one of the human knee, combining rotation movements to sliding movements, but remaining in the flexion-extension plane, these mechanisms are usually applied in the development of external prosthesis. Recent researches, focused in the development of internal prosthesis or surgical procedures, use 3D mechanisms and parallel mechanisms delivering advances with a trajectory closer to experimental data (WILSON, D. R. *et al.*, 1998; OTTOBONI *et al.*, 2010; PONCE SALDIAS, 2014).

The advance of knee mechanisms with accurate kinematics is very important to improve the contribution and precision since with a reliable kinematic the mechanism will present closer behavior to the real knee.

The internal forces in the human knee are mostly studied to contribute in the development of internal prosthesis or surgical procedures. These studies are usually divided into 3D knees models using Finite Element Analysis (FEA) and analysis of equivalent mechanisms using Theory of Mechanisms.

The studies using FEA demand more resources and compute power than the studies using the Theory of Mechanisms, delivering accurate results but being restricted to resourceful applications. The approach using Theory of Mechanism, generates a mechanism with equivalent kinematics of the human knee and then the internal forces can be analyzed, with low demand for computing power.

There are two ways to represent the human knee as a mechanism, by using a passive or an active knee. The active knee is the one subjected to muscle activation or external forces having six degrees of freedom (DoF), while the passive knee it is not subjected to any kind or force presenting only one DoF.

Representing a passive knee with one DoF mechanism it is possible to achieve the knee flexion-extension trajectory, hence studies indicate that the human knee trajectory has one DoF within a three-dimensional (3D) space.

The passive motion of human knee is determined by anatomical structures, being possible to identify and analyze the constraints imposed by every structure resulting in the knees kinematic. Additionally, a mechanism with one DoF has a simplest kinematic analysis than a six DoF one (PONCE SALDIAS, 2014).

Using the theory of mechanisms, some studies proposed different mechanisms improving the representation of the passive human knee (WILSON, D. R. *et al.*, 1998; FEIKES *et al.*, 2003; OTTOBONI *et al.*, 2010; PARENTI-CASTELLI; SANCISI, Nicola, 2013; PONCE SALDIAS, 2014). These studies assimilate the human knee with parallel mechanisms, usually analyzing the femur, tibia and main ligaments. These mechanisms present one DoF and rigid links, using optimization of the links' length and joints position to improve the resulting kinematics.

Formed by four bones and several soft structures, as ligaments and menisci, the status of knees' different structures can change from taut to lax during the flexion-extension movement, impacting in the distribution of forces and probably changing the equivalent kinematic chain.

In this regard, it is proposed to identify the constraints imposed by the main ligaments of the human knee, to contribute in the development of future mechanisms representing the human knee considering the status of its soft structures.

The main goal of this thesis, is to analyze the different kinematic chains contained in the human knee, generating equivalent mechanisms in an attempt to represent the redundant constraints imposed by the main ligaments.

These mechanisms will assist in the better understanding of redundant constraints in the human knee, contributing for the development of mechanical representations by theory of mechanisms.

1.1 JUSTIFICATION

The knee's representation by Theory of Mechanisms brings several advantages to the analysis of the knee kinematics and statics, hence it is a simplest approach than the one using Finite Element Analysis, comparing anatomical structures to equivalent mechanical joints and links, identifying the constraints and the distribution of forces.

Being an extremely complex joint, the human knee can present different demands to each one of its structures during the flexion-extension. As an example, analyzing the contact between tibia and femur, at the firsts degrees of flexion there is a pure rotation movement, followed by a rotation combined with a sliding movement, and ending with only a sliding movement at the lasts degrees of flexion. This change occurs due to anatomical structures, their shapes and imposed constraints (KAPANDJI, 2000).

Other changes can be noticed in the main ligaments, while the cruciate ligaments remain taut during flexion-extension, the collateral ligaments vary from taut to lax, no longer constraining the knee after a certain range of flexion.

Considering the changes in the human knee during the flexion-extension movement it is possible to discuss if the human knee joint behaves as a reconfigurable mechanism, changing its kinematic chain or the equivalent type of joint in a mechanical representation during the flexion-extension.

The need to investigate the possibility of the human knee presenting different equivalent kinematic chains depending on its range of flexion justifies further studies to represent the knee as a reconfigurable mechanism.

1.2   RESEARCH OBJECTIVES

The research objectives were divided into general and specific.

1.2.1   General objective

The general objective of this research is to identify the ligaments constraints in the human knee during the flexion-extension movement, analyzing the behavior of each main ligament and proposing equivalent mechanisms to each range of flexion-extension. Then it is proposed to analyze the kinematic trajectory and the static behavior of the designed mechanisms comparing the *in situ* forces of the anterior cruciate ligament representation to experimental data.

1.2.2   Specific objectives

The specific objectives are:

- Review the anatomy and biomechanics of the human knee, exploring its different representations;

- Identify the ligaments constraints in different ranges of flexion-extension proposing equivalent mechanical kinematic pairs to each ligaments freedom;

- Assemble the kinematic chains of the mechanisms equivalent to each range of flexion-extension and calculate the position of the joints during the respective range of flexion;

- To analyze the mechanisms trajectory and the static behavior of the equivalent Anterior Cruciate Ligament, comparing the results to experimental data.

2 THE HUMAN KNEE JOINT

This chapter presents an introduction to anatomy standard terms, anatomical structures of the human knee joint and its biomechanics.

2.1 HUMAN KNEE AND STANDARD TERMS

The human knee is the largest synovial joint of the human body and is capable of performing extremely complex movements (STANDRING *et al.*, 2016; FLOYD, 2011).

A joint is called synovial when the articulating surfaces of the bones are covered in articular cartilage and separated by a film of viscous synovial fluid that serves as a lubricant. The stability in synovial joints is provided by a fibrous capsule and by internal or external ligaments (STANDRING *et al.*, 2016).

The knee joint has six DoF therefore it can perform translational and rotational movements in three different planes. The anatomical planes of motion are the median, frontal and horizontal planes. The median plane divides the body into right and left halves, any plane parallel to median plane is named sagittal plane. The frontal (or coronal) plane divides the body into anterior (front) and posterior (back) halves. The horizontal (or transverse) plane divides the body into superior (upper) and inferior (lower) halves. All anatomical assumptions are made considering that the body is in anatomical position which is described as standing erect and facing forwards, as shown in Figure 1 (STANDRING *et al.*, 2016; NEUMANN, 2010).

Figure 1 – Anatomical planes of motion
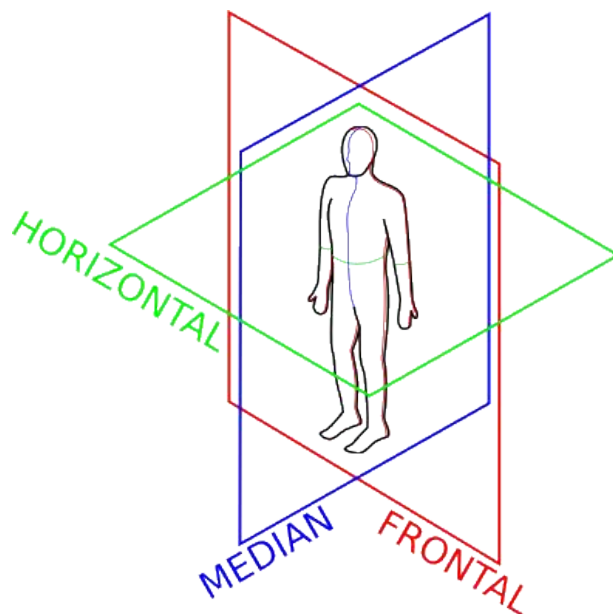
Source – own construction

Movements occur in a given plane, a joint or a part of interest moves or turns around an axis. The axis of rotation of median plane is called mediolateral axis (or frontal axis), the axis of rotation of frontal plane is called anteroposterior axis and the axis of rotation of horizontal plane is the vertical axis (FLOYD, 2011; NEUMANN, 2010).

To describe the position of structures relative to anatomical planes, some direction terms are particularly used. Referring to median plane the term "medial" is used to indicate that something is closer and "lateral" that something is distant. Referring to frontal plane "anterior" is used to indicate that something is in front of the frontal plane and "posterior" that something is behind it. Referring to horizontal plane the term "proximal" is used to indicate that something is closer to a joint or a point of interest whereas "distal" is used to indicates that something is distant, shown in Figure 2 (STANDRING *et al.*, 2016; NEUMANN, 2010).

Figure 2 – Anatomical planes: Axes of rotation and directions
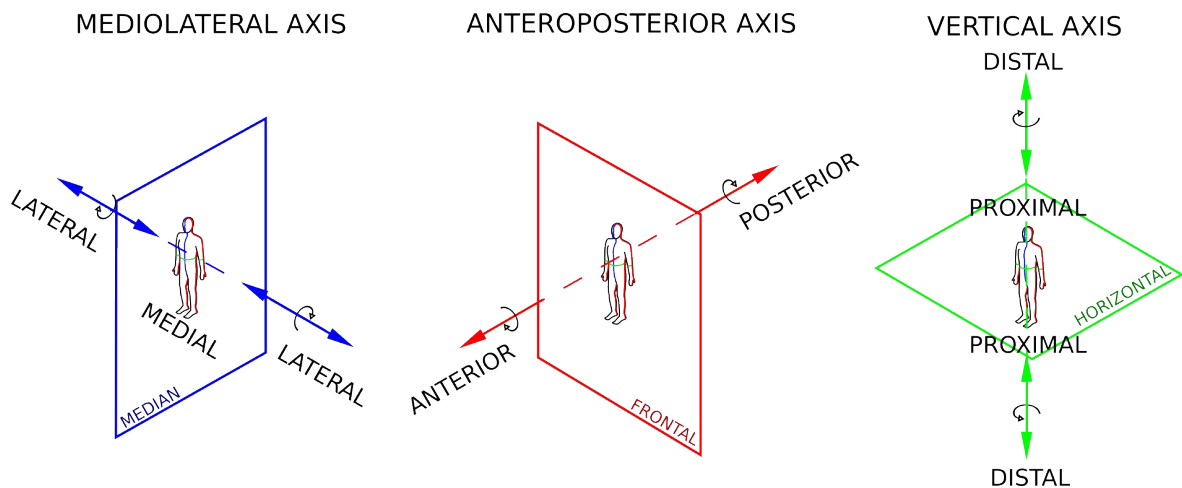
Source – own construction

Anatomical planes of motion, axes of rotation and direction terms are used during the analysis of joints, a point of interest or other anatomical structures, including the knee joint (Figure 3).

Figure 3 – Right human knee anatomical planes and directions
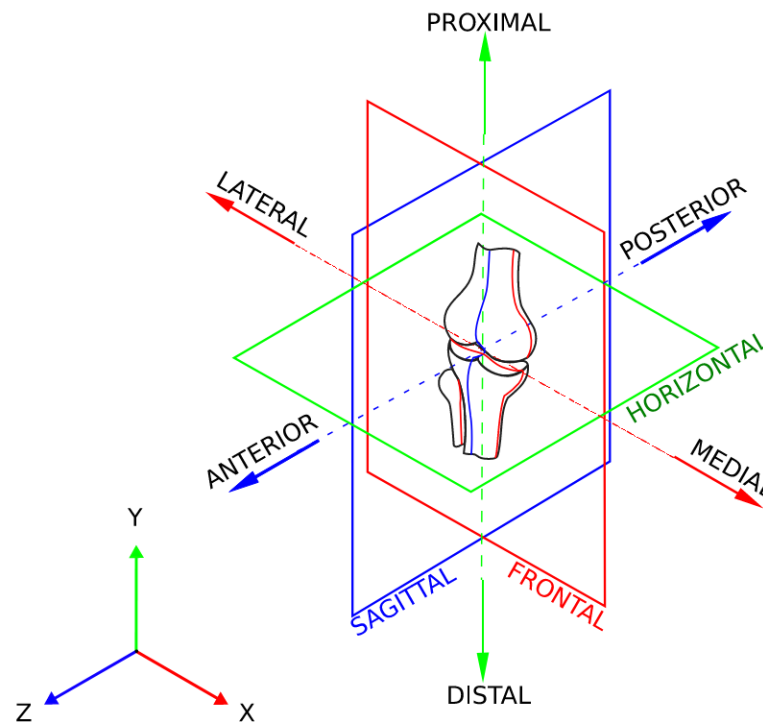
Source – own construction

2.2 KNEE ANATOMICAL STRUCTURES

The knee joint is composed by several structures which contribute to joint control and performance. Its unique movements are the result of a combination of bone geometry, muscles, menisci, ligaments and other soft structures. Stability of the knee joint is maintained by the shape of each of its components (KAKARLAPUDI; BICKERSTAFF, 2000; FLOYD, 2011).

2.2.1 Bone geometry and joints

Formed by the distal extremity of the femur, the patella and the proximal extremities of tibia and fibula, the human knee joint can be subdivided in three minor joints, petellofemoral, tibiofibular and tibiofemoral joint, respectively.

Patella is the lagest sesamoid bone of the human body, it is triangular shaped and lies anteriorly to femur condyles (Figure 4). The patella is surrounded by the quadriceps femoris tendon and its articular surface combined to the femurs patellar surface form the patellofemoral joint. During knee flexion there is a sliding movement in the patellofemoral joint, hence, from 0 to 20 degrees of flexion, the patella remains in front of the femoral intercondylar groove (Figure 5 A) and at 135 degrees of flexion the patella remains below it, as shown in Figure 5 B (NEUMANN, 2010; STANDRING *et al.*, 2016).

Figure 4 – Patella
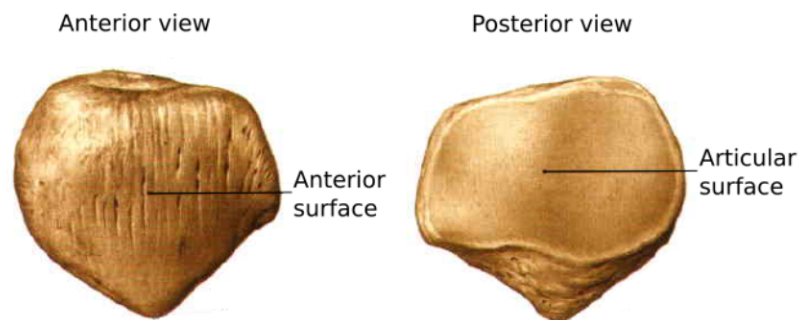
Figure 5 – Movement of patellofemoral joint
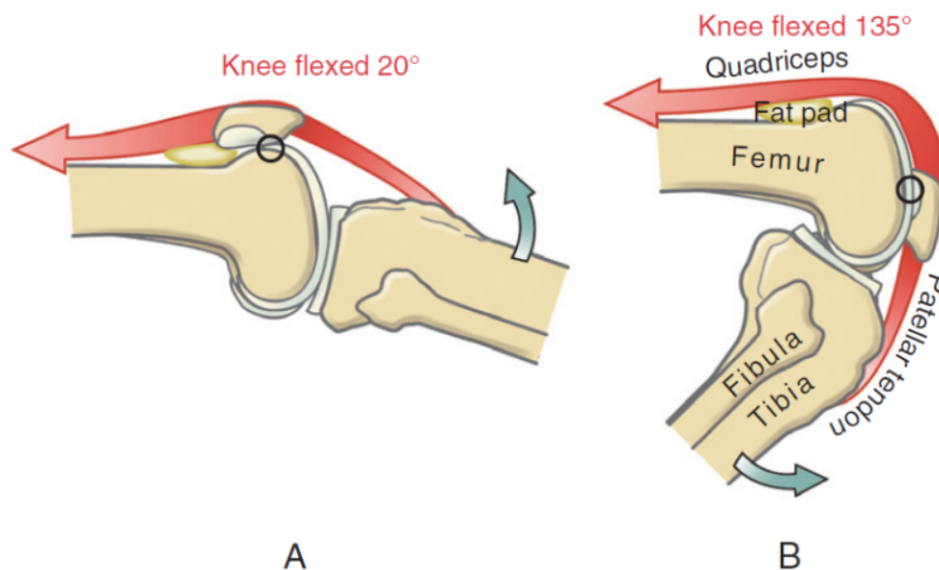
Besides connecting hip movements to knees, femur geometry plays an essential role in knee joint movements. The distal extremity of the femur bears two large convex condyles, lateral and medial, respectively. The lateral condyle is larger than the medial, and each of them possess epicondyles where the latteral ligaments are attached, (Figure 6). Posteriorly, the condyles are separated by the intercondylar fossa where the cruciate ligaments are attached. Anteriorly, the condyles form the intercondylar groove which articulates with patella in the patellofemoral joint (NEUMANN, 2010; STANDRING *et al.*, 2016).

The proximal extremity of the tibia articulates with the femur in the tibiofemoral joint and bears the transmitted load. It comprises medial and lateral condyles which

Figure 6 – Distal extremity of femur (right leg): A - Lateral view, B - Inferior view
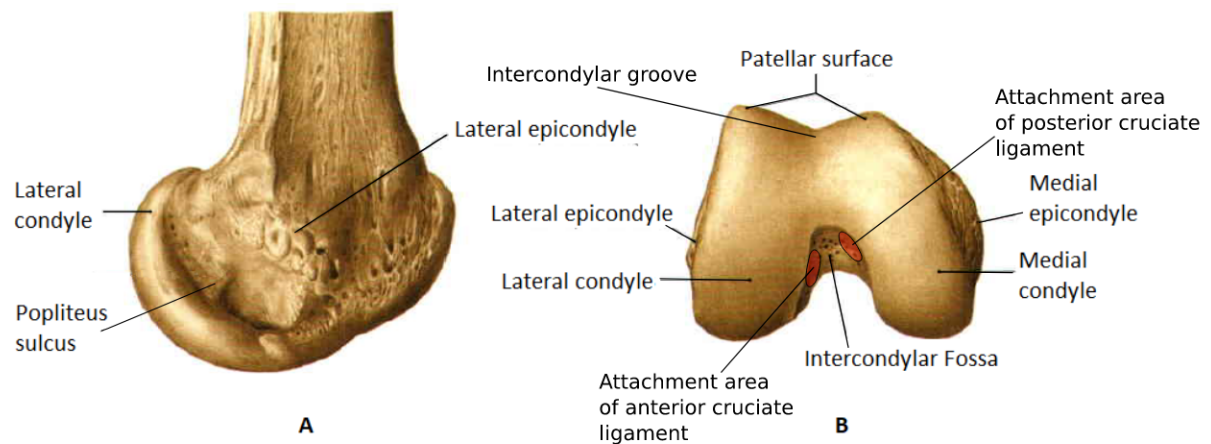
Source – Adapted from (SOBOTTA *et al.*, 2006)

superior surfaces form the articular surface often referred to as the tibial plateau. The medial surface is rather convex than the lateral which is almost flat, and they are separated by posterior and anterior intercondylar areas where the cruciate ligaments as well as the menisci are attached (Figures 7 and 8). From the anterior surface of the tibia projects the tibial tuberosity which is near to smooth areas where patellar tendon and patellar ligaments are attached, as shown in Figure 7) (NEUMANN, 2010; STANDRING *et al.*, 2016).

The fibula lies in the lateral side of the tibia, its proximal head is irregular shaped and projects a proximomedial facet which articulates with the lateral condyle of tibia forming the proximal tibiofibular joint. This joint has minor gliding movements which occurs mutually to movements at the distal tibiofibular joint, as shown in Figure 7 (STANDRING *et al.*, 2016).

The tibiofemoral joint consist of the articulation formed by the distal extremity of femur and the proximal extremity of tibia. The distal extremity of femur posses two almost wholly convex condyles considering the articular cartilage. The proximal extremity of tibia is smaller and posses two concave and nearly flat condyles (NEUMANN, 2010; STANDRING *et al.*, 2016).

According to Standring et al. (2016), the tibiofemoral congruence is improved by the menisci, which produces concavity in tibial surface increasing the contact area with femur condyles.

Figure 7 – Tibia and Fibula parts
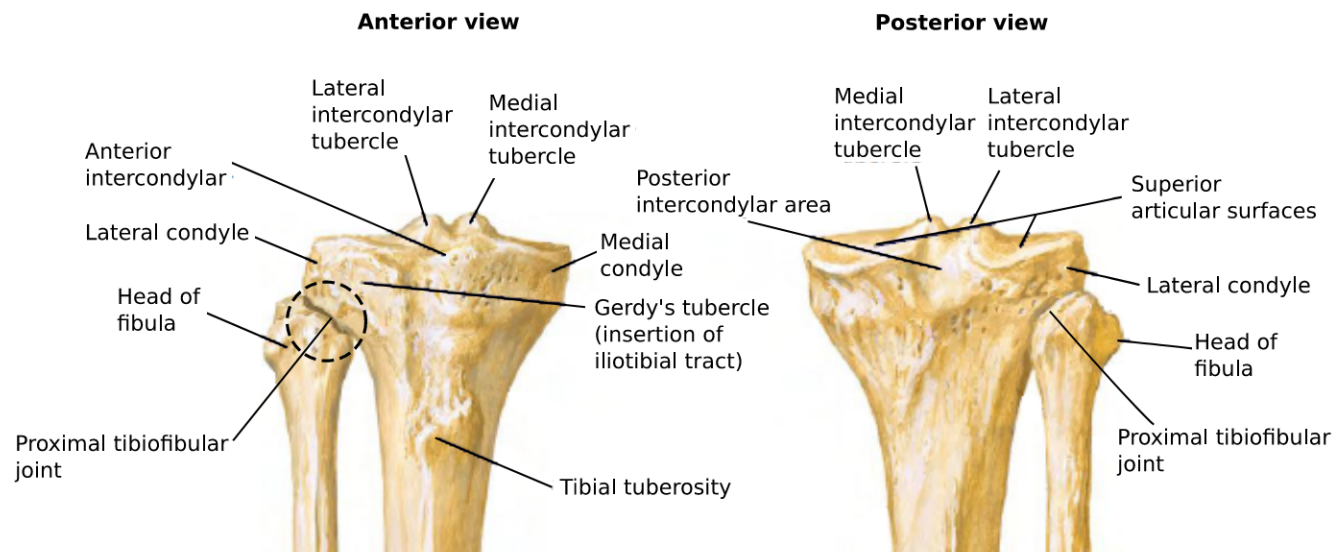
Source – Adapted from (NETTER, 2014)

Figure 8 – Tibia's attachment areas
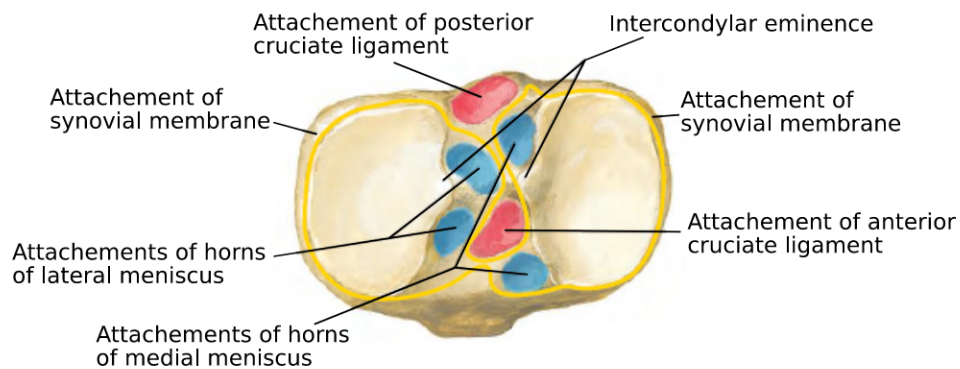
Source – Adapted from (NETTER, 2014)

2.2.2 Menisci

The menisci are two semilunar shaped fibrocartilaginous laminae that prepare the tibial plateau to receive femoral condyles, each covering approximately two-thirds of its tibial articular surface (medial and lateral), represented in Figure 9. They increase the articulation congruence contributing to spread the joint load and providing stability by their physical presence (STANDRING *et al.*, 2016).

The most studied menisci ligaments are the deep fibers of the medial collateral ligament (dMCL) and the two meniscofemoral ligaments, anterior and posterior, also

Figure 9 – Menisci superior view
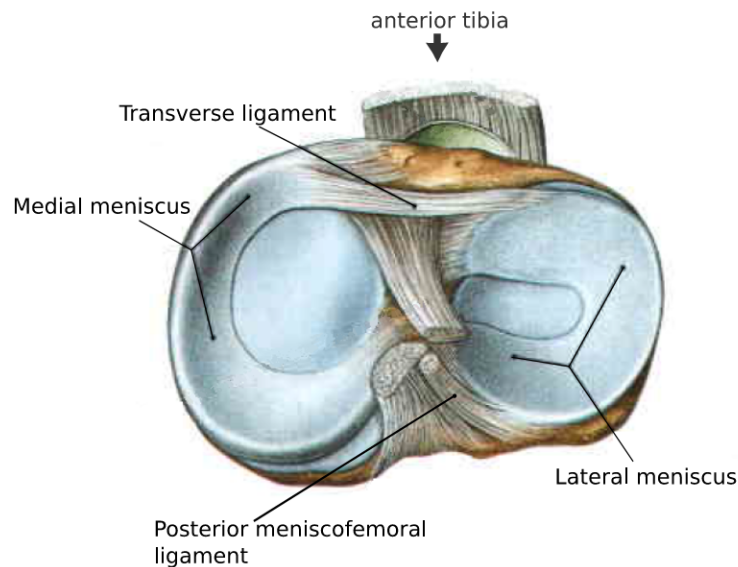
Source – Adapted from (SOBOTTA *et al.*, 2006)

known as ligament of Humphrey and ligament of Wrisberg, respectively (HALEWOOD, 2016).

The medial meniscus is attached to the fibrous capsule and the deep medial collateral ligament, this dMCL attachment acts constraining medial meniscus movements (STANDRING *et al.*, 2016).

The lateral meniscus is attached to meniscofemoral ligaments which act as secondary constraints to posterior translation of the tibia supporting the posterior cruciate ligament (STANDRING *et al.*, 2016; GUPTE *et al.*, 2003).

2.2.3   Ligaments

The ligaments act constraining movements and increasing knee stability. Usually there is more than one ligament constraining the same movement, resisting together an applied load and preventing failure.

The major ligaments in the knee joint are the cruciate ligaments which are the main responsible for constraining the sliding movement between tibia and femur in the sagittal plane, and the collateral ligaments which constrain the movement in the frontal and horizontal plane increasing knee stability. But there are also ligaments connecting the minisci, tendons attaching muscles and membranes involving all joint, each part contributing to preserve stability and well performed movements (Figure 10).

Figure 10 – Right knee ligaments
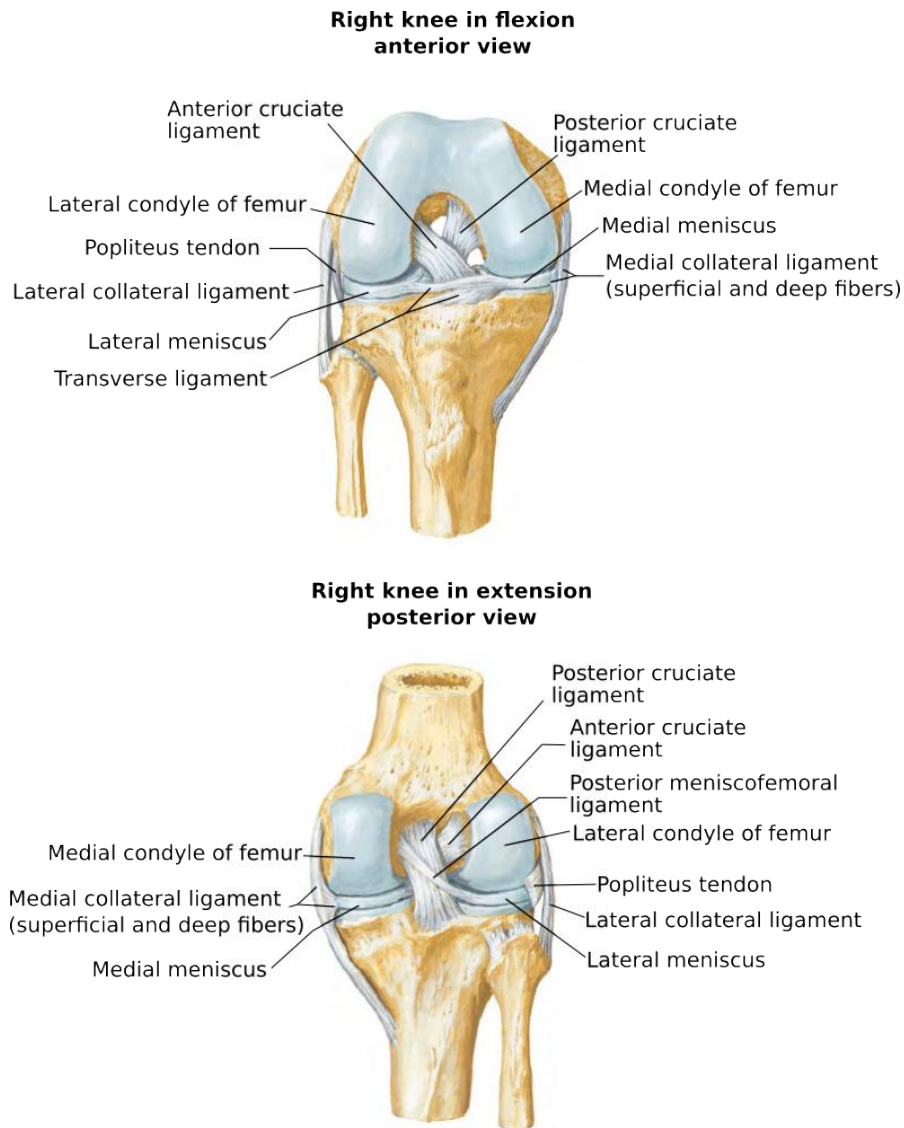
Source – Adapted from (NETTER, 2014)

2.2.3.1 Cruciate ligaments

The Anterior Cruciate Ligament (ACL), shown in Figure 10, is attached to the posterior medial side of lateral femoral condyle and the anterior intercondylar area of tibia. From one attachment to another it twist itself and it is formed by two to three functional bundles (NETTER, 2014; STANDRING *et al.*, 2016).

Taut when knee is fully extended, the ACL prevents posterior displacement of femur on tibia as well as hyperextension of knee joint (NETTER, 2014).

The Posterior Cruciate Ligament (PCL) is attached to the lateral surface of medial condyle of femur and the posterior intercondylar region of tibia. It is formed by two bundles named anterolateral and posteromedial (NETTER, 2014; STANDRING *et al.*,

2016).

Netter (2014) considers that PCL is taut during flexion and Standring et al. (2016) analyze its bundles separately, concluding that anterolateral bundle is taut during flexion while posteromedial bundle tightens in extension of the knee joint. The main function of PCL is to prevent displacement of the femur on tibia.

2.2.3.2 Collateral ligaments

The collateral ligaments are known as Medial Collateral Ligament (MCL) and Lateral Collateral Ligament (LCL), they impose movement constraint of rotation in the anteroposterior axis direction.

The MCL , also known as tibial collateral ligament, is a flat and band shaped ligament which prevent valgus and is attached from medial femoral epicondyle to medial tibial condyle. It can be divided in superficial and deep surfaces. The deep surface is attached to medial meniscus providing it more stability (NETTER, 2014; STANDRING *et al.*, 2016).

The medial ligament complex is composed by the MCL , the posterior oblique ligament, which is posterior to the MCL , and the medial capsular ligament, which is immediately deep to the MCL (KAKARLAPUDI; BICKERSTAFF, 2000).

The LCL , also known as fibular collateral ligament, is a strong and cord shaped ligament attached from lateral femoral epicondyle to fibular head, it limits extension and adduction, preventing varus forces on the knee joint (NETTER, 2014; STANDRING *et al.*, 2016).

From femur to tibia the MCL has an oblique downward and forward direction, whereas the knee is in full extension. In the same situation the LCL has an oblique downward and backward direction, so their directions intersect in space (KAPANDJI, 2000).

2.3 BIOMECHANICS

The geometry of knee joint permits motion to occur in six DoF (Figure 11). The primary motion is constrained to sagittal plane and it is called flexion-extension movement. Flexion-extension is connected to a secondary rotation movement known as screw-home movement in the horizontal plane (external/internal rotation shown in Figure 11). The screw-home rotation is known to be responsible for locking the knee while it is in extension and, in almost every situation, it cannot be performed independently. While in flexion, the knee joint can also perform a minor degree of movement of rotation in the transverse plane due to geometry and ligaments laxity (STANDRING *et al.*, 2016; LIPPERT, 2006; NEUMANN, 2010).

Knee motion is often defined as starting from 0°of flexion, which means that

Figure 11 – The Human knee six DoF movements
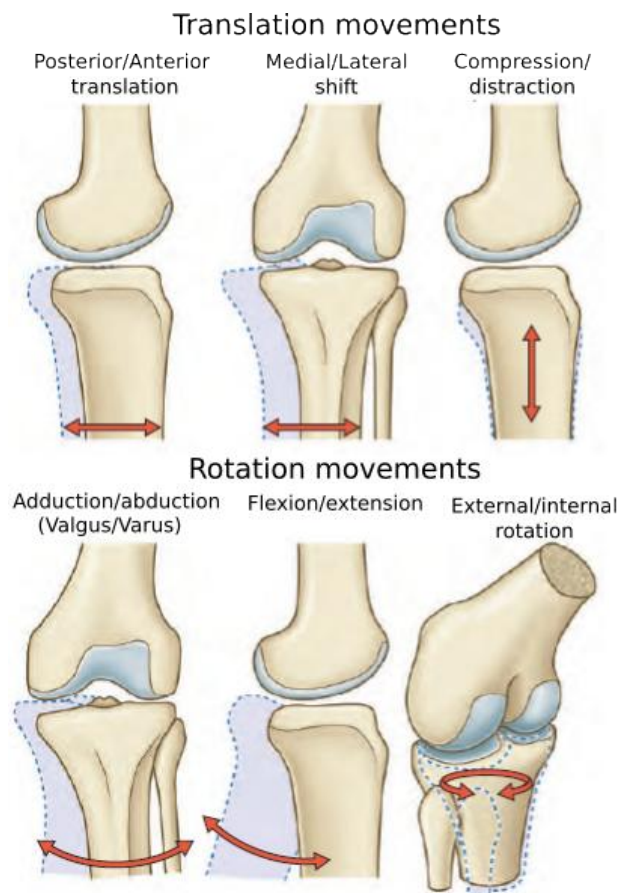
Source – Adapted from (STANDRING *et al.*, 2016)

the joint is fully extended therefore tibia and femur are aligned in the sagittal plane (STANDRING *et al.*, 2016).

The knee flexion-extension movement can be defined as a complex movement being the subject of many studies (OTTOBONI *et al.*, 2010). The flexion-extension involves rotational and translational (or sliding) motions. Experiments produced by Strasse (1917, *apud* Kapanji, 2000) demonstrated that even the proportion of rotation of femurs condyles differs from one another at the same degree of flexion. Beginning at full-extension the condyles present pure rotation but as they are flexed the posteriorly rotational motion (flexion as in Figure 11) occurs combined with the anteriorly sliding movement (anterior translation as in Figure 11) and at the end of flexion only the sliding movement occurs (Figure 12).

The movement of pure rotation in medial condyle occurs from full-extension to 10°to 15°of flexion and in the lateral condyle it occurs until 20 degrees (KAPANDJI, 2000).

A healthy adult knee can perform from 10°to 5°of hyper-extension (or -10°to -5°of

Figure 12 – Human knee flexion movement
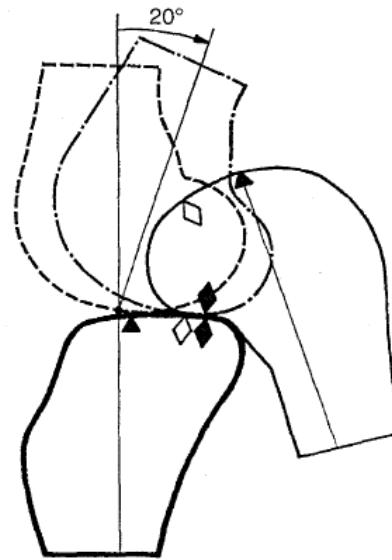
Fig. 2-62

Source – Image from (KAPANDJI, 2000)

flexion) to 130°to 150°of passive flexion (NEUMANN, 2010).

According to the degree of flexion different ligaments became taut or lax, working together as primary or secondary constraints to maintain stability throughout the flexion movement. Hyper-extension movements are primary constrained by ACL ligament and the Oblique Popliteal Ligament (OPL) and secondary constrained by collateral ligaments and menisci (NETTER, 2014).

As previously discussed, cruciate ligaments prevent displacement of femur on tibia (posterior and anterior translations) acting as primary constraints, but they also act as secondary constraints preventing rotations in the horizontal and frontal planes of motion. Collateral ligaments prevent rotation in the frontal plane (adduction and abduction) imposing primary constraints and act as secondary constraints preventing rotation in the horizontal plane (external and internal rotations) and translation in the sagittal plane (posterior and anterior translations). However, the collateral ligaments became more slack according to the flexion angle of the knee (generally, the more flexed the knee is, the more slack the collateral ligaments are).

There are different clinical laxity tests applied to exam the clinical conditions of ligaments and soft structures of the knee joint and they are usually performed to identify possible tear of a ligament or any instability.

The *anterior drawer test* is performed with the knee flexed at 90°and the *Lachman test* is performed from 20°to 30°of flexion but both apply forces in the direction of anterior translation of the tibia. This tests are usually performed to exam the anterior cruciate

ligament integrity (LUBOWITZ *et al.*, 2008).

Accordingly, the *posterior drawer test* is performed with the knee flexed at 90°and the *posterior Lachman test* is performed from 20°to 30°of flexion, both applying forces in the direction of posterior translation of the tibia and usually performed to exam the posterior cruciate ligament integrity (LUBOWITZ *et al.*, 2008).

Valgus and *varus tests* are performed applying movements of abduction and adduction, respectively, while performing flexion movement. The Valgus test has as primary constraint the medial collateral ligament followed by the anterior cruciate ligament and the posterior oblique ligament. The major constraints to *varus test* are the lateral collateral ligament and the posterior cruciate ligament (LUBOWITZ *et al.*, 2008).

The *pivot-shift test* and the *reverse pivot-shift test* apply internal and external rotation, respectively, combined with valgus rotation while flexing the knee. These tests are often used to confirm injuries in cruciate ligaments (LUBOWITZ *et al.*, 2008).

During *dial test*, the tibia is forced to perform movements of external rotation from 30°to 90°of flexion, to compare the knees and indicate abnormal laxity.

Compression and distraction movements of tibia are apply during *Apley's test* which is performed to detect minisci injury or chondral lesion (defect in femur condyles) (ROSSI *et al.*, 2011).

Other tests used to evaluate knees injuries are a combination of the presented tests and are usually performed to corroborate with the initial diagnosis of possible injuries.

2.4 FORCES AND CONSTRAINTS ANALYSIS

The ligaments are essential for proper knee function. Each ligament provides stability in more than one DoF, playing an important role as an individual constraint and also interacting with one another, maintaining the knee stability (WOO *et al.*, 1998).

To better understand the function of each knee's structure during gait or passive motion, some studies analyzed the distribution of internal forces and the constraints within the knee joint.

Ligaments and other knees structures play different roles during flexion-extension movement. Halewood (2015), presents the analysis of active constraints in the human knee during different ranges of flexion when submitted to different clinical tests, during a study comparing different total knee replacement (TKR) and test methods (HALEWOOD; AMIS, 2015).

Conconi et al. (2019), discuss the main structures responsible for constraining knees motion, presenting a geometrical characterization of the knee motion, applying the principle of virtual work and demonstrating the necessity of the intersection of the lines of each resultant force with the instantaneous helical axis, allowing a one DoF unresisted motion at the knee (CONCONI *et al.*, 2019).

One of the causes of the singular motion of the human knee, is the change of

orientation and elongation of fibers that compose the ligaments of the human knee. In this regard, a study compare the data obtained in tests using ten cadavers to analyze the changes in the cruciate and collateral ligaments, as well as in the patellar tendon during flexion-extension, comparing the elongation and orientation of fibers (BELVEDERE *et al.*, 2012).

Being one of the major ligaments of the human knee and associated with one of most common injuries, the ACL is the focus of diverse studies. In order to evaluate the *in situ* forces of the ACL ligament, a robotic manipulator was used in experiments involving nine human cadaver knee joints, analyzing the ligaments behavior under stress in different ranges of flexion (WOO *et al.*, 1998).

The experimental data of researches that analyzed the kinematics and the distribution of forces within the structures of the human knee were used to compare and validate different mechanisms aiming to replicate the knees kinematic and force distribution, in order to contribute in the development of prosthesis or in surgical procedures of ligament reconstruction (PARENTI-CASTELLI; GREGORIO, 2000; OTTOBONI *et al.*, 2010; SANCISI *et al.*, 2011; PARENTI-CASTELLI; SANCISI, Nicola, 2013; PONCE SALDIAS, 2014)

2.5   MECHANICAL REPRESENTATION

Different mechanical representations of the human knee where developed and applied in diverse areas. This section is focus on the research developed to replicate the human knee trajectory and contribute in surgical procedures, focusing on ligaments' mechanical representation and *in situ* forces.

To represent ligaments in mechanisms different approaches can be made. Wilson *et al.* (1998) present distinct equivalent connections using either higher pairs or one DoF pairs, proposing a 3D mechanism model of the knee (WILSON, D.; O'CONNOR, 1997; WILSON, D. R. *et al.*, 1998).

Parenti-Castelli and Di Gregorio (2000) develop variants of the one-DoF mechanism proposed by Wilson et al. (1997) presenting other mathematical solutions to forward kinematics for passive knee motion (PARENTI-CASTELLI; GREGORIO, 2000; WILSON, D.; O'CONNOR, 1997), and in further work (PARENTI-CASTELLI *et al.*, 2004), demonstrating the validation of the use of one DoF spatial mechanisms to the kinematic modelling of the knee.

Carrying on the representation of the human knee by the theory of mechanisms, Sancisi (2011) proposed a 1 DoF spherical mechanism, validating the proposal as a possible alternative solution as a kinematic model, presenting satisfactory results with a lower mechanical complexity (SANCISI *et al.*, 2011).

Most recent research proposed a model of a 5-5 parallel mechanisms, with five parallel rigid links connecting the platform to the base by spherical joints, representing

with high accuracy the knee passive motion (SANCISI, Nicola; PARENTI-CASTELLI, 2011). Afterwards, this model was improved by the addition of the patello-femoral joint mechanical representation (PARENTI-CASTELLI; SANCISI, Nicola, 2013). This latest model was successfully applied and customized in the replication of the knee motion of a volunteer, comparing the trajectory obtained by clinical images (NARDINI *et al.*, 2020).

The knee representation by theory of mechanism has a great value in the development of prosthesis and surgical procedures. Aiming to contribute on decision-making during ACL reconstruction a new mechanism was proposed and validated by Ponce (2014). Inspired by the 5-5 parellel mechanism (SANCISI, Nicola; PARENTI-CASTELLI, 2011), the new proposal is a reshaped 5-5 parallel mechanism developed considering the anatomical constraints, and optimized to besides delivering a kinematic model, also obtaining the *in situ* forces in the ACL during passive motion. This research brings multiple contributions expanding the possibilities of application of theory of mechanisms contributing to surgical procedures (PONCE SALDIAS, 2014).

2.6   FINAL CONSIDERATIONS

All developed models assume rigid links as joint structures during passive motion, simplifying each ligament as a single rigid link. As pointed by the reviewed literature, the ligaments suffer elongation and alterations in the direction of its fibers during flexion-extension, imposing different constraints to the human knee.

3 KINEMATIC AND STATIC ANALYSIS

This chapter introduces fundamental tools used in this thesis to analyze the kinematic and static of mechanisms, as Graph Theory, Screw Theory, Davies Method and Position Analysis.

3.1 GRAPH THEORY

Graph Theory is applied in problems of different areas. In the representation of mechanisms, each element of the graph corresponds to an element of the mechanism, representing the connection between links, as forces, motion, velocity and other properties (TSAI, 1999) (MENEGHINI, 2020).

A graph is a structure that consists in *vertices* and *edges*. In the representation of mechanisms, each graph vertex represents a link of a mechanism, and each graph edge can represent a joint of a mechanism, a group of actions, or properties connecting two links (MARTINS, 2002).

If the graph is represented assigning a direction to each edge, it is called a *directed graph* or a *digraph*, and the directed edges are called *arcs*.

A kinematic chain can be represented as a coupling graph (G_c), where each link will be represented as a vertex and each joint as an arc with an arbitrary direction.

Action graph (G_A) is a graph where the arcs represent single constraints. In static analysis, each joint can be represented as multiple arcs equivalent to the number of joint's constraints (Figure 13 (a)).

Opposite to a action graph, a movement graph (G_M) is a graph where the arcs represent single freedoms. In kinematic analysis, each joint of a mechanism can be represented as an arc with a number of arrows equal the number of joint's freedom (Figure 13 (b)) (MARTINS, 2002).

Considering the Stephenson kinematic chain with only revolute joints R_x, within a

Figure 13 – Graph representation for a cylindrical joint in Y axis: (a) Action Graph (G_A) (b) Movement graph (G_M).
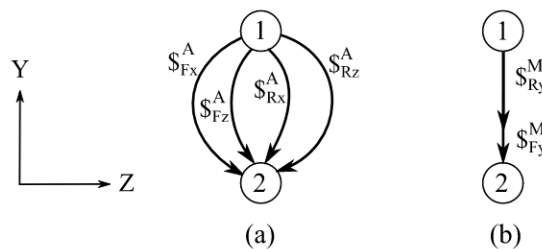
Source – own construction

Figure 14 – (a) Stephenson kinematic chain; (b) Coupling Graph and (c) Action Graph.

(a)   (b)   (c)
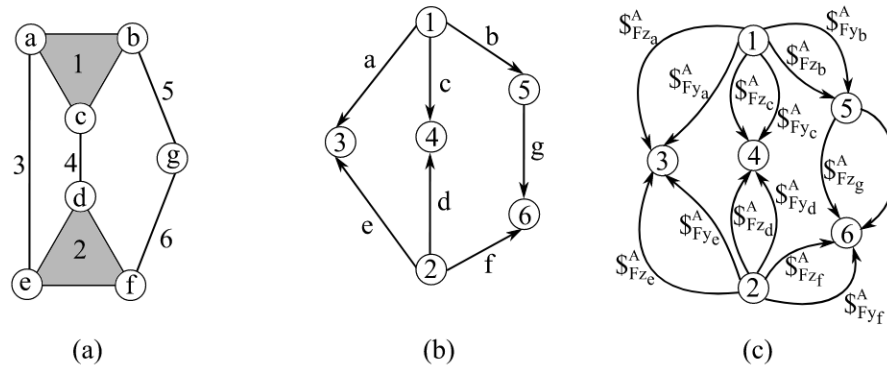
Source – own construction

planar workspace, the kinematic chain, coupling graph (G_c) and action graph (G_M) can be represented as Figure 14 (a), (b) and (c), respectively.

Every graph is composed by a *tree, branches* and *chords*. A tree is a subgraph that connects all vertices without closing any circuit. The edges that take part in the tree are called branches and the ones that do not take part are called chords (Figure 15 (a and b)).

After defining the tree, branches and chords, it is possible to define the *cutsets*. A cutset is formed by a group of branches and arcs that can be circled in the graph without crossing more than one branch, spliting the graph into disjoint subgraphs (Figure 15 (c)). The number of cutsets equals the number of branches and the number of chords equals the number of circuits of a graph (MARTINS, 2002).

Figure 15 – (a) Coupling graph with circuits identification (G_c) ; (b) Action Graph (G_A) and (c) Cutsets. Branches are identified in black, chords in dashed red and cutsets in dashed blue.

(a)   (b)   (c)
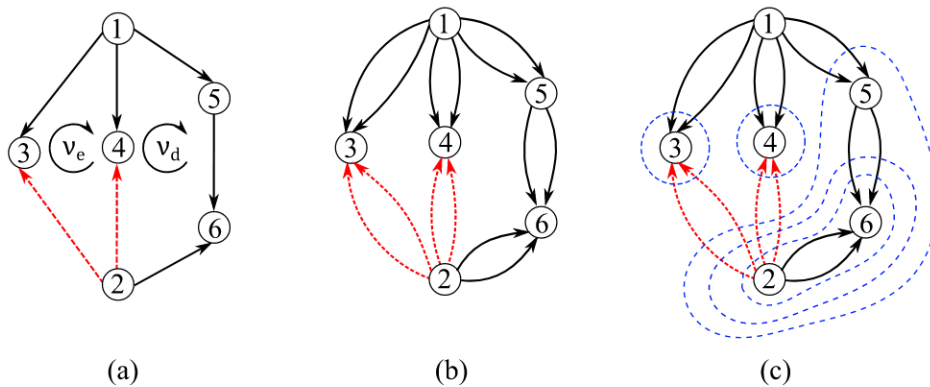
Source – own construction

The coupling graph, movement graph and the cutsets, can be represented by matrices. The incidency matrix (I_C) (1) is a representation of the coupling graph, their elements are -1's, 1's or 0's, according to the direction of each edge (e) towards each vertex (v). Being 1 if the edge is pointing out of the vertex, -1 if the edge is pointing towards the vertex and 0 if the edge is not connected to the vertex.

$$[I_C]_{v \times e} = \begin{pmatrix} i_{1,1} & \cdots & i_{1,e} \\ \vdots & \vdots & \vdots \\ i_{v,1} & \cdots & i_{v,e} \end{pmatrix} \tag{1}$$

The circuit matrix B_M (2), is the representation of the movement graph, identifying the mechanism circuits. This matrix is composed by -1's, 1's and 0's elements according to the direction of each edge and the direction of each circuit (v). Being 1 if the edge is pointing towards the same direction of the circuit, -1 if the edge is pointing against the circuit's direction and 0 if the edge is not on the circuit.

$$[B_M]_{l \times e} = \begin{pmatrix} b_{1,1} & \cdots & b_{1,e} \\ \vdots & \vdots & \vdots \\ b_{l,1} & \cdots & b_{l,e} \end{pmatrix} \tag{2}$$

The cutset matrix Q_A (3), is the representation of each cutset (s) of the mechanism. The Q_A matrix is also composed by -1's, 1's and 0's elements according to the direction of each edge contained in the cutset when compared to the direction of the branch that is being cut, defining the direction of the cutset. The element is equal to 1 if the edge is pointing towards the same direction of the branch that defines the cutset, -1 if the edge is pointing against the branch and 0 if the edge is not on the cutset.

$$[Q_A]_{s \times e} = \begin{pmatrix} q_{1,1} & \cdots & q_{1,e} \\ \vdots & \vdots & \vdots \\ q_{s,1} & \cdots & q_{s,e} \end{pmatrix} \tag{3}$$

3.2   SCREW THEORY

Screw theory is a powerful tool to represent and analyze the instantaneous kinematic and static of a given mechanism in space, based on the idea that any motion can be represented by a rotation and a translation in the same axis corresponding to the analyzed object. The theory was first reasoned by Mozzi (1763), introducing its first concepts and later structured by Ball (1900) (CAZANGI, 2008; MOZZI, 1763; BALL, 1900).

A screw ($) is a geometrical element, an axis with a determined pitch. It can be represented in axial form, when the free vector is in the second part of $ (Eq. 4), or radial

form when the free vector is in the first part of $ (CAZANGI, 2008).

$$\$ = \begin{pmatrix} \vec{S} \\ \\ \vec{S}_0 \times \vec{S} + h\vec{S} \end{pmatrix} \tag{4}$$

Regarding instantaneous kinematic the screw is referred to as a twist, formed by the combination of angular velocities about axes and linear-velocity components of points. Regarding statics, the screw is referred to as a wrench, formed by a combination of forces and couples (HUNT, 2003).

A twist is composed by the angular velocity (w) about the instantaneous axis of rotation of a body, and the linear velocity (Vp) of a point (P) attached to the same body and related to the same coordinate system. A twist pitch (h) is described as a relation between the angular velocity and the linear velocity (MARTINS, 2002; CAZANGI, 2008). The twist can be represented as Eq. (5).

$$\$^{M} = \begin{pmatrix} \vec{w} \\ \\ \vec{V}_p \end{pmatrix} = \begin{pmatrix} \vec{w} \\ \\ \vec{S}_0 \times \vec{w} + h\vec{w} \end{pmatrix} \tag{5}$$

Normalizing the twist, it is possible to obtain a geometrical element ($\hat{S}^{M}$) and a related magnitude of velocity (ψ^{M}) (Eq. 6).

$$\$^{M} = \begin{pmatrix} \vec{S}^{M} \cdot \psi^{M} \\ \\ (\vec{S}_0 \times \vec{S}^{M} + h\vec{S}^{M}) \cdot \psi^{M} \end{pmatrix} = \begin{pmatrix} \vec{S}^{M} \\ \\ \vec{S}_0 \times \vec{S}^{M} + h\vec{S}^{M} \end{pmatrix} \cdot \psi^{M} = \hat{S}^{M} \cdot \psi^{M} \tag{6}$$

A wrench (Eq. 7) is composed by the resultant force $\vec{F}_R$ applied to a body and the resultant couple moment $\vec{T}_P$ at a specific point P of the body (MARTINS, 2002; CAZANGI, 2008). The resultant couple moment $\vec{T}_P$ is formed by a binary vector, parallel to the wrench's axis and the resultant couple in a point P due the application of the

resultant force $\vec{F}_R$.

$$
\$^M = \begin{pmatrix} \vec{T}_P \\ \\ \vec{F}_R \end{pmatrix} = \begin{pmatrix} \vec{S}_0 \times \vec{F}_R + h\vec{F}_R \\ \\ \vec{F}_R \end{pmatrix} \tag{7}
$$

Normalizing the wrench, related to the direction of the screw, it is possible to obtain a geometrical element ($\hat{S}^A$) and a related magnitude of load (ψ^A) (Eq. 8).

$$
\$^A = \begin{pmatrix} (\vec{S}_0 \times \vec{S}^A + h\vec{S}^A) \cdot \psi^A \\ \\ \vec{S}^A \cdot \psi^A \end{pmatrix} = \begin{pmatrix} \vec{S}_0 \times \vec{S}^A + h\vec{S}^A \\ \\ \vec{S}^A \end{pmatrix} \cdot \psi^A = \hat{S}^A \cdot \psi^A \tag{8}
$$

3.3 DAVIES METHOD

A tool to analyze the static and kinematic of complex mechanisms, the Davies Method is based on Kirchhoff's first law (Kirchhoff's junction rule), Kirchhoff's second law (Kirchhoff's voltage law) and the topology of kinematic chains. Through Graph Theory and Screw Theory, Davies adapted Kirchhoff's laws to the analysis of mechanisms, originating the Davies Method (DAVIES, 1995).

Davies Method solves the instantaneous actions and movements of each kinematic pair in a given kinematic chain. The method represents the related magnitudes through screws, being possible to apply the method to solve either static or kinematic of a mechanism.

The method was detailed and applied in different thesis, analyzing the differential kinematics or static of mechanisms (MARTINS, 2002; CAZANGI, 2008; WEIHMANN, 2011; MEJIA RINCON, 2016; MORENO CONTRERAS, 2017; MENEGHINI, 2020).

3.4 POSITION ANALYSIS

A serial manipulator is formed by a joint in a fix base followed by a sequence of links connected in series by joints, the last link is called end-effector. A parallel manipulator usually consists of a fixed base connected to a moving platform by "*limbs*" or "legs" consisting of a series of links connected by joints.

To calculate the position and orientation of the joints in a given mechanism, position kinematic analysis is used. The position analysis can be made by forward kinematics (also known as direct kinematics) or inverse kinematics.

In problems involving forward kinematics, variables of actuated joints are known and some methods can be applied to calculate the position of non-actuated joints and the end-effector or the platform. Forward kinematics of serial manipulators is generally straightforward, it is usual to apply the Denavit-Hartenberg Method, though is also possible to apply the Method of Sucessive Screw Displacement (TSAI, 1999; SIMAS, 2008; MENEGHINI, 2020). Whereas for a parallel manipulator, the forward kinematics becomes difficult, depending on the number of DoF, being an option to use the Geometric Method (TSAI, 1999).

In problems of inverse kinematics, the position and orientation of the end-effector of the serial manipulator, or a specific point of the platform for a parallel manipulator, is known, and the problem is to find the joint variables resulting in the given position of the end-effector. Depending on the type of the mechanism, it is possible to have several solutions for a inverse kinematics problem (TSAI, 1999).

3.5   FINAL CONSIDERATIONS

This chapter introduced theoretical basis of different tools used during the development of this thesis to study and analyze the motion and the static of the proposed mechanisms. Graph Theory was also used during early stages of this research and is applied in Section 4.2 during the calculus of mechanisms mobility.

4 BIOMECHANICAL AND MOBILITY ANALYSIS

A mechanism capable of changing its topological structure or configuration during operation is usually called as a reconfigurable mechanism (KUO *et al.*, 2009). Kuo et al. (2009) describe four conditions that indicates the ability of a mechanism change its topology or configuration: *"the effective number of its links and/or joints are changeable, the kinematic types of certain joints are changeable, the adjacency and incidence of links and joints are changeable, and the relative arrangement between joints is changeable"*. If a given mechanism met at least one of these conditions, it can be called as reconfigurable.

As well as in some reconfigurable mechanisms, the human knee joint suffers alterations on its kinematic chain during flexion-extension movements. This occurs due to the geometry of its soft structures which can vary from taut to lax throughout the movement.

A lax ligament can be mechanically seen as a non existing joint because, at that instant, it does not imposes any constraint to the knee joint, not contributing to stability nor impacting on knees trajectory. The same occurs to cable joints, the only constraint imposed by this type of joint is translation in the direction of its own axis, but when lax the cable joint can not impose any constraint, therefore it does not cause any kinematic impact on the mechanism. In this regard, it is proposed to analyze the kinematic chains contained in the human knee flexion-extension movement, formed by its main structures.

4.1 BIOMECHANICAL ANALYSIS

In order to analyze the knee joint as a mechanism, one must understand the source of its movements' constraints.

The study developed by Halewood (2015) identifies primary and secondary constraints for different flexion angles of the knee during different clinical tests.

As previously discussed in chapter 2 (Pag. 33), there are standard tests applied to the knee joint in order to evaluate the integrity of ligaments. These tests consider the movement of tibia in relation to a stationary femur. Each test perform a movement corresponding to one DoF, resulting in the analysis of existing constraints in that movement direction. Therefore all considerations made in this regard are presented in Table 1 given Figure 16, based on axis defined in Figure 2.

Figure 16 – Right knee reference axis of motion.
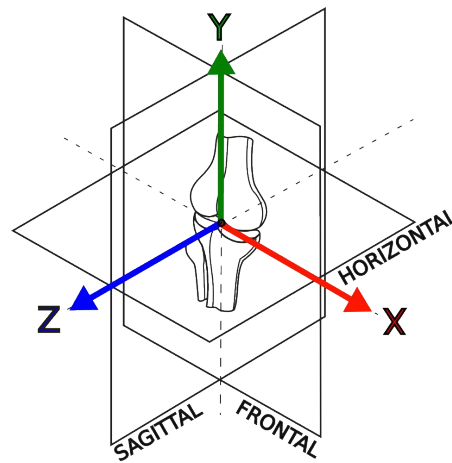
Source – own construction

Table 1 – Knee standard exams and DoF equivalence considering a fixed femur and a mobile tibia

Test	Direction
Anterior drawer	Tz(+)
Posterior drawer	Tz(-)
Internal Rotation	Ry(+)
External Rotation	Ry(-)
Varus	Rz(+)
Valgus	Rz(-)
Flexion	Rx(+)
Hyperextension	Rx(-)

(+) Positive direction of translation or counterclockwise direction of rotation; (-) Negative direction of translation or clockwise direction of rotation; T - Translation; R - Rotation; x, y and z stand for its respective axis.

Based on Table 1 considerations and the discussed literature, Table 2 was developed, dividing the flexion movement into eight ranges of flexion degrees due to the variation of tautness of each studied ligament.

Table 2 – Mechanical constraints imposed by ligaments during flexion-extension movement.

Flexion range	Ligament	constraints
< 0	OPL	Rx(-)
	ACL	Rx(-)
	PCL	Rx(-)
	PFL	Rx(-)
	POL	Rx(-)
0 - 30	ACL	Ry(+), Rz(-), Tz(+)
	PCL	Rz(+), Tz(-)
	LCL	Ry(-), Rz(+), Tz(-), Tz(+)
	MCL	Ry(+), Ry(-), Rz(-), Tz(+)
	OPL	Rz(-), Tz(-)
	PFL	Ry(-), Tz(-)
	MFL	Tz(-)
	POL	Ry(+), Rz(-), Tz(-)
	Menisci	Ry(+), Ry(-), Tz(+)
30 - 40	ACL	Ry(+), Rz(-), Tz(+)
	PCL	Ry(-), Rz(+), Tz(-)
	LCL	Ry(-), Rz(+), Tz(-)
	MCL	Ry(+), Ry(-), Rz(-), Tz(+)
	OPL	Tz(-)
	PFL	Ry(-), Tz(-)
	MFL	Tz(-)
	POL	Ry(+), Tz(-)
	Menisci	Ry(+), Ry(-)
40 - 60	ACL	Ry(+), Rz(-), Tz(+)
	PCL	Ry(-), Rz(+), Tz(-)
	LCL	Ry(-), Rz(+)
	MCL	Ry(+), Ry(-), Rz(-)
	PFL	Tz(-), Ry(-)
	MFL	Tz(-)
	POL	Ry(+)
	Menisci	Ry(+), Ry(-)
60 - 90	ACL	Ry(+), Tz(+)
	PCL	Ry(-), Rz(+), Tz(-)
	LCL	Ry(-), Rz(+)
	MCL	Ry(+), Ry(-), Rz(-)
	Continued on next page	

Table 2 – continued from previous page

Flexion range	Ligament	constraints
	PFL	Tz(-)
60 - 90	MFL	Tz(-)
	Menisci	Ry(+), Ry(-)
	ACL	Tz(+)
	PCL	Ry(-), Tz(-)
	LCL	Ry(-)
90 - 120	MCL	Ry(-)
	PFL	Tz(-)
	MFL	Tz(-)
	Menisci	Ry(-)
120 - 140	ACL	Tz(+)
	PCL	Tz(-)

ACL - Anterior Cruciate Ligament, PCL - Posterior Cruciate Ligament,

LCL - Lateral Collateral Ligament, MCL - Medial Collateral Ligament,

OPL - Oblique Popliteal Ligament, PLC - Popliteofibular Ligament

Complex, MFL - Meniscofemoral Ligaments

Regarding translation in the direction of y-axis, by analyzing the knee structure it is possible to assume that all ligaments and soft structures constraint the movement of tibia in negative translation (distraction) whereas tibia itself and the menisci prevent the positive translation (compression).

Regarding translation in the directions of x-axis, the same ligaments that provide resistance to rotation about z-axis may act as constraints in the translation in x-axis. In the human knee, this may occur as a combination of dimensional constraints align with the constraint of translation in y-axis.

The constraints presented in Table 2 are mostly the result of ligaments geometry and position. When the tibia perform a movement in one direction a group of ligaments became taut, consequently these ligaments present constraints regarding that movement. However analyzing the ligament by itself as a single joint, it does not provide the same amount of constraints.

Therefore, in order to represent and analyze the constraints of each ligament of the knee as a mechanism there are different approaches. Some approaches may consider anatomical factors as geometry and shapes and others focuses in the constraints imposed by each ligament which are responsible for constraining the knee mechanism.

This second kind of approach tries to translate the anatomical constraints present in the human knee to mechanical constraints, preserving its redundancies. This approach aims to better understand the mechanical behavior of ligaments in the human knee using

theory of mechanism, presenting a different perspective of the human knee as a mechanism and for this reason it was chosen for the development of the present work.

4.1.1 Human knee by Theory of Mechanisms

From now on, ligaments will not be seen as their anatomy or as cable joints, but as the raw constraints and freedoms that each one of them imposes for each movement of Tibia. This approach is proposed to evaluate the *in situ* forces of each ligament, focusing in the static analysis.
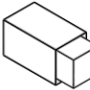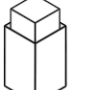
When a ligament presents a constraint, the equivalent mechanism will not allow this DoF, but when the ligament does not constraint a movement, the equivalent mechanism will have a joint representing this DoF. Consequently, when external forces are applied on the mechanism in a specific direction, ligaments representation that allows movement in the force direction will not present constraining forces.

The constraints presented in Table 2 enable the division of the knee mechanism in distinct kinematic chains. This approach provides the possibility of working with rigid links since all considered ligaments in that range of flexion stay taut throughout the range.

Initially, the contact between the femur and tibia was considered as constraining translation in the y-axis and x-axis, representing the anatomical constraints between the femur, tibia, menisci and other soft structures. This consideration is then validated or amended when the mobility of each mechanism is calculated, since all mechanisms must have mobility equal to one and other anatomical parts may present constraints on the knee regarding its degree of flexion.

To develop the mechanisms for each range of flexion, only joints with one DoF were considered (Figure 17). Then each ligament was represented as one arm of the mechanism containing the constraints presented in Table 2 and resulting in different parallel mechanisms.

Figure 17 – Joints representation

The resulting mechanisms for each range of flexion are illustrated in Figure 18 and its respective kinematic chains in Figure 19.

Figure 18 – Mechanisms for each range of flexion. Ligaments represented by the mechanisms arms: LCL - Lateral Collateral Ligament (yellow), ACL - Anterior Cruciate Ligament (blue), Contact point (black), PCL - Posterior Cruciate Ligament (red), MCL - Medial Collateral Ligament (green)
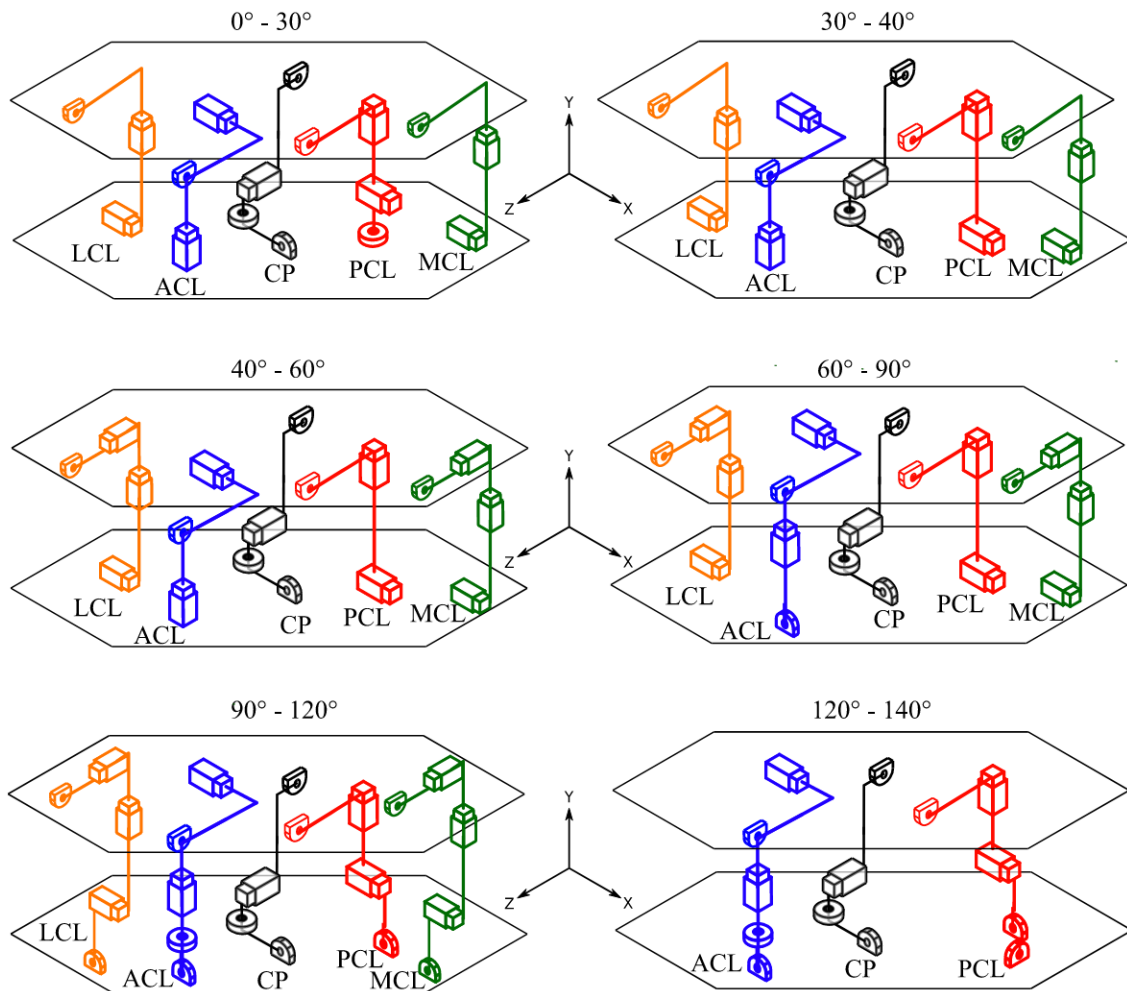
Source – own construction

The proposed representation has its limits, since as shown in Table 2, sometimes in a single axis the ligaments present constraints in one direction and freedom in other, this is due to the laxity of the ligament and it is not represented in rigid links. In the proposed approach, if a ligament presents a constraint regarding one DoF, this constraint will be considered regardless the direction of the movement.

Figure 19 – Kinematic chains for each range of flexion.
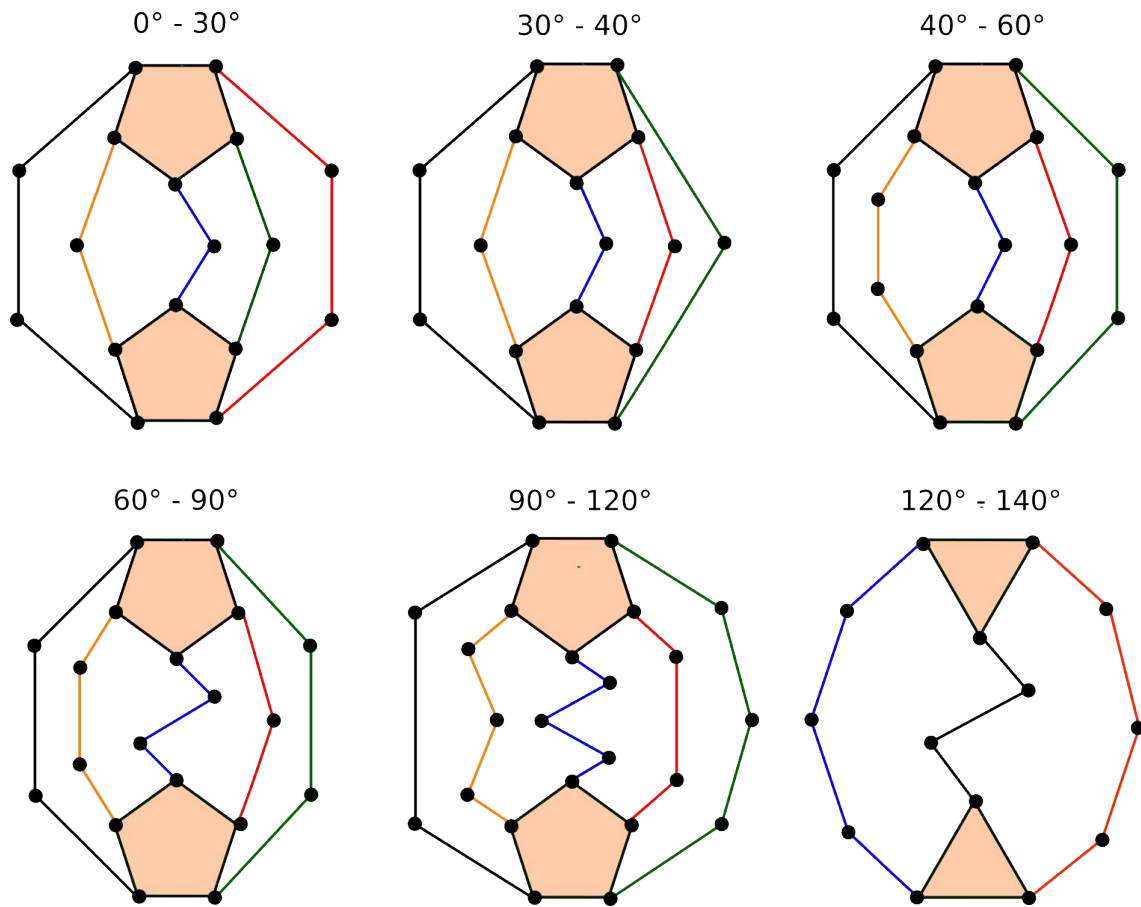
Source – own construction

4.2 MOBILITY ANALYSIS

The mobility or DoF of a mechanism is "the number of independent parameters required to completely specify the configuration of the mechanism in space" (TSAI, 2001).

By using the Grübler or Kutzbach Criterion (9) it is possible to obtain the mobility of a mechanism (TSAI, 2001).

$$M = \lambda(n - j - 1) + \sum_{i=1}^{j} f_i \tag{9}$$

Where:

- M is the mechanism DoF

- λ refers to the DoF of the space which comprises the motions of the mechanism

- n is the number of links

- j the number of kinematic pairs

- f_i degrees of relative motion permited by a joint

However, the Grübler criterion can not be used to obtain the mobility of overconstrained mechanisms. For these mechanisms, Huang et al. (2013) developed the Modified Grübler-Kutzbach Criterion (Eq. 10), which considers the mechanisms redundant constraints (C_N) in the mobility calculus.

$$M = \lambda(n - j - 1) + \sum_{i=1}^{j} f_i + C_N \tag{10}$$

A redundant constraint is the one that does not change the mechanism mobility, therefore when removed the mechanism remains with the same DoF.

To analyze the constraints of a given mechanism, Reshetov's method can be used (RESHETOV, 1979). In this method, first it is necessary to evaluate the mechanism graph dividing its kinematic pairs among its loops. An example of a four-bar mechanism is shown in Figure 20. Then, for each loop, a mobility table is elaborated and filled in with the freedoms of each kinematic pair.

Figure 20 – Four-bar mechanism, kinematic chain and graph representation.

MECHANISM   STRUCTURAL   GRAPH
                  REPRESENTATION
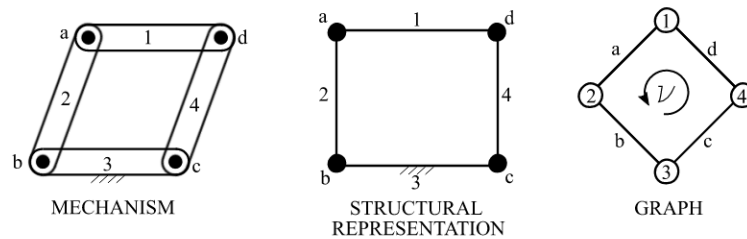
Source – own construction

The four-bar mechanism is formed by four links and four revolute joints, it is a planar mechanism, which means that its movements are within a space of three DoF ($\lambda = 3$). As a four-bar mechanism has one loop, only one table is necessary to analyze its mobility by using Reshetov's method.

In Reshetov's method, a mechanism with mobility and overconstraints equal to zero is translated in a table where for each DoF a single joint freedom is distributed. Each joint's freedom must fill the table of its respective loop, in the four-bar example the single loop (ν_1) is formed by the joints a, b, c and d. In Table 3 the columns that list the DoF are marked with a red rectangle and the columns that correspond to the freedom of each joint are marked with a blue dashed square. It is possible to observe that the four joints in the four-bar mechanism present only the freedom of rotation about the x-axis (R_x).

After fill in the table with the joints freedoms, one must distribute the spare freedoms. Each spare rotation freedom can compensate the lack of freedom in one of the

Table 3 – Reshetov's method applied to a four-bar mechanism

Loop (a, b, c, d)			
R_X	a, b, c, d	T_X	0
R_y	0	T_y	0
R_z	0	T_z	0

translations, as long as the translation is not contained on the same axis of the respective rotation.

In the four-bar mechanism, the freedoms of joints c and d (Table 4), can be redistributed to T_y and T_z, respectively, compensating the redundant constraints.

Table 4 – Permutation in Reshetov's method applied to a four-bar mechanism

Loop (a, b, c, d)			
R_X	a, b, c, d	T_X	0
R_y	0	T_y	0 (d)
R_z	0	T_z	0 (c)
	M = 1	C_N = 3	

Ultimately, the table lines that do not present a DoF (zeros with arrows pointing down) represent the redundant constraints (C_N) of the mechanism. The lines that received more than one freedom (arrows pointing up) represent the mobility (M). Each spare freedom is summed resulting in the mechanism mobility. The same goes to the zeros which represent the number of redundant constraints.

As a result, the four-bar mechanism presents mobility equal to one (M = 1) and three redundant constraints (C_N = 3). Disregarding the redundant constraints and applying the Grübler or Kutzbach Criterion (9) a mobility equal to one is found (Equation 11).

$$M = 3 \cdot (4 - 4 - 1) + 4$$
$$M = 1$$
(11)

Applying the Modified Grübler-Kutzbach Criterion (10), and considering the redundant constraints equal to three (C_N = 3), as obtained by applying Reshetov's method, the mobility is also equal to one (Equation 12).

$$M = 6 \cdot (4 - 4 - 1) + 4 + 3$$
$$M = 1$$
(12)

Observe that using the Modified Grübler-Kutzbach Criterion and the redundant constraints obtained by using Reshetov's method, the DoF of the workspace must be considered equal to six ($\lambda = 6$), since Reshetov's method analyzes all six DoF.

Besides the DoF, and especially to overconstrained mechanisms, the motion capability depends not only on its kinematic chain and type of kinematic pairs but also on the position of its kinematic pairs and length of its links.

In the subsequent sections, the mobility analysis of the mechanisms presented in Chapter 4.1 are developed by applying the Reshetov's method and the Modified Grübler-Kutzbach Criterion.

4.2.1   From $0°$ to $30°$ of flexion

The mechanism representing the human knee from $0°$ to $30°$ of flexion is formed by 14 links and 17 joints (Figure 21). To analyze the mechanism by Reshetov's method, it is necessary to identify its loops and distribute the joints freedom in the table.

Figure 21 – Mechanism correspondent to the flexion-extension range of 0°to 30°.
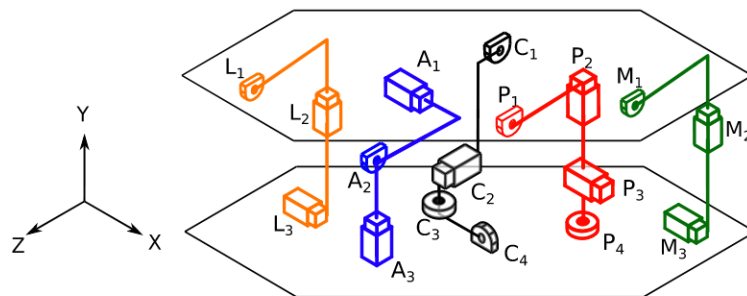
Source – own construction

The mechanism graph is obtained from its kinematic chain (Figure 22 (a)) and its respective loops are shown in Figure 22 (b). The loop ν_l is formed by the joints L_1, L_2 and L_3. The loop ν_a is formed by the joints A_1, A_2, A_3, C_1, C_2, C_3 and C_4. The loop ν_p is formed by the joints P_1, P_2, P_3 and P_4. The loop ν_m is formed by the joints M_1, M_2 and M_3. The mobility analysis by Reshetov's method is presented in Table 5.

Figure 22 – Mechanism 0°to 30°: (a) Kinematic chain and (b) graph and loops.

(a)   (b)
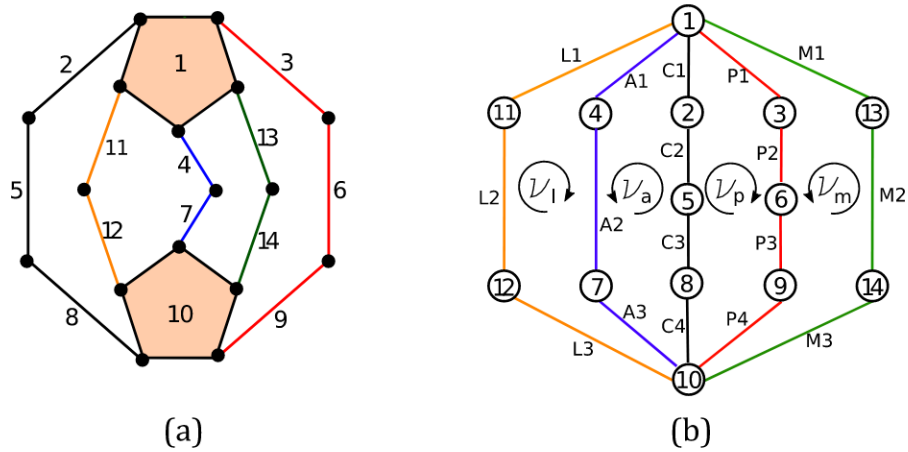
Source – own construction

Table 5 – Mechanism correspondent to the flexion-extension range of 0°to 30°: Mobility analysis by Reshetov's method.

Joints				

Loop l (L_1, L_2, L_3)				
R_x	L_1		T_x	L_3
R_y	0		T_y	L_2
R_z	0		T_z	0
	M = 0		C_N = 3	

Loop a (A_1, A_2, A_3, C_1, C_2, C_3, C_4)				
R_x	C_1, A_2		T_x	A_1
R_y	C_3		T_y	A_3
R_z	C_4		T_z	C_2
	M = 1		C_N = 0	

Loop p (P_1, P_2, P_3, P_4)				
R_x	P_1		T_x	P_3
R_y	P_4		T_y	P_2
R_z	0		T_z	0
	M = 0		C_N = 2	

Loop m (M_1, M_2, M_3)				
R_x	M_1		T_x	M_3
R_y	0		T_y	M_2
R_z	0		T_z	0
	M = 0		C_N = 3	

To validate the mobility analysis made by using the Reshetov's method (Table 5) it is possible to calculate the mechanism mobility using the Modified Grübler-Kutzbach Criterion (Eq. 10). Thus, the mobility of the respective mechanism is calculated in Equation 13 using the number of redundant constraints determined in Reshetov's method (C_N = 8).

$$M = 6 \cdot (14 - 17 - 1) + 17 + 8$$
$$M = 1$$

(13)

As the results achieved in Reshetov's method and in the Modified Grübler-Kutzbach Criterion converged, it is possible to conclude that the proposed mechanism has one DoF.

The mechanism motion depends on the length and position of its joints. If the revolute joints are misaligned, it is probable that the mechanism will not move. As the human knee ligaments are located in different spots in a 6 DoF workspace, and the mechanism will replicate the position of the ligaments insertion areas by placing the revolute joints in equivalent spots, it is foreseen that overconstraints may prevent the

motion. To overcome this problem it is proposed to eliminate some overconstraints.

Focusing in the Anterior Drawer test, to overcome motion difficulties imposed by the mechanism overconstraints, it is proposed to adjust the mechanism preserving the representation of the ACL ligament, seen in Figure 22, and preserving the DoF. To do so, three revolute joints about the x-axis are add on the mechanism, L_4, P_5 and M_4, respectively. The adapted mechanism $0°$to$30°$ is presented in Figure 23.

Figure 23 – Adapted Mechanism correspondent to the flexion-extension range of $0°$to $30°$.
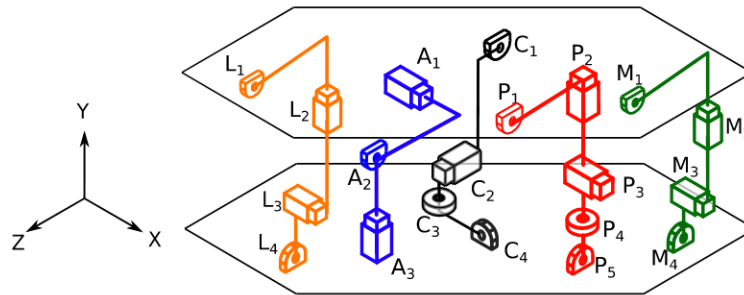
Source − own construction

The adapted mechanism kinematic chain and graph are shown in Figure 24 (a) and (b), respectively.

Figure 24 – Adapted Mechanism correspondent to the flexion-extension range of $0°$to $30°$: (a) Kinematic chain and (b) graph and loops.
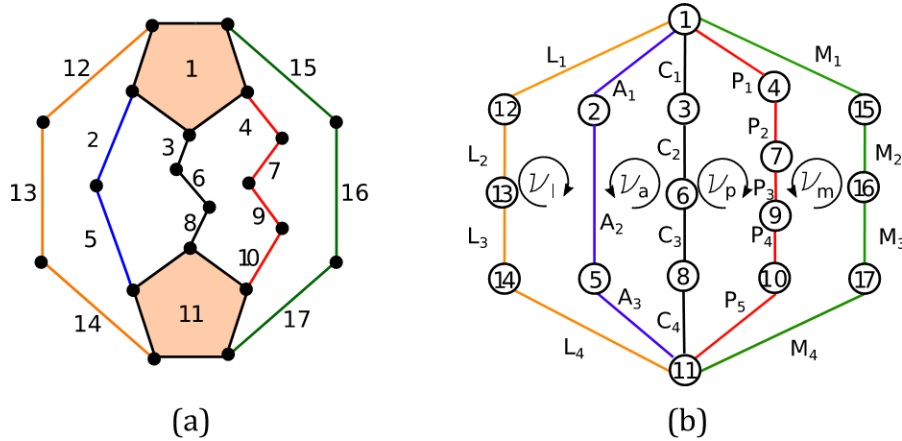
Source − own construction

The mobility analysis by Reshetov's method is presented in Table 6.

Table 6 – Adapted Mechanism correspondent to the flexion-extension range of 0° to 30°: Mobility analysis by Reshetov's method.

Joints

Loop l (L_1, L_2, L_3, L_4)

R_X	L_1, L_4	T_X	L_3
R_Y	0	T_Y	L_2
R_Z	0	T_Z	0 (L_4)

M = 0 C_N = 2

Loop a (A_1, A_2, A_3, A_4, C_1, C_2, C_3, C_4)

R_X	C_1, A_2	T_X	A_1
R_Y	C_3	T_Y	A_3
R_Z	C_4	T_Z	C_2

M = 1 C_N = 0

Loop p (P_1, P_2, P_3, P_4, P_5)

R_X	P_1, P_5	T_X	P_3
R_Y	P_4	T_Y	P_2
R_Z	0	T_Z	0 (P_5)

M = 0 C_N = 1

Loop m (M_1, M_2, M_3, M_4)

R_X	M_1, M_4	T_X	M_3
R_Y	0	T_Y	M_2
R_Z	0	T_Z	0 (M_4)

M = 0 C_N = 2

Applying the Modified Grübler-Kutzbach Criterion to validate the result obtained in Table 6, the mobility is calculated (Eq. 14) using the number of redundant constraints determined on Reshetov's method ($C_N = 5$).

$$M = 6 \cdot (17 - 20 - 1) + 20 + 5$$
$$M = 1$$

(14)

This analysis validate the mechanical representation of the mechanism. As obtained in Reshetov's method, the expected DoF is a rotation about the x-axis, as in a passive human knee.

4.2.2 From $30°$ to $40°$ of flexion

The mechanism representing the human knee from $30°$ to $40°$ of flexion is formed by 13 links and 16 joints (Figure 25).

Figure 25 – Mechanism correspondent to the flexion-extension range of 30°to 40°.
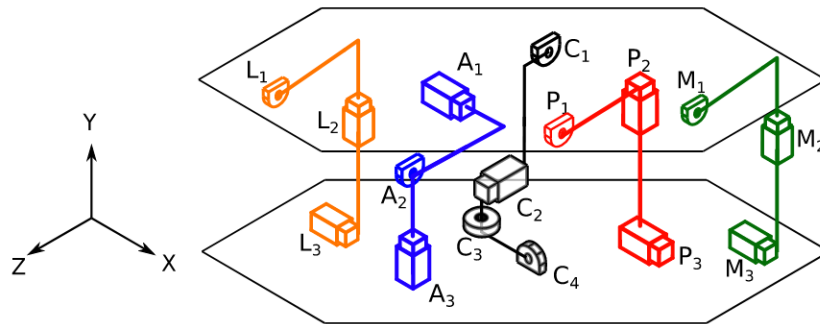
Source – own construction

The mechanism graph is obtained from its kinematic chain (Figure 26 (a)) and its respective loops are presented in Figure 26 (b). The loop ν_l is formed by the joints L_1, L_2 and L_3. The loop ν_a is formed by the joints A_1, A_2, A_3, C_1, C_2, C_3 and C_4. The loop ν_p is formed by the joints P_1, P_2 and P_3. The loop ν_m is formed by the joints M_1, M_2 and M_3.

Figure 26 – Mechanism correspondent to the flexion-extension range of 30°to 40°: (a) Kinematic chain and (b) graph and loops.
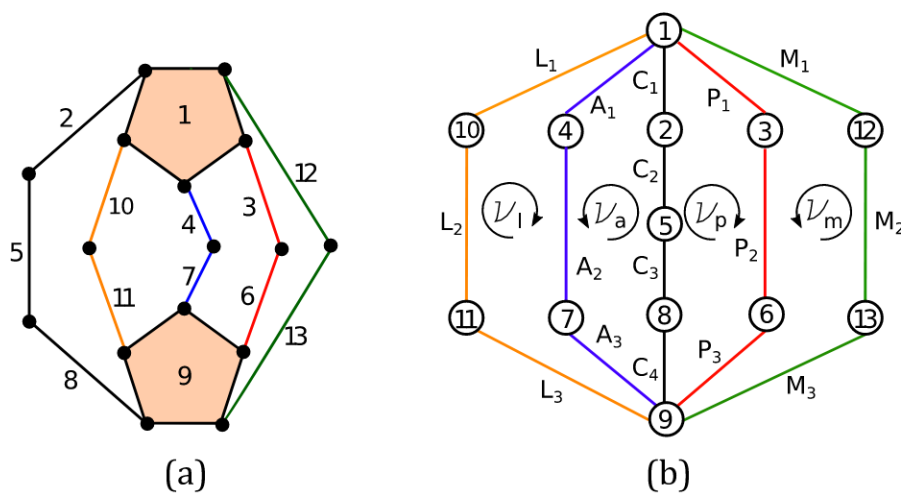
Source – own construction

The mobility analysis by Reshetov's method (Table 7) shows that the mechanism has one DoF and nine redundant constraints.

Table 7 – Mechanism correspondent to the flexion-extension range of 30°to 40°: Mobility analysis by Reshetov's method.
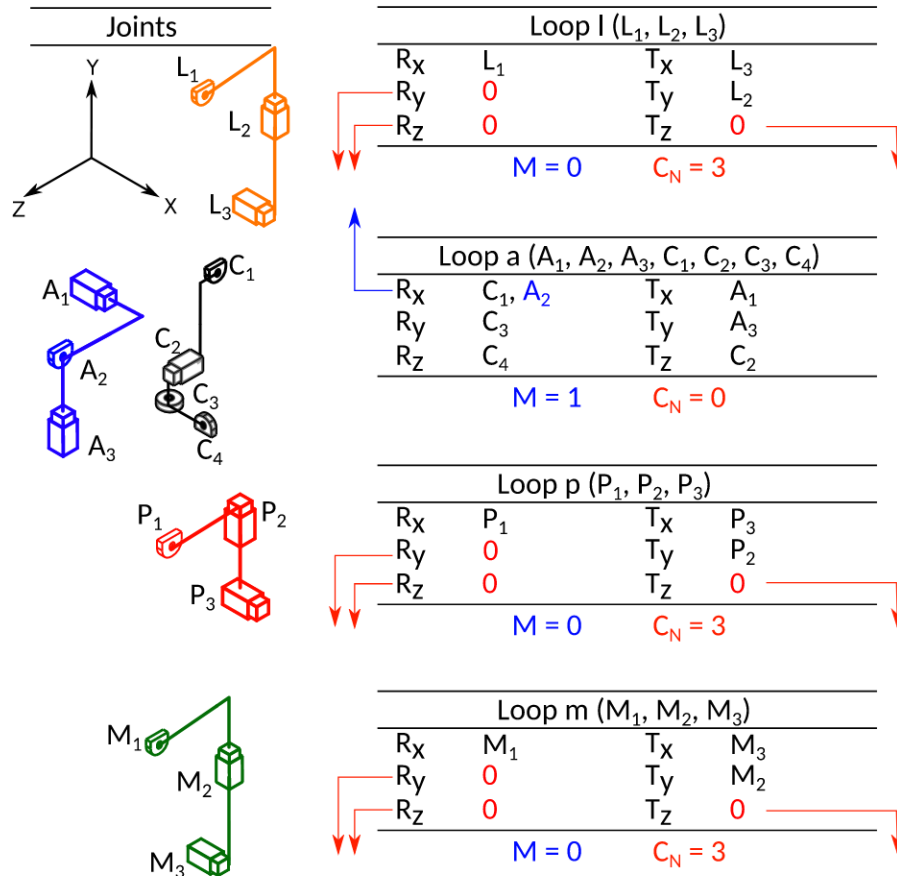
Applying the Modified Grübler-Kutzbach Criterion (Equation 10) with the number of redundant constraints determined in Reshetov's method ($C_N = 9$), the mechanism mobility is equal to one (Eq. 15).

$$M = 6 \cdot (13 - 16 - 1) + 16 + 9$$
$$M = 1$$

(15)

As exposed in Section 4.2.1, the redundant constraints together with the ligaments insertion points variation may result in a static structure. Thus, to decrease the number of redundant constraints it is proposed to add three revolute joints about the x-axis, L_4, P_4 and M_4, respectively, as shown in Figure 27, maintaining the DoF as presented in Table 9.

Figure 27 – Adapted Mechanism correspondent to the flexion-extension range of 30°to 40°
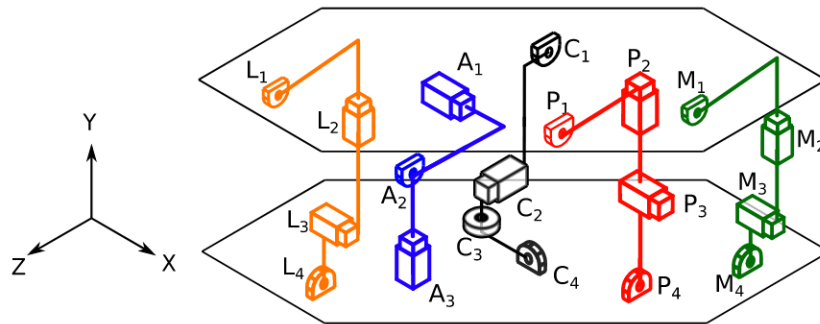
Source – own construction

The kinematic chain and graph with the identification of its loops is presented in Figure 8

Table 8 – Adapted Mechanism correspondent to the flexion-extension range of 30°to 40°: (a) Kinematic chain and (b) graph and loops.

(a)   (b)

The mobility is calculated by applying the Modified Grübler-Kutzbach Criterion (equation 16).

$$M = 6 \cdot (16 - 19 - 1) + 19 + 6$$
$$M = 1$$

(16)

Table 9 – Adapted Mechanism correspondent to the flexion-extension range of 30°to 40°: Mobility analysis by Reshetov's method.
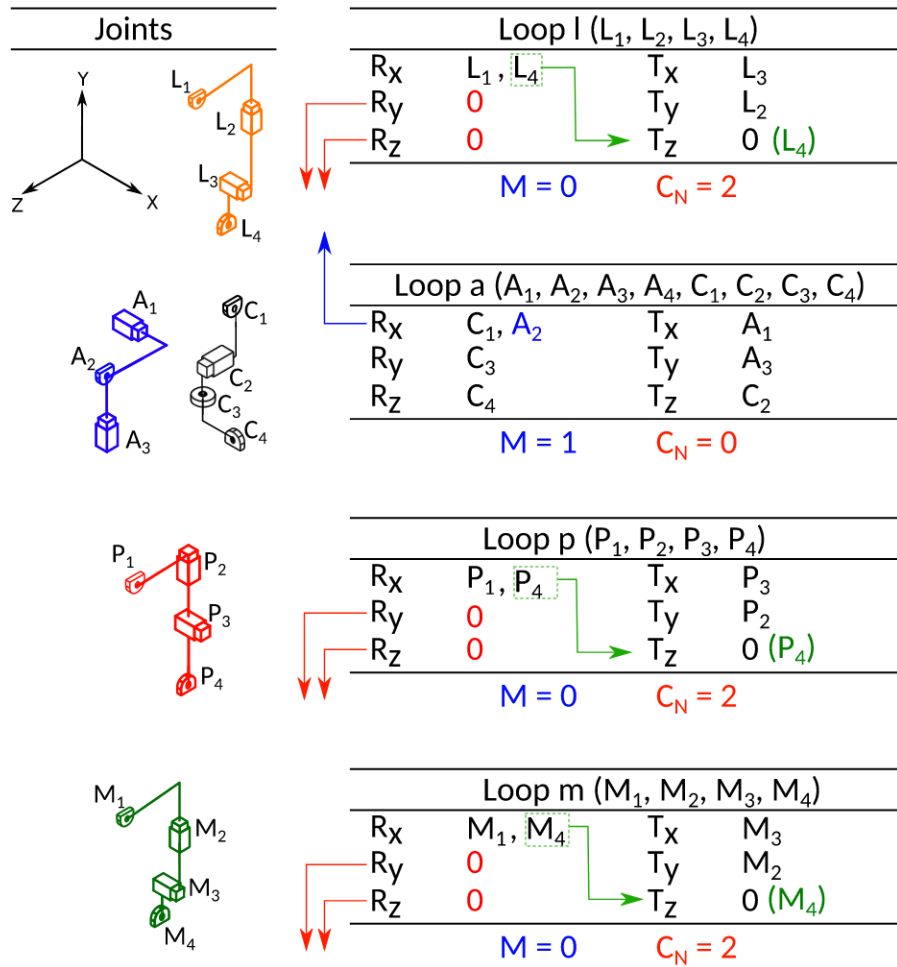
As the results achieved in Reshetov's method and the Modified Grübler-Kutzbach Criterion converged it is possible to conclude that the proposed mechanism has one DoF.

4.2.3   From 40° to 60° of flexion

The mechanism representing the human knee from 40° to 60° of flexion is formed by 15 links and 18 joints (Figure 28).

Figure 28 – Mechanism correspondent to the flexion-extension range of 40°to 60°.
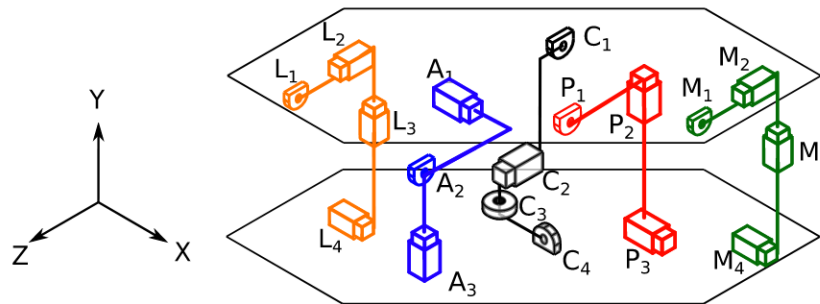
Source – own construction

The mechanism graph is obtained from its kinematic chain (Figure 29 (a)) and its respective loops are presented in Figure 29 (b). The loop ν_l is formed by the joints L_1, L_2, L_3 and L_4. The loop ν_a is formed by the joints A_1, A_2, A_3, C_1, C_2, C_3 and C_4. The loop ν_p is formed by the joints P_1, P_2 and P_3. The loop ν_m is formed by the joints M_1, M_2, M_3 and M_4.

Figure 29 – Mechanism correspondent to the flexion-extension range of 40°to 60°: (a) Kinematic chain and (b) graph and loops.

Source – own construction

The mobility analysis by Reshetov's method (Table 10) shows that the mechanism has one DoF and seven redundant constraints ($C_N = 7$).

Table 10 – Mechanism correspondent to the flexion-extension range of 40°to 60°: Mobility analysis by Reshetov's method.

Joints		Loop l (L_1, L_2, L_3, L_4)			
		R_X	L_1	T_X	L_4
		R_y	0	T_y	L_3
		R_z	0	T_z	L_2
			M = 0	C_N = 2	

		Loop a (A_1, A_2, A_3, C_1, C_2, C_3, C_4)			
		R_X	C_1, A_2	T_X	A_1
		R_y	C_3	T_y	A_3
		R_z	C_4	T_z	C_2
			M = 1	C_N = 0	

		Loop p (P_1, P_2, P_3)			
		R_X	P_1	T_X	P_3
		R_y	0	T_y	P_2
		R_z	0	T_z	0
			M = 0	C_N = 3	

		Loop m (M_1, M_2, M_3, M_4)			
		R_X	M_1	T_X	M_4
		R_y	0	T_y	M_3
		R_z	0	T_z	M_2
			M = 0	C_N = 2	

By using the Modified Grübler-Kutzbach Criterion (Equation 10) and the number of redundant constraints determined in Reshetov's method ($C_N = 7$), the mechanism mobility is equal to one (Equation 17).

$$M = 6 \cdot (15 - 18 - 1) + 18 + 7$$
$$M = 1$$

(17)

Following the same line of reasoning of the anterior mechanisms presented in Sections 4.2.1 and 4.2.2, to decrease the number of redundant constraints it is proposed to add a revolute joint about the x-axis, P_4, as in Figure 30, maintaining the DoF as shown in Table 12.

Figure 30 – Adapted Mechanism correspondent to the flexion-extension range of 40°to 60°.
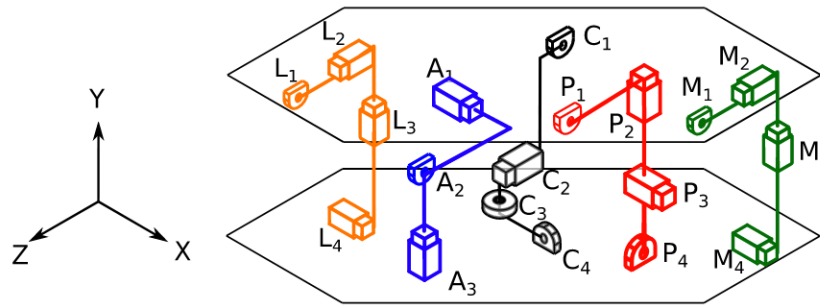
Source – own construction

The kinematic chain of the adapted mechanism and the graph with loops is presented inf Figure 11.

Table 11 – Adapted Mechanism correspondent to the flexion-extension range of 40°to 60°: (a) Kinematic chain and (b) graph and loops.

(a)   (b)

Table 12 – Adapted Mechanism correspondent to the flexion-extension range of 40°to 60°: Mobility analysis by Reshetov's method.

Joints		Loop l (L_1, L_2, L_3, L_4)			
	R_X	L_1	T_X	L_4	
	R_y	0	T_y	L_3	
	R_z	0	T_z	L_2	
		M = 0	C_N = 2		

Loop a (A_1, A_2, A_3, C_1, C_2, C_3, C_4)				
R_X	C_1, A_2	T_X	A_1	
R_y	C_3	T_y	A_3	
R_z	C_4	T_z	C_2	
	M = 1	C_N = 0		

Loop p (P_1, P_2, P_3, P_4)				
R_X	P_1, P_4	T_X	P_3	
R_y	0	T_y	P_2	
R_z	0	T_z	0 (P_4)	
	M = 0	C_N = 2		

Loop m (M_1, M_2, M_3, M_4)				
R_X	M_1	T_X	M_4	
R_y	0	T_y	M_3	
R_z	0	T_z	M_2	
	M = 0	C_N = 2		

The mobility is calculated by applying the Modified Grübler-Kutzbach Criterion 16.

$$M = 6 \cdot (16 - 19 - 1) + 19 + 6$$
$$M = 1 \tag{18}$$

This result is consistent with the DoF in a passive human knee and it validates the proposed mechanism for posterior analysis in this range of motion.

4.2.4 From 60° to 90° of flexion

The mechanism representing the human knee from 60° to 90° of flexion is formed by 16 links and 19 joints (Figure 31).
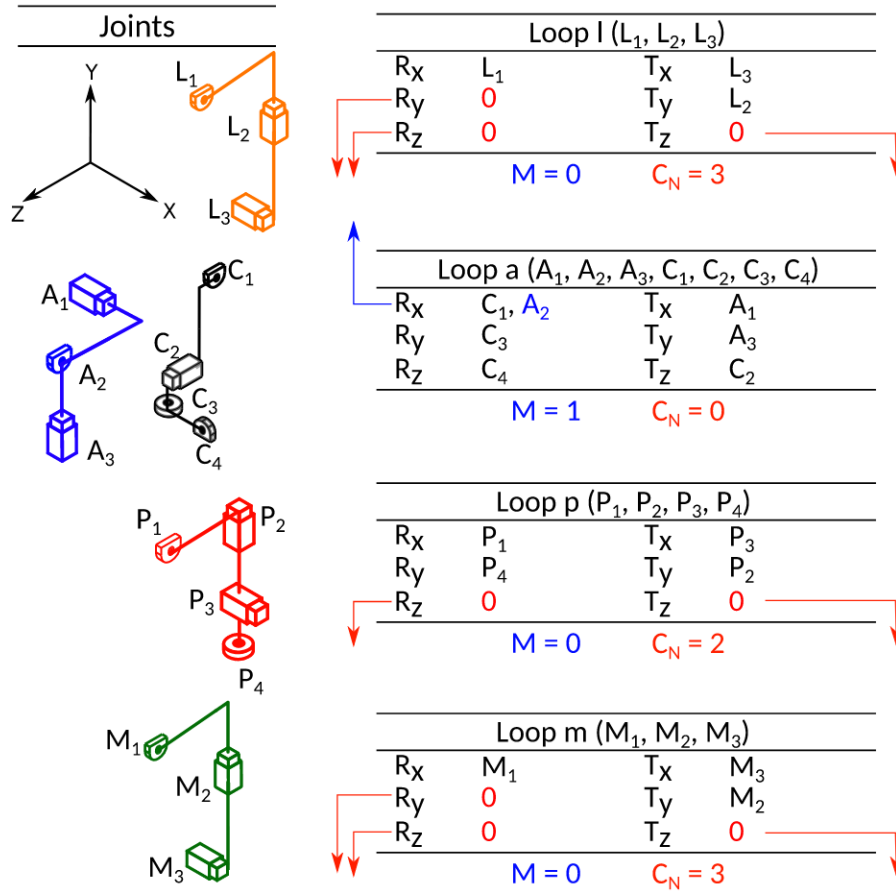
The mechanism graph is obtain from its kinematic chain (Figure 32 (a)) and its respective loops are presented in Figure 32 (b). The loop ν_l is formed by the joints L_1, L_2, L_3 and L_4. The loop ν_a is formed by the joints A_1, A_2, A_3, A_4, C_1, C_2, C_3 and C_4.

Figure 31 – Mechanism correspondent to the flexion-extension range of 60°to 90°.
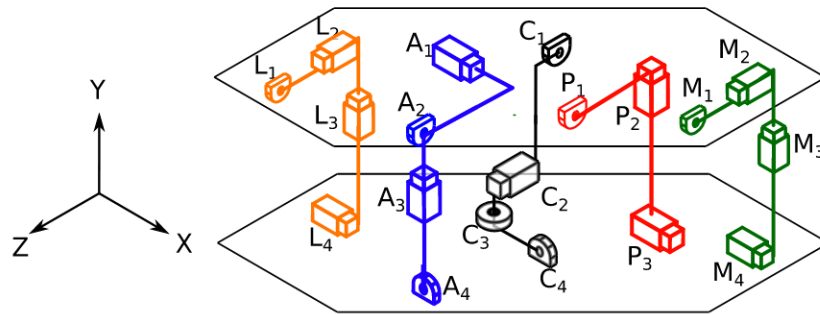
Source – own construction

The loop ν_p is formed by the joints P_1, P_2 and P_3. The loop ν_m is formed by the joints M_1, M_2, M_3 and M_4.

Figure 32 – Mechanism correspondent to the flexion-extension range of 60°to 90°: (a) Kinematic chain and (b) graph and loops.
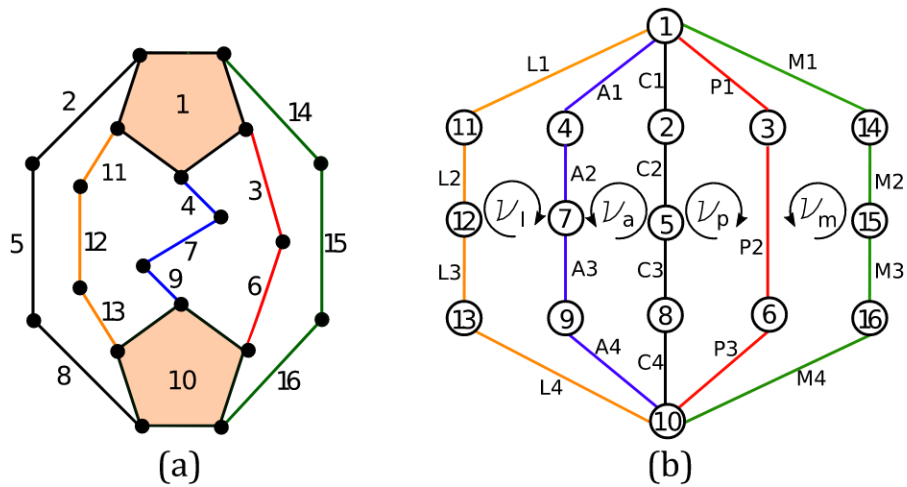
Source – own construction

The mobility analysis by Reshetov's method (Table 13) shows that the mechanism has 1 DoF and 6 redundant constraints.

Table 13 – Mechanism correspondent to the flexion-extension range of 60°to 90°: Mobility analysis by Reshetov's method.

Joints

Loop I (L_1, L_2, L_3, L_4)

R_X	L_1	T_X	L_4
R_y	0	T_y	L_3
R_z	0	T_z	L_2

M = 0 C_N = 2

Loop a (A_1, A_2, A_3, C_1, C_2, C_3, C_4)

R_X	C_1, A_2	T_X	A_1
R_y	C_3	T_y	A_3
R_z	C_4, A_4	T_z	C_2

M = 1 C_N = 0

Loop p (P_1, P_2, P_3)

R_X	P_1	T_X	P_3
R_y	0	T_y	P_1
R_z	0	T_z	0 (A_2)

M = 0 C_N = 2

Loop m (M_1, M_2, M_3, M_4)

R_X	M_1	T_X	M_4
R_y	0	T_y	M_3
R_z	0	T_z	M_2

M = 0 C_N = 2
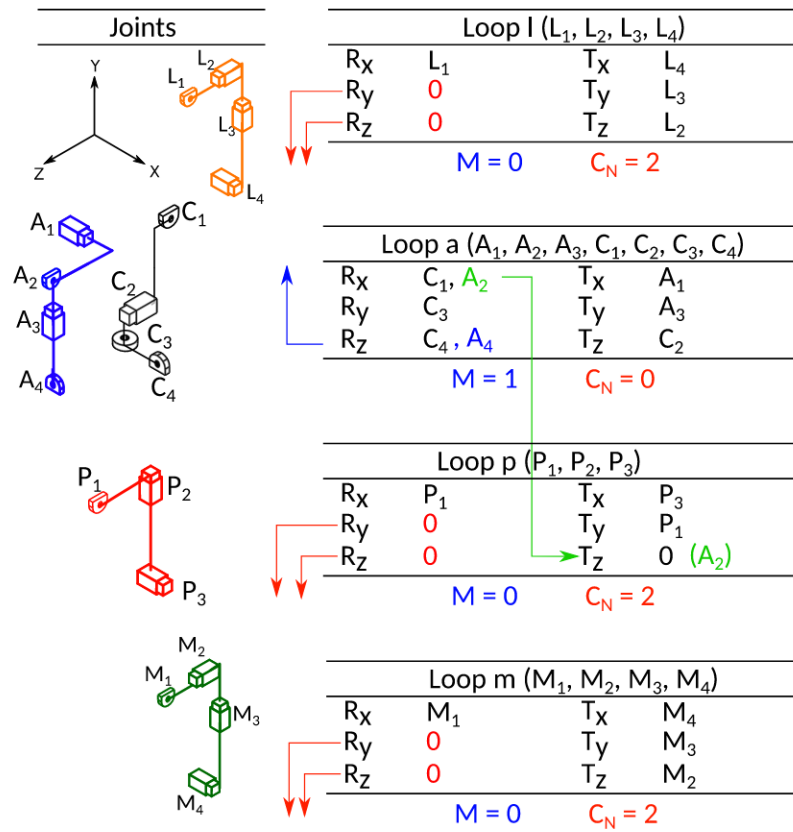
The mobility of the respective mechanism is also calculated in the Equation 19 by using the Modified Grübler-Kutzbach Criterion (Equation 10) and the number of redundant constraints determined in Reshetov's method ($C_N = 6$).

$$M = 6 \cdot (16 - 19 - 1) + 19 + 6$$
$$M = 1 \tag{19}$$

This result can be put into question, since the Reshetov's Method does not allow mobility permutes between rotations about the same axis after defining the loops and can present different results depending on the distribution of joints in the loops. This would be the case if the C_4 join was in the loop l instead of in the loop a, for example. However, this thesis will not enter this merit, proposing only an adjustment of kinematic pairs, removing C_4 and adding the P_4 joint as shown in Figure 33. The mobility is analyzed in Table 14.

Figure 33 – Adapted Mechanism correspondent to the flexion-extension range of 60°to 90°.
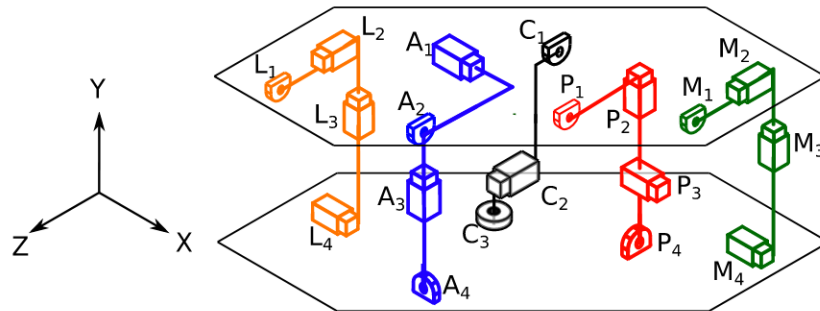
Source – own construction

Analyzing its joints, the adapted mechanism has the same number of constraints. As the representation of the PCL has now two revolute joints, it does not imposes a dimensional constraint in the construction of the mechanism. The new mechanism graph is obtained from its new kinematic chain (Figure 34 (a)) and its respective loops are represented in Figure 34 (b).

The mobility analysis by Reshetov's method (Table 14) indicates that the proposed mechanism has only one DoF.
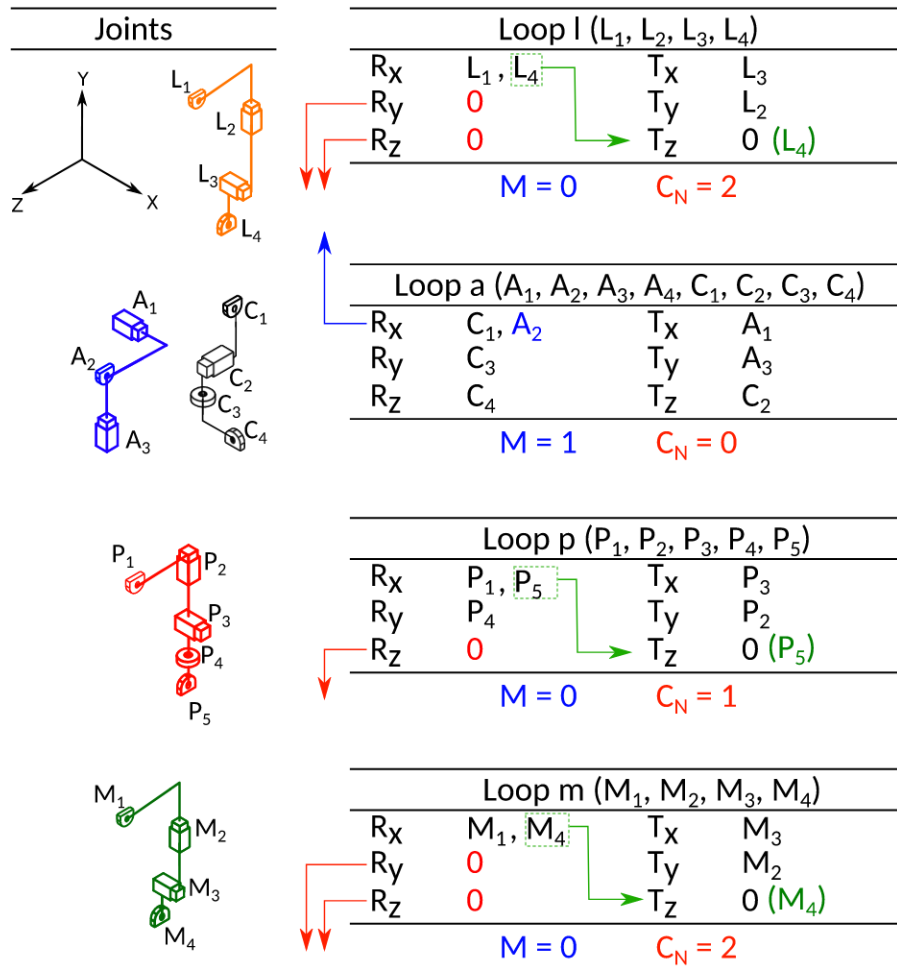
Figure 34 – Adapted Mechanism correspondent to the flexion-extension range of 60°to 90°: (a) kinematic chain and (b) graph and loops.
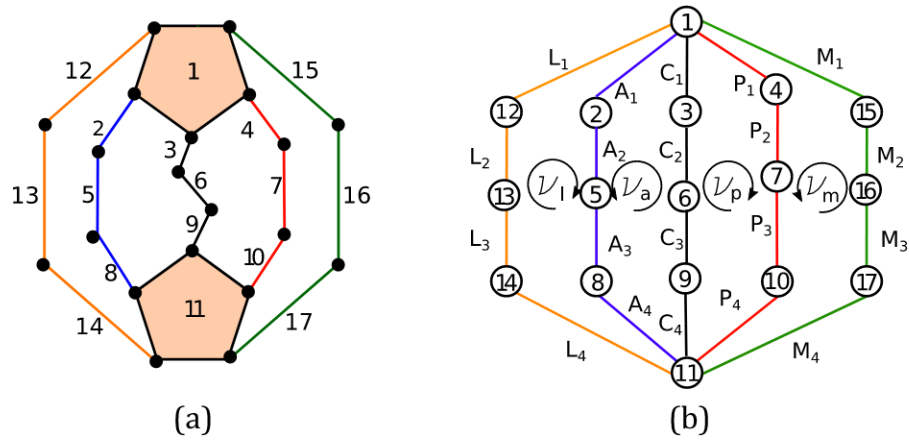
Source – own construction

Table 14 – Adapted Mechanism correspondent to the flexion-extension range of 60°to 90°: Mobility analysis by Reshetov's method.

Joints	Loop l (L_1, L_2, L_3, L_4)			
	R_x	L_1	T_x	L_4
	R_y	0	T_y	L_3
	R_z	0	T_z	L_2
	M = 0		C_N = 2	

	Loop a (A_1, A_2, A_3, C_1, C_2, C_3)			
	R_x	C_1, A_2	T_x	A_1
	R_y	C_3	T_y	A_3
	R_z	A_4	T_z	C_2
	M = 1		C_N = 0	

	Loop p (P_1, P_2, P_3, P_4)			
	R_x	P_1 , P_4	T_x	P_3
	R_y	0	T_y	P_1
	R_z	0	T_z	0 (P_4)
	M = 0		C_N = 2	

	Loop m (M_1, M_2, M_3, M_4)			
	R_x	M_1	T_x	M_4
	R_y	0	T_y	M_3
	R_z	0	T_z	M_2
	M = 0		C_N = 2	

Applying the Modified Grübler-Kutzbach Criterion (Equation 10) and using the number of redundant constraints determined in Reshetov's method ($C_N = 5$), the new mechanism mobility is calculated (Equation 20).

$$M = 6 \cdot (16 - 19 - 1) + 19 + 6$$
$$M = 1$$

(20)

The achieved results converged confirming that the proposed mechanism has one DoF.

4.2.5   From 90° to 120° of flexion

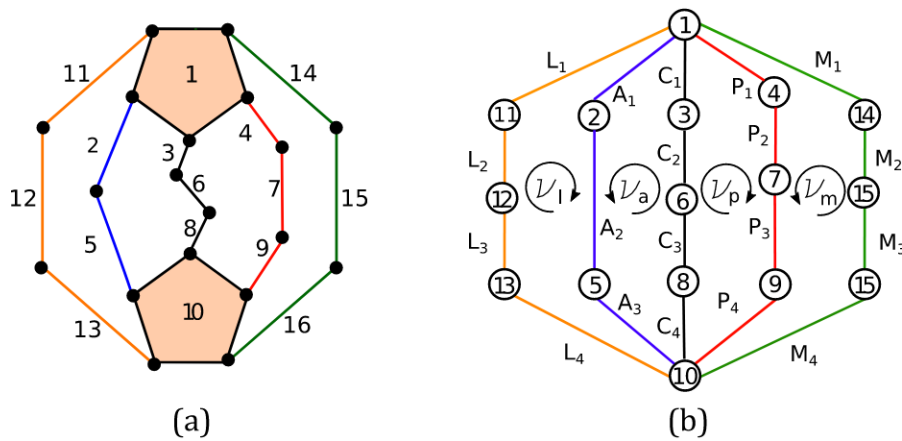The mechanism representing the human knee from 90° to 120° of flexion is formed by 17 links and 20 joints (Figure 35).

Figure 35 – Mechanism correspondent to the flexion-extension range of 90°to 120°.
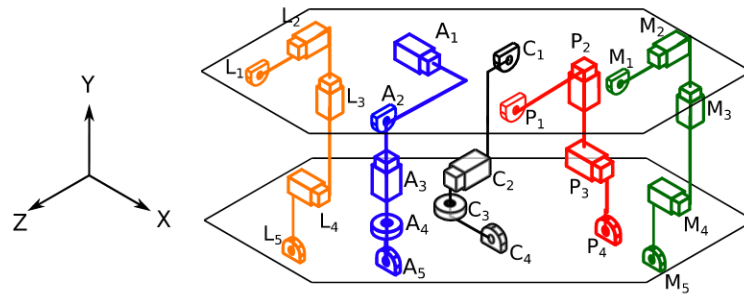
Source – own construction

The mechanism graph is obtain from its kinematic chain (Figure 36 (a)) and its respective loops are shown in Figure 36 (b). The loop ν_l is formed by the joints L_1, L_2, L_3, L_4 and L_5. The loop ν_a is formed by the joints A_1, A_2, A_3, A_4, A_5, C_1, C_2, C_3 and C_4. The loop ν_p is formed by the joints P_1, P_2, P_3 and P_4. The loop ν_m is formed by the joints M_1, M_2, M_3, M_4 and M_5.

Figure 36 – Mechanism correspondent to the flexion-extension range of 90°to 120°: (a) Kinematic chain and (b) graph and loops.
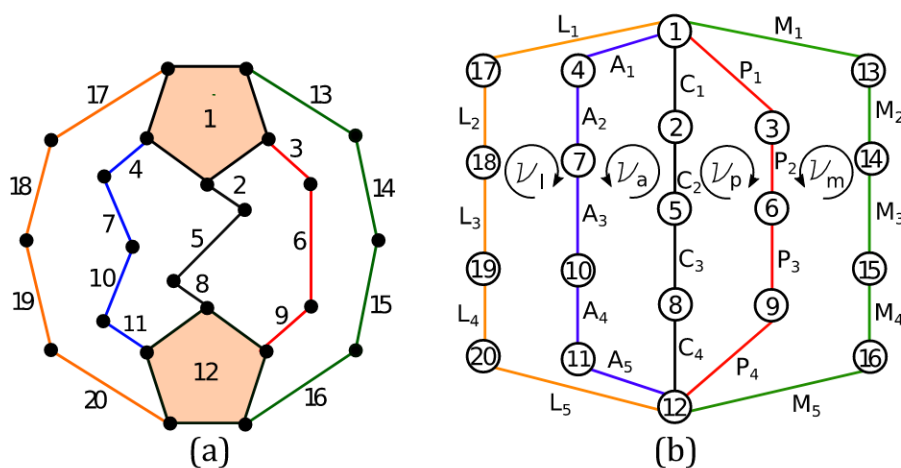
Source – own construction

The mobility analysis by Reshetov's method (Table 15) shows that the mechanism has three DoF and four redundant constraints.

Table 15 – Mechanism correspondent to the flexion-extension range of 90°to 120°: Mobility analysis by Reshetov's method.
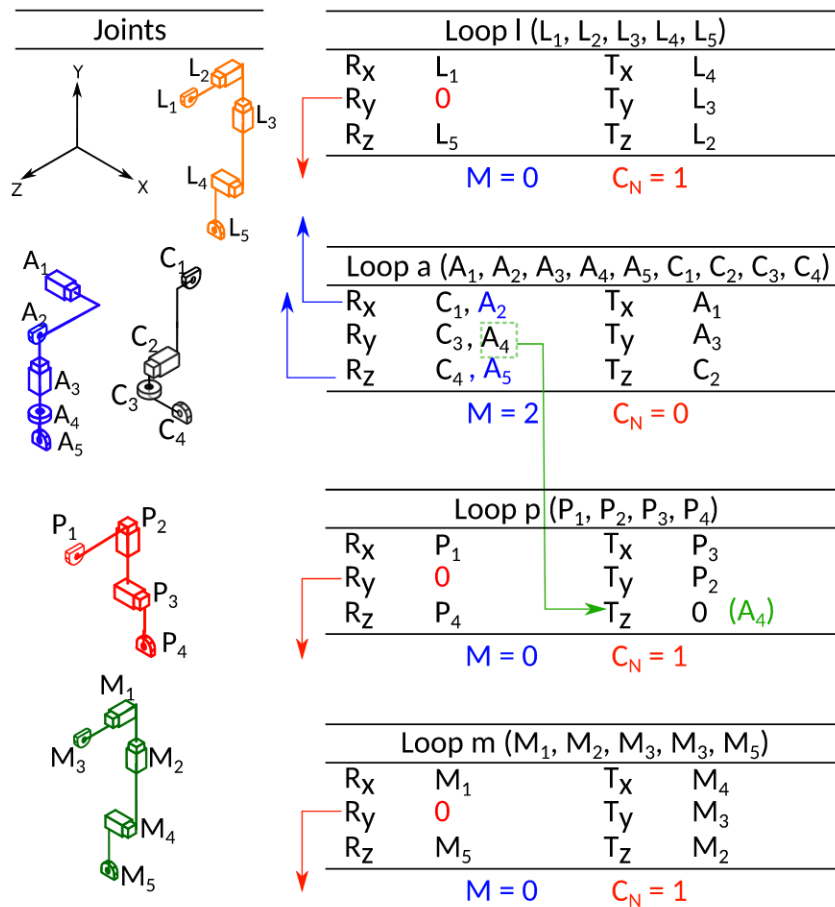
The mobility of the respective mechanism is calculated (Equation 21) by applying the Modified Grübler-Kutzbach Criterion (Equation 10) and considering the number of redundant constraints determined in Reshetov's method ($C_N = 3$).

$$M = 6 \cdot (20 - 23 - 1) + 23 + 3$$
$$M = 2$$

(21)

This result is similar to the one obtained in the mechanism from 60° to 90° of flexion, since it is possible to obtained a result of mobility equal to one, depending on the distribution of the joints.

The extra mobility may also be the result of an anatomical condition, suggesting that the contact point or the interference from other structures considered in Section 4.1 has changed and now presents different constraints.

Adapting the mechanism to represent the extra constraints, the joints C_1 and C_2 shown in Figure 35 were removed. The new mechanism is formed by 18 links and 21 joints (Figure 37).

Figure 37 – Adapted Mechanism correspondent to the flexion-extension range of 90°to 120°.
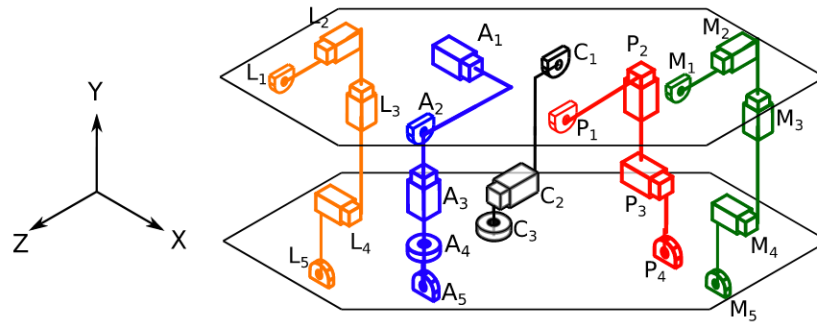
Source − own construction

The new mechanism graph is obtain from its new kinematic chain and its respective loops are presented in Figure 38.

Figure 38 – Adapted Mechanism correspondent to the flexion-extension range of 90°to 120°: (a) kinematic chain and (b) graph and loops.
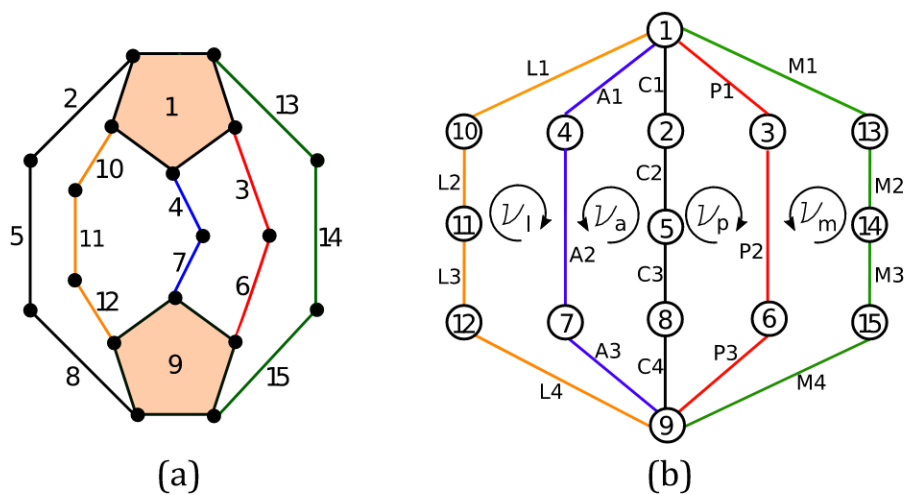

(a)   (b)
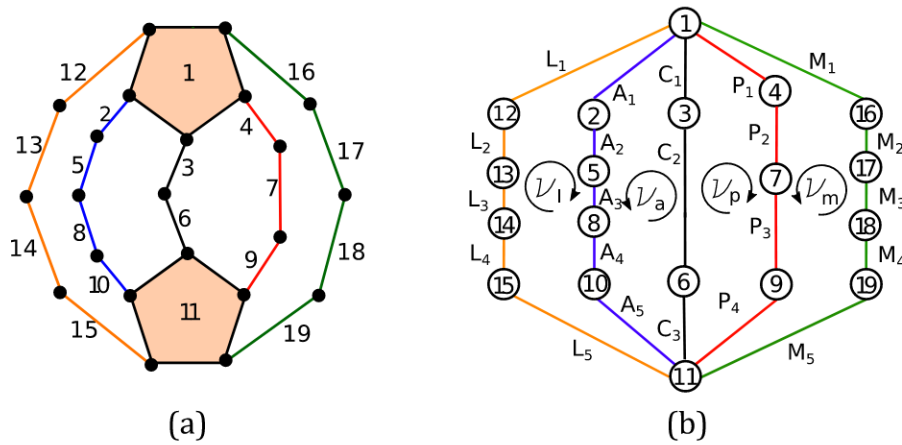
Source − own construction

The mobility analysis by Reshetov's method (Table 16) shows that the proposed mechanism has now one DoF.

Table 16 – Adapted Mechanism correspondent to the flexion-extension range of 90°to 120°: Mobility analysis by Reshetov's method.
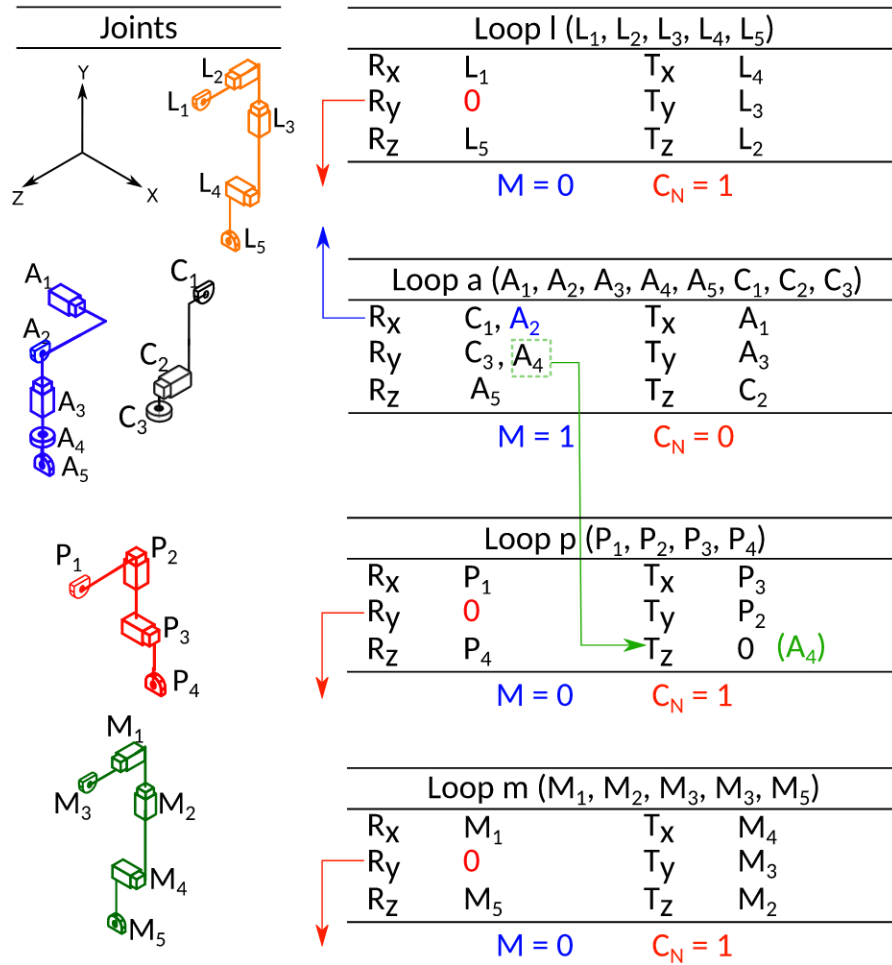
Applying the Modified Grübler-Kutzbach Criterion (Equation 10) and cosidering the redundant constraints obtained by applying Reshetov's method, the mechanism mobility is calculated (Equation 22).

$$M = 6 \cdot (19 - 22 - 1) + 22 + 3$$
$$M = 1$$

(22)

The achieved results converged, confirming that the proposed mechanism has one DoF, preserving the ligaments constraints as shown in anatomical analysis (Table 2).

4.2.6 From 120° to 140° of flexion

The mechanism representing the human knee from 120° to 140° of flexion is formed by 13 links and 14 joints (Figure 39).

The kinematic chain of the mechanism is used to obtain its graph representation (Figure 40 (a)) and its respective loops are shown in Figure 40 (b). The loop ν_a is formed

Figure 39 – Mechanism correspondent to the flexion-extension range of 120°to 140°.
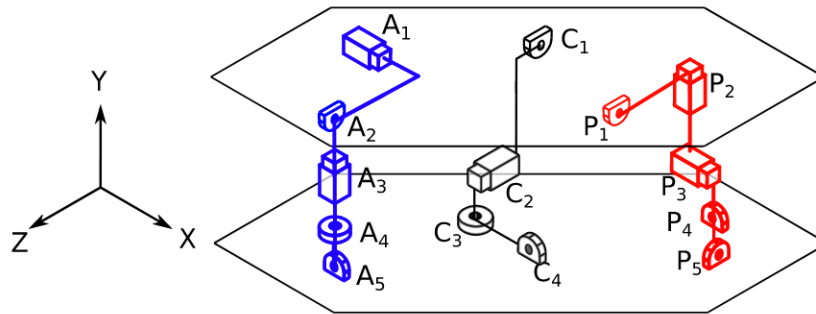
Source – own construction

by the joints A_1, A_2, A_3, A_4, A_5, C_1, C_2, C_3 and C_4, and the loop ν_p is formed by the joints P_1, P_2, P_3, P_4 and P_5.
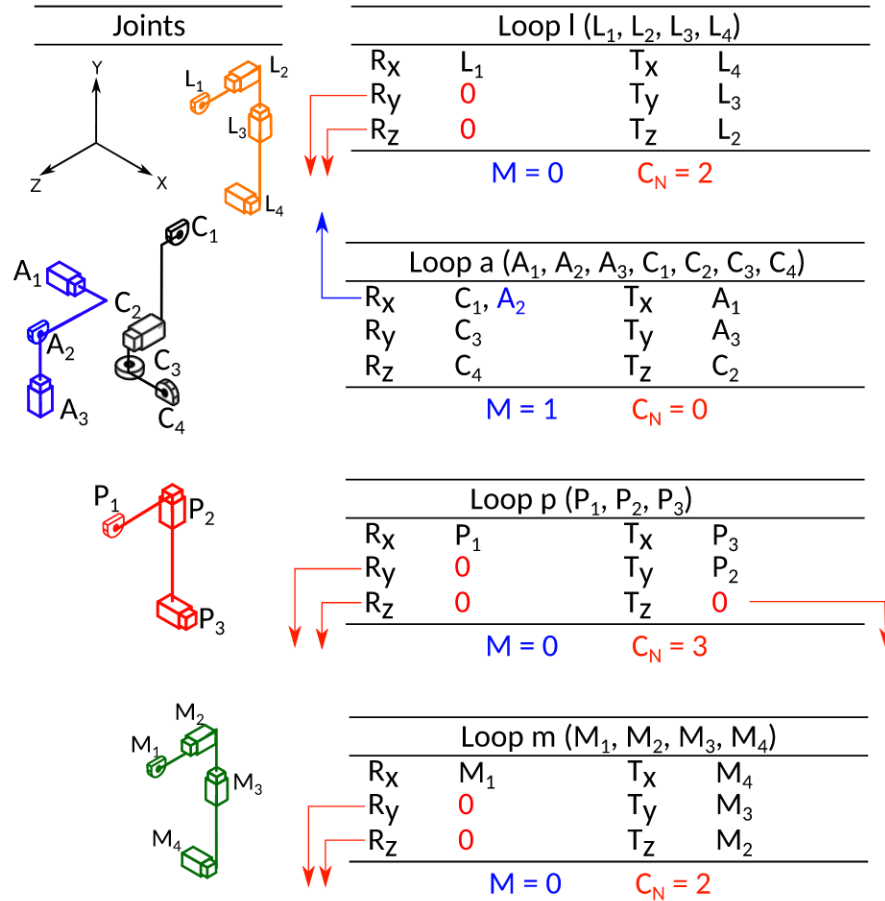
Figure 40 – Mechanism correspondent to the flexion-extension range of 120°to 140°: (a) Kinematic chain and (b) graph and loops.
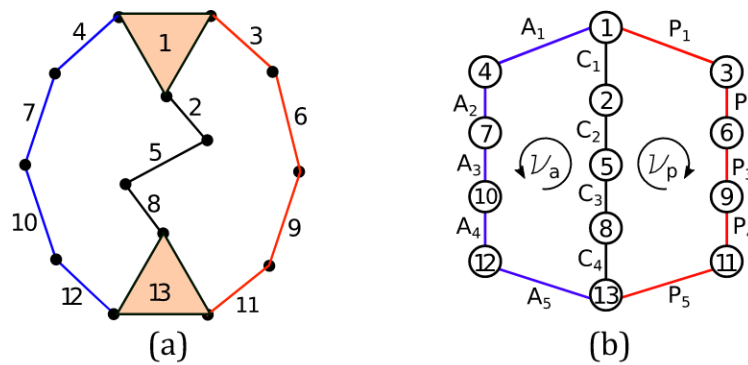
Source – own construction
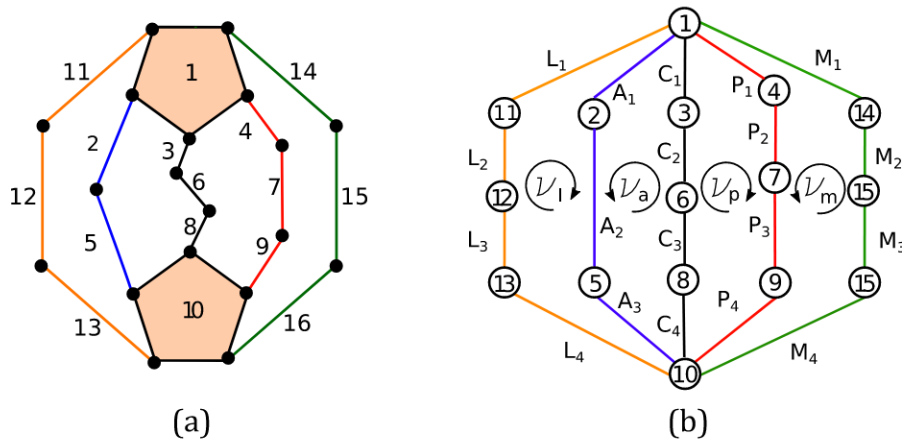
Applying the Reshetov's method (Table 17) it is possible to observe that the mechanism has three DoF and only one redundant constraint.

Table 17 – Mechanism correspondent to the flexion-extension range of 120°to 140°: Mobility analysis by Reshetov's method.
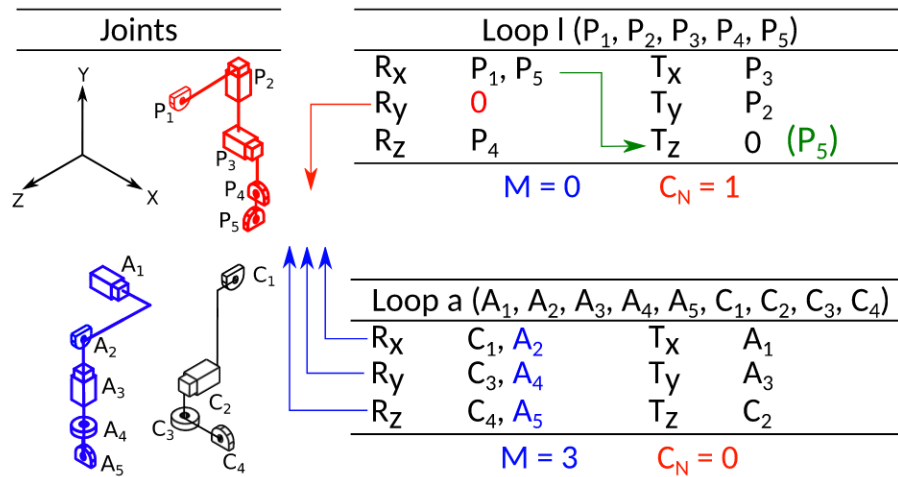
Using the Modified Grübler-Kutzbach Criterion (Equation 10) the mobility of the respective mechanism is calculated (Equation 23).

$$M = 6 \cdot (13 - 14 - 1) + 14 + 1$$
$$M = 3$$

(23)

The achieved results indicates that the proposed mechanism has three DoF. As previously discussed, the human knee can be considered as presenting its mobility equal to one through all flexion-extension motion, this result suggest that the contact point or the interference from other soft structures considered in Section 4.1 has changed and now presents different constraints.

In order to adapt the mechanism representing the change in its constraints the joint C_4 and A_4 were removed. The resultant mechanism is formed by 11 links and 12 joints (Figure 41).

The mechanism graph is obtain from its new kinematic chain (Figure 42 (a)) and its respective loops are presented in Figure 42 (b).

Figure 41 – Adapted Mechanism correspondent to the flexion-extension range of 120°to 140°.
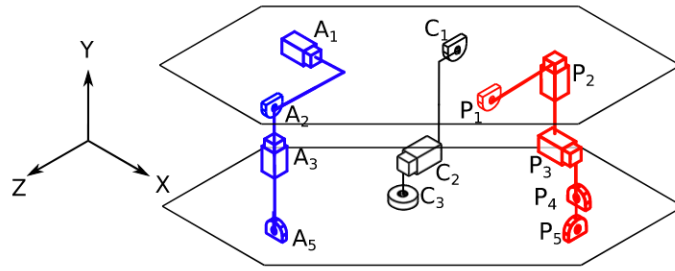
Source – own construction

Figure 42 – Adapted Mechanism correspondent to the flexion-extension range of 120°to 140°: (a) kinematic chain and (b) graph and loops
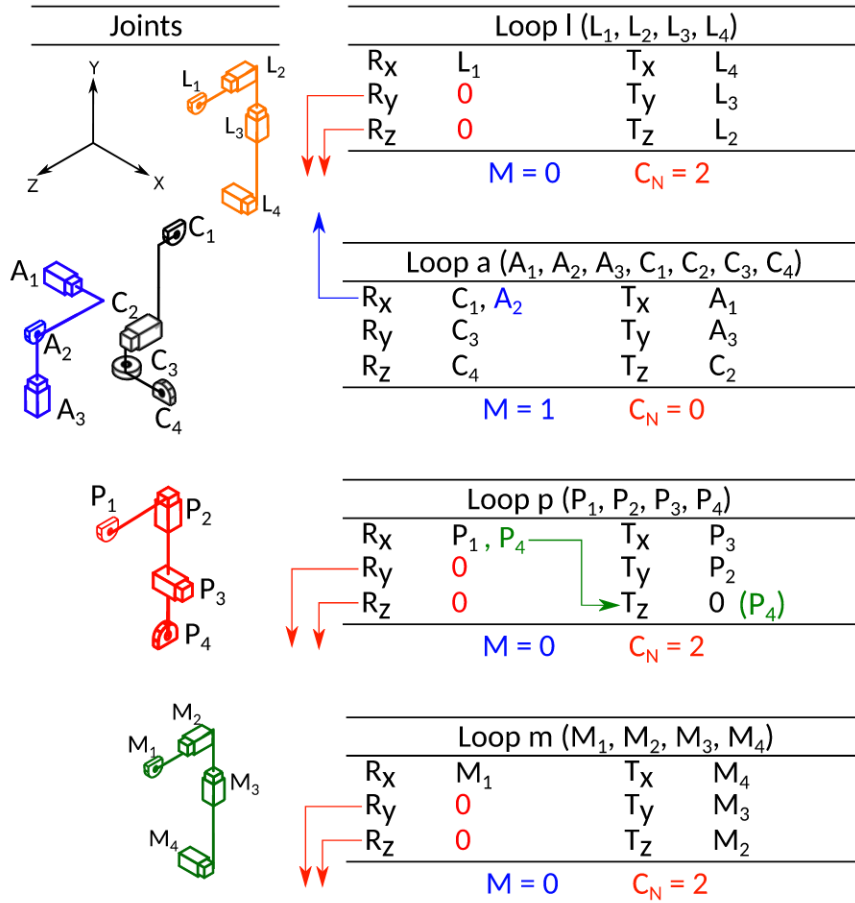

(a)   (b)
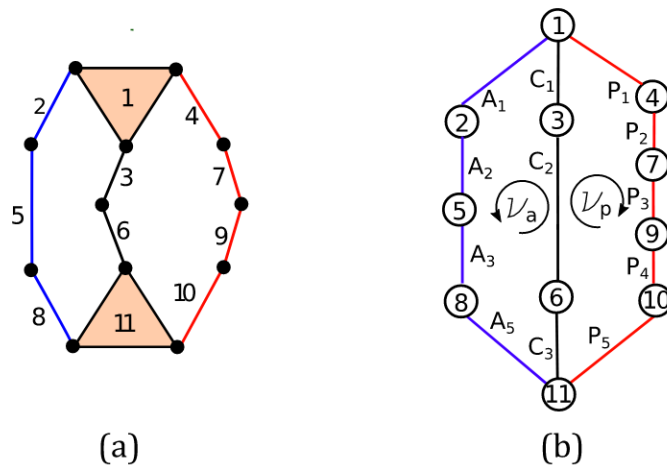
Source – own construction

The Reshetov's method applied in the mechanism (Table 18) shows that it has one DoF and no redundant constraints.

Table 18 – Adapted Mechanism correspondent to the flexion-extension range of 120°to 140°: Mobility analysis by Reshetov's method.

The mobility of the new mechanism is now calculated (Equation 24).

$$M = 6 \cdot (11 - 12 - 1) + 12 + 1$$
$$M = 1$$

$$(24)$$

The achieved results converged, confirming that the proposed mechanism has one DoF.

4.3 FINAL CONSIDERATIONS

The human knee suffers alteration on the condition of its joints during flexion-extension movement. Main ligaments can vary from lax to taut or even bend, changing the axis of its imposed constraint. This chapter analyzes the knee main structures for each tibia movement, discretizing the imposed constraints by DoF and range of flexion. Then it is proposed equivalent mechanisms, to represent the behavior of the main ligaments to each range of flexion of the knee.

Regarding the mobility analysis, some considerations were made to preserve the DoF of each mechanism equal to one. These considerations reflect mostly on changes of kinematic pairs that represent the contact joint between femur and tibia or in the addition of revolute joints in the ligaments representation. This change can also be seen in the human knee, regarding each degree of flexion where the contact joint begins with full rotation at the firsts degrees of flexion-extension and ends up with pure translation at the latest degrees, or in ligaments that became more lax allowing more flexibility but still supporting the movements.

5 POSITION AND STATIC ANALYSIS

The trajectory of the human knee can vary from person to person. Some studies involving experiments with different knees of healthy subjects resulted in approximations of the knee trajectory during flexion (OTTOBONI *et al.*, 2010; PARENTI-CASTELLI; SANCISI, Nicola, 2013). Data of the knee ligaments insertion areas are also the focus of different studies (PARENTI-CASTELLI; SANCISI, Nicola, 2013; WILSON, D. R. *et al.*, 1998; ENGIN; TUMER, 1993; CROWNINSHIELD *et al.*, 1976).

The studies developed by Gasparutto et al. (2015) and by Ponce Saldias (2014) used as reference the data obtained by Ottoboni et al. (2010) and by Parenti-Castelli and Sancisi (2013) which used a coordinate system defined by Wu (1995).

All the experimental data of the knee ligaments insertion areas, ligaments length and trajectory are presented in the studies made by Ottoboni et al. (2010) and by Parenti-Castelli and Sancisi (2013), and by consequence are available in the study made by Gasparutto *et al.* (2015). This chapter and the following steps of this research will rely upon the experimental data obtained in these studies, as insertion areas of the ligaments and its expected trajectory (Annex A), (GASPARUTTO *et al.*, 2015; OTTOBONI *et al.*, 2010; PARENTI-CASTELLI; SANCISI, Nicola, 2013; WU; CAVANAGH, 1995).

In forward kinematics, joints variables and length of links are given thus one can determine the position and orientation of the end-effector or, in a parallel mechanism, the center point of the mobile platform (or any other chosen point). In inverse kinematics, the position of a specific point or end-effector is known as well as the length of the links and one must determine the joints variables (angles and positions).

For the mechanism 0°-30° developed and analyzed in Sections 4.1 and 4.2, the initial position of the joints in the femur and tibia (mobile and fix platform) will be considered equivalent to the insertion areas of the experimental data obtained by (PARENTI-CASTELLI; SANCISI, Nicola, 2013) and (OTTOBONI *et al.*, 2010). The other mechanisms (30°to 40°, 40°to 60°, 60°to 90°, 90°to 120°, 120°to 140°) will consider as initial position of its joints, the final position of the mechanism joints previous to them.

The input data of the mechanisms are the knees flexion angle and the insertion areas of each ligament, thus it is proposed the use of forward kinematics, in order to obtain the knees trajectory. This approach is applied to obtain the angles of revolute joints and the position of prismatic joints. The length of the links is initially estimate by using experimental data and linear algebra.

Then, the trajectory obtained by applying forward kinematics is compared with the corresponding experimental data presented by (PARENTI-CASTELLI; SANCISI, Nicola, 2013) and (OTTOBONI *et al.*, 2010), for each range of flexion.

5.1   FORWARD KINEMATICS

In order to achieve a continuous trajectory line throughout flexion, regardless of the variation of the kinematic chains in each range of flexion, the initial position of the joints in the mechanism's fix platform and mobile platform is passed sequentially from one to another.

The initial position of joints connected to fix and mobile platforms of the proposed mechanism $0°$ to $30°$ (Fig. 43) is equivalent to experimental data of the main ligaments insertion areas and the midpoint between the center of femurs condyles and tibial plateaus (PARENTI-CASTELLI; SANCISI, Nicola, 2013; OTTOBONI *et al.*, 2010), representing the contact between tibia and femur.

Figure 43 – General mechanism.
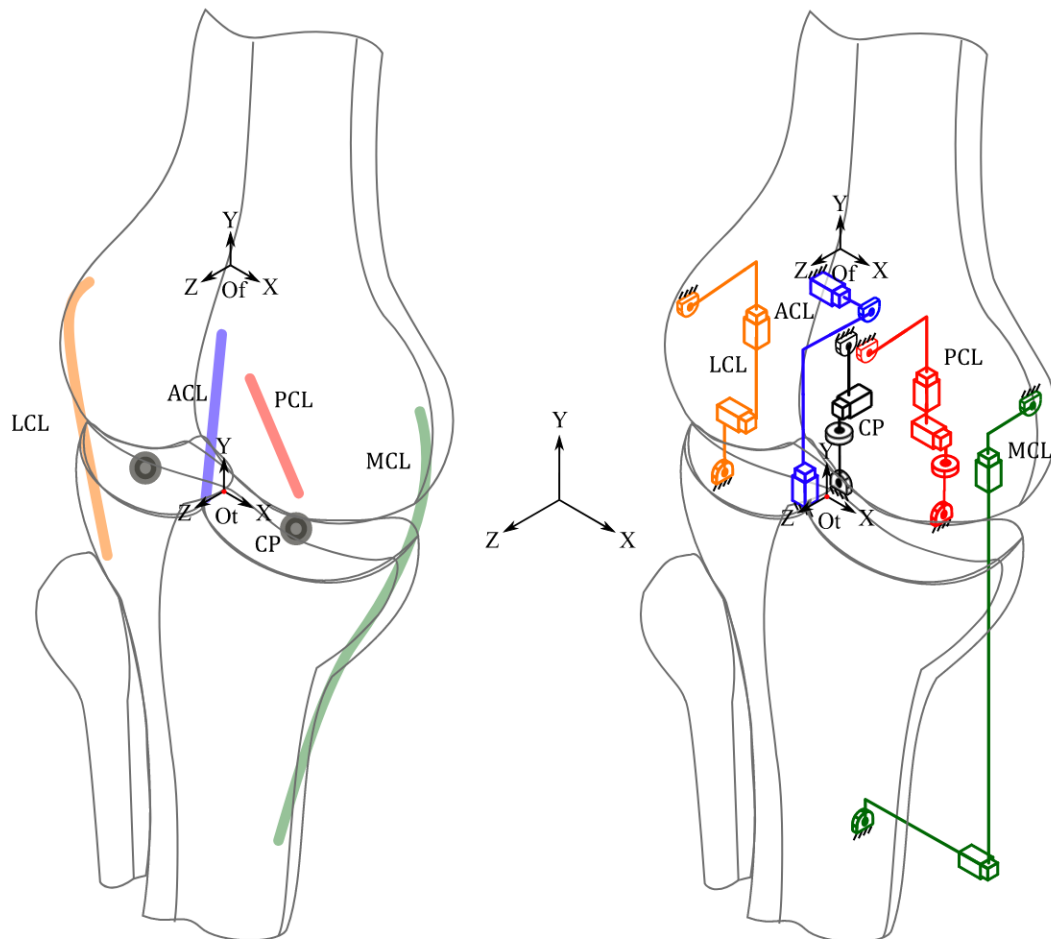
Source – own construction

Considering the experimental data of the origin of tibia (O_t), femur (O_f), and the insertion area of each ligament on tibia and femur, in millimeters [mm]:

$$O_t = \begin{bmatrix} 0.00 \\ 0.00 \\ 0.00 \end{bmatrix} \quad O_f = \begin{bmatrix} 4.00 \\ 20.35 \\ 2.32 \end{bmatrix}$$

$$ACL_t = \begin{bmatrix} 0.90 \\ -26.10 \\ 12.80 \end{bmatrix} \quad ACL_f = \begin{bmatrix} -9.20 \\ 7.50 \\ -6.80 \end{bmatrix} \quad PCL_t = \begin{bmatrix} 3.50 \\ -38.10 \\ -25.80 \end{bmatrix} \quad PCL_f = \begin{bmatrix} 2.20 \\ -1.10 \\ -2.70 \end{bmatrix}$$

$$MCL_t = \begin{bmatrix} 5.80 \\ -117.10 \\ 2.10 \end{bmatrix} \quad MCL_f = \begin{bmatrix} 47.60 \\ 5.80 \\ 2.70 \end{bmatrix} \quad LCL_t = \begin{bmatrix} -37.10 \\ -48.00 \\ -24.30 \end{bmatrix} \quad LCL_f = \begin{bmatrix} -36.20 \\ 2.30 \\ 3.20 \end{bmatrix}$$

$$CP_t = \begin{bmatrix} -2.65 \\ -27.35 \\ -2.45 \end{bmatrix} \quad CP_f = \begin{bmatrix} -1.50 \\ 2.75 \\ -1.55 \end{bmatrix}$$

The initial position of the mechanism's joints ($0°$ to $30°$) are the same as the experimental data.

$$A1_{i_{0° to 30°}} = ACL_f \quad A3_{0° to 30°} = ACL_t$$

$$P1_{i_{0° to 30°}} = PCL_f \quad P4_{0° to 30°} = PCL_t$$

$$M1_{i_{0° to 30°}} = MCL_f \quad M4_{0° to 30°} = MCL_t$$

$$L1_{i_{0° to 30°}} = LCL_f \quad L4_{0° to 30°} = LCL_t$$

$$C1_{i_{0° to 30°}} = CP_f \quad C4_{0° to 30°} = CP_t$$

The initial position of the mechanism's joints ($30°$ to $40°$) are equal to the final position of the joints of the mechanism $0°$ to $30°$.

$$A1_{i_{30° to 40°}} = A1_{f_{0° to 30°}} \qquad A3_{i_{30° to 40°}} = A3_{f_{0° to 30°}}$$

$$P1_{i_{30° to 40°}} = P1_{f_{0° to 30°}} \qquad P4_{i_{30° to 40°}} = P5_{f_{0° to 30°}}$$

$$M1_{i_{30° to 40°}} = M1_{f_{0° to 30°}} \qquad M4_{i_{30° to 40°}} = M4_{f_{0° to 30°}}$$

$$L_{1i_{30°to40°}} = L_{1f_{0°to30°}} \qquad L_{4i_{30°to40°}} = L_{4f_{0°to30°}}$$

$$C_{1i_{30°to40°}} = C_{1f_{0°to30°}} \qquad C_{4i_{30°to40°}} = C_{4f_{0°to30°}}$$

The initial position of the mechanism's joints (40°to 60°) are equal to the final position of the joints of the mechanism 30°to 40°.

$$A_{1i_{40°to60°}} = A_{1f_{30°to40°}} \qquad A_{3i_{40°to60°}} = A_{3f_{30°to40°}}$$

$$P_{1i_{40°to60°}} = P_{1f_{30°to40°}} \qquad P_{4i_{40°to60°}} = P_{4f_{30°to40°}}$$

$$M_{1i_{40°to60°}} = M_{1f_{30°to40°}} \qquad M_{4i_{40°to60°}} = M_{4f_{30°to40°}}$$

$$L_{1i_{40°to60°}} = L_{1f_{30°to40°}} \qquad L_{4i_{40°to60°}} = L_{4f_{30°to40°}}$$

$$C_{1i_{40°to60°}} = C_{1f_{30°to40°}} \qquad C_{4i_{40°to60°}} = C_{4f_{30°to40°}}$$

The initial position of the mechanism's joints (60°to 90°) are equal to the final position of the joints of the mechanism 40°to 60°.

$$A_{1i_{60°to90°}} = A_{1f_{40°to60°}} \qquad A_{4i_{60°to90°}} = A_{3f_{40°to60°}}$$

$$P_{1i_{60°to90°}} = P_{1f_{40°to60°}} \qquad P_{4i_{60°to90°}} = P_{4f_{40°to60°}}$$

$$M_{1i_{60°to90°}} = M_{1f_{40°to60°}} \qquad M_{4i_{60°to90°}} = M_{4f_{40°to60°}}$$

$$L_{1i_{60°to90°}} = L_{1f_{40°to60°}} \qquad L_{4i_{60°to90°}} = L_{4f_{40°to60°}}$$

$$C_{1i_{60°to90°}} = C_{1f_{40°to60°}} \qquad C_{4i_{60°to90°}} = C_{4f_{40°to60°}}$$

The initial position of the mechanism's joints (90°to 120°) are equal to the final position of the joints of the mechanism 60°to 90°.

$$A_{1i_{90°to120°}} = A_{1f_{60°to90°}} \qquad A_{5i_{90°to120°}} = A_{4f_{60°to90°}}$$

$$P_{1i_{90°to120°}} = P_{1f_{60°to90°}} \qquad P_{5i_{90°to120°}} = P_{4f_{60°to90°}}$$

$$M_{1i_{90°to120°}} = M_{1f_{60°to90°}} \qquad M_{5i_{90°to120°}} = M_{4f_{60°to90°}}$$

$$L_{1i_{90°to120°}} = L_{1f_{60°to90°}} \qquad L_{5i_{90°to120°}} = L_{4f_{60°to90°}}$$

$$C_{1i_{90°to120°}} = C_{1f_{60°to90°}} \qquad C_{3i_{90°to120°}} = C_{4f_{60°to90°}}$$

The initial position of the mechanism's joints ($120°$to $140°$) are equal to the final position of the joints of the mechanism $90°$to $120°$.

$$A_{1i_{120°to140°}} = A_{1f_{90°to120°}} \qquad A_{4i_{120°to140°}} = A_{5f_{90°to120°}}$$

$$P_{1i_{120°to140°}} = P_{1f_{90°to120°}} \qquad P_{5i_{120°to140°}} = P_{5f_{90°to120°}}$$

$$C_{1i_{120°to140°}} = C_{1f_{90°to120°}} \qquad C_{3i_{120°to140°}} = C_{3f_{90°to120°}}$$

Considering the origin of the fix platform equal to the origin of tibia (O_t), the origin of the mobile platform equal to the origin of femur (O_f). For all mechanisms, the actuated joint is the revolute joint A_2 about the x-axis. The position of this joint will dictate the position of all other joints through all the range of flexion (Fig. 44).

Figure 44 – Mechanisms throughout flexion, in the respective ranges: (A) 0° to 30°, (B) 30° to 40°, (C) 40° to 60°, (D) 60°to 90°, (E) 90° to 120° and (F) 120° to 140°.
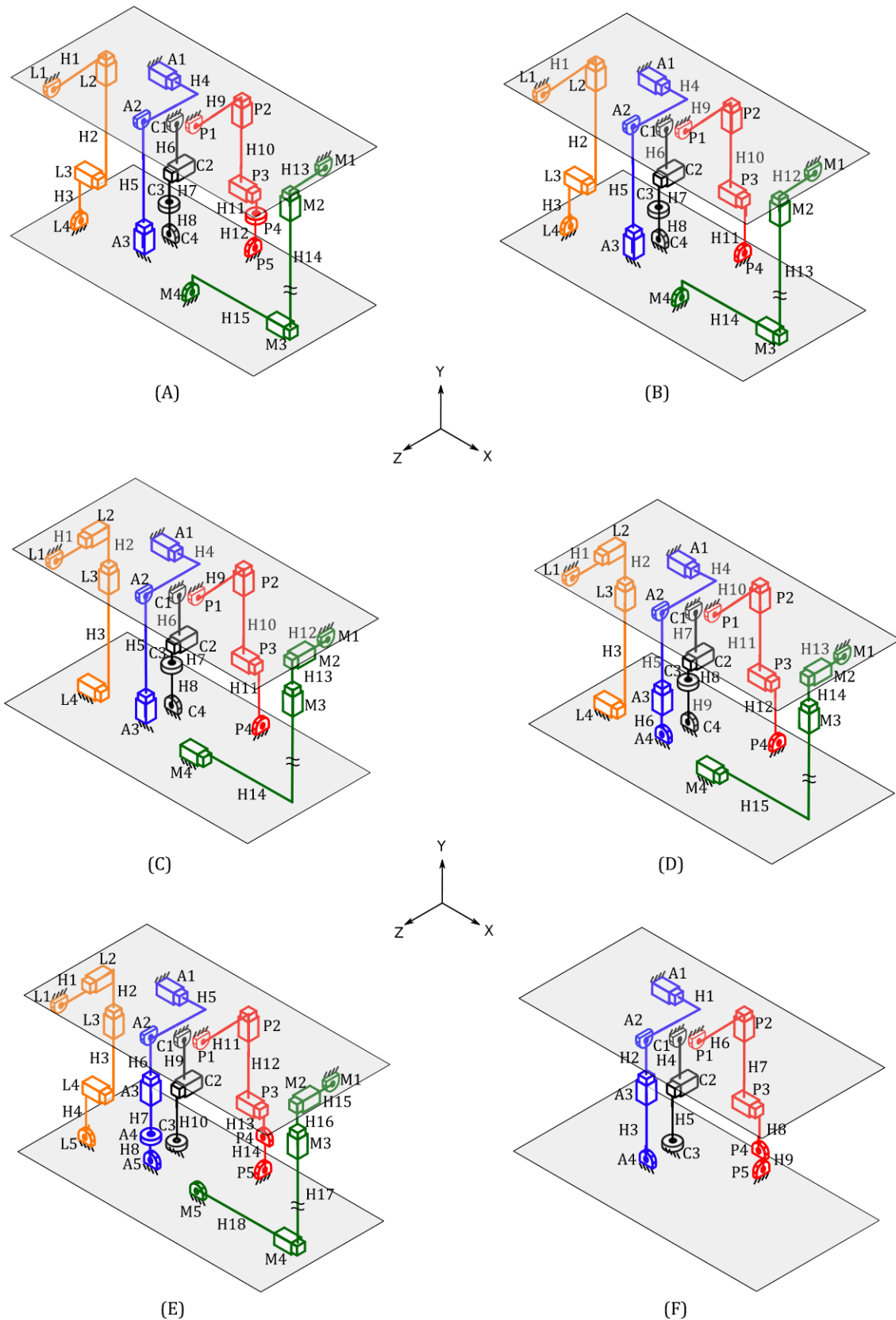
Source – own construction

Using algebra it is possible to obtain the equations that define the position of each joint for each degree of flexion that the A_2 joint may represent. This equations are called the position vectors of each joint (Appendix A).

Through the position vectors it is possible to calculate the mechanism trajectory throughout the flexion-extension range, comparing the results with experimental data of femurs trajectory in the y-axis and z-axis, shown in Figure 45 and Figure 46, respectively.

Figure 45 – Proposed mechanisms and experimental data trajectories in the y-axis.
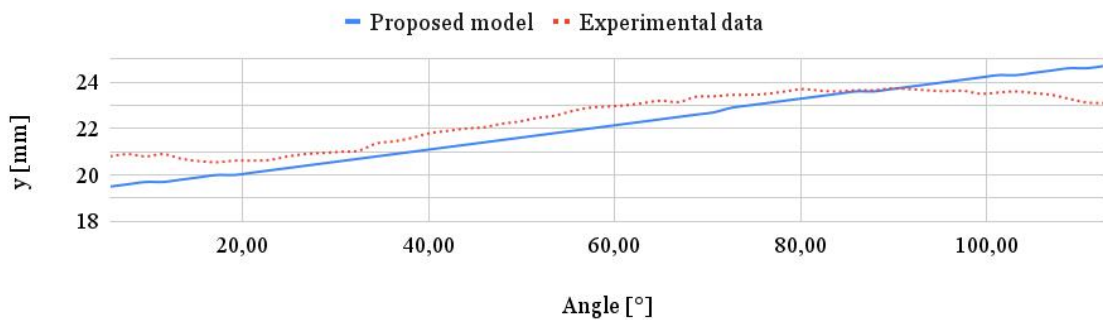
Source – own construction

Figure 46 – Proposed mechanisms and experimental data trajectories in the z-axis.
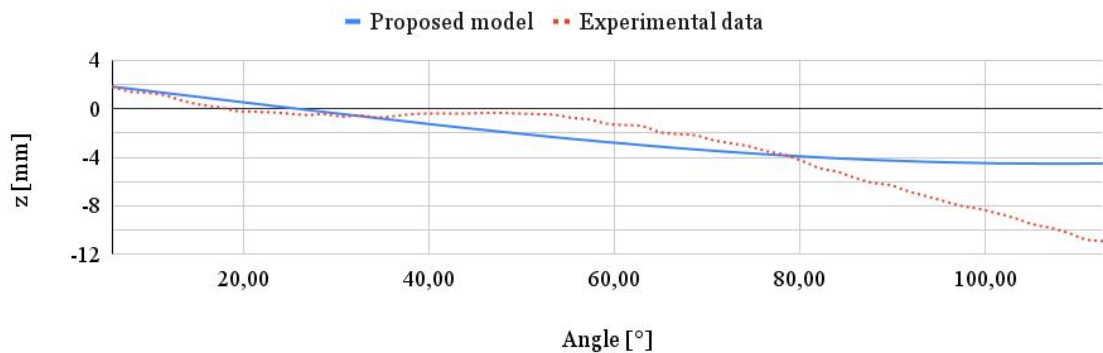
Source – own construction

The X-axis is not compared, since the mechanism is planar, not presenting a translation in the x-axis. This is a limitation of the proposed mechanism that presented a kinematic behavior close to a four bar mechanism.

5.2 STATIC ANALYSIS BY DAVIES METHOD

When an external force is applied on tibia, as during an anterior drawer test, the reaction forces are distributed between the ligaments and soft structures. A good distribution of forces between ligaments indicates that they will provide stability during other activities that require its strength and function.

In this chapter, the mechanisms is positioned and a force is applied in the link correspondent to tibia, replicating the experiment made by (WOO *et al.*, 1998) at 9 human knee joints and comparing the results. During the experiment, a force in the z-axis is applied on tibia in different levels (22N, 44N, 66N, 88N and 110N) and at different degrees of knees flexion (0°, 15°, 30°, 60°and 90°).

As all experimental data analyzes the knee from 0°to 30°and 60°to 90°, only the correspondent mechanisms of 0-30° and 60°-90° of flexion will be analyzed.

To analyze the *in situ* forces of the ligaments, Davies' Method was applied first on the Mechanism 0°to 30°. The position vectors and wrenches are available in appendix A and B, respectively.

The matrix of actions (A_D) (Eq. 25) is formed by the wrenches of all actions (constraints of joints and external forces). The number of lines is equal to the workspace and the number of columns is equal to the number of actions (λxA).

$$
[A_D]_{6\text{x}102} = \Big[\$^A_{L_{4_{Fx}}} \ \$^A_{L_{4_{Fy}}} \ \$^A_{L_{4_{Fz}}} \ \$^A_{L_{4_{My}}} \ \$^A_{L_{4_{Mz}}} \ \$^A_{A_{3_{Fx}}} \ \$^A_{A_{3_{Fz}}} \ \$^A_{A_{3_{Mx}}} \ \$^A_{A_{3_{My}}} \ \$^A_{A_{3_{Mz}}} \cdots
$$

$$
\$^A_{P_{5_{Fx}}} \ \$^A_{P_{5_{Fy}}} \ \$^A_{P_{5_{Fz}}} \ \$^A_{P_{5_{My}}} \ \$^A_{P_{5_{Mz}}} \ \$^A_{M_{4_{Fx}}} \ \$^A_{M_{4_{Fy}}} \ \$^A_{M_{4_{Fz}}} \ \$^A_{M_{4_{My}}} \ \$^A_{M_{4_{Mz}}} \cdots
$$

$$
\$^A_{L_{1_{Fx}}} \ \$^A_{L_{1_{Fy}}} \ \$^A_{L_{1_{Fz}}} \ \$^A_{L_{1_{My}}} \ \$^A_{L_{1_{Mz}}} \ \$^A_{L_{2_{Fx}}} \ \$^A_{L_{2_{Fz}}} \ \$^A_{L_{2_{Mx}}} \ \$^A_{L_{2_{My}}} \ \$^A_{L_{2_{Mz}}} \cdots
$$

$$
\$^A_{L_{3_{Fy}}} \ \$^A_{L_{3_{Fz}}} \ \$^A_{L_{3_{Mx}}} \ \$^A_{L_{3_{My}}} \ \$^A_{L_{3_{Mz}}} \ \$^A_{A_{1_{Fy}}} \ \$^A_{A_{1_{Fz}}} \ \$^A_{A_{1_{Mx}}} \ \$^A_{A_{1_{My}}} \ \$^A_{A_{1_{Mz}}} \cdots
$$

$$
\$^A_{A_{2_{Fx}}} \ \$^A_{A_{2_{Fy}}} \ \$^A_{A_{2_{Fz}}} \ \$^A_{A_{2_{My}}} \ \$^A_{A_{2_{Mz}}} \ \$^A_{C_{1_{Fx}}} \ \$^A_{C_{1_{Fy}}} \ \$^A_{C_{1_{Fz}}} \ \$^A_{C_{1_{My}}} \ \$^A_{C_{1_{Mz}}} \cdots
$$

$$
\$^A_{C_{2_{Fx}}} \ \$^A_{C_{2_{Fy}}} \ \$^A_{C_{2_{Mx}}} \ \$^A_{C_{2_{My}}} \ \$^A_{C_{2_{Mz}}} \ \$^A_{C_{3_{Fx}}} \ \$^A_{C_{3_{Fy}}} \ \$^A_{C_{3_{Fz}}} \ \$^A_{C_{3_{Mx}}} \ \$^A_{C_{3_{Mz}}} \cdots
$$

$$
\$^A_{C_{4_{Fx}}} \ \$^A_{C_{4_{Fy}}} \ \$^A_{C_{4_{Fz}}} \ \$^A_{C_{4_{Mx}}} \ \$^A_{C_{4_{My}}} \ \$^A_{L_{1_{Fx}}} \ \$^A_{P_{1_{Fy}}} \ \$^A_{P_{1_{Fz}}} \ \$^A_{P_{1_{My}}} \ \$^A_{P_{1_{Mz}}} \cdots
$$

$$
\$^A_{P_{2_{Fx}}} \ \$^A_{P_{2_{Fz}}} \ \$^A_{P_{2_{Mx}}} \ \$^A_{P_{2_{My}}} \ \$^A_{P_{2_{Mz}}} \ \$^A_{P_{3_{Fy}}} \ \$^A_{P_{3_{Fz}}} \ \$^A_{P_{3_{Mx}}} \ \$^A_{P_{3_{My}}} \ \$^A_{P_{3_{Mz}}} \cdots
$$

$$
\$^A_{P_{4_{Fx}}} \ \$^A_{P_{4_{Fy}}} \ \$^A_{P_{4_{Fz}}} \ \$^A_{P_{4_{Mx}}} \ \$^A_{P_{4_{Mz}}} \ \$^A_{M_{1_{Fx}}} \ \$^A_{M_{1_{Fy}}} \ \$^A_{M_{1_{Fz}}} \ \$^A_{M_{1_{My}}} \ \$^A_{M_{1_{Mz}}} \cdots
$$

$$
\$^A_{M_{2_{Fx}}} \ \$^A_{M_{2_{Fz}}} \ \$^A_{M_{2_{Mx}}} \ \$^A_{M_{2_{My}}} \ \$^A_{M_{2_{Mz}}} \ \$^A_{M_{3_{Fy}}} \ \$^A_{M_{3_{Fz}}} \ \$^A_{M_{3_{Mx}}} \ \$^A_{M_{3_{My}}} \ \$^A_{M_{3_{Mz}}} \cdots
$$

$$\$^{A}_{F'_z} \$^{A}_{M'_x}\,](25)$$

The cutset matrix (Q_A) (Appendice C) is formed, as explained in Chapter 3, by analyzing the cutset graph (Fig. 47).

Figure 47 – Cutset graph and identification of the strings of the mechanism 0°to 30°.
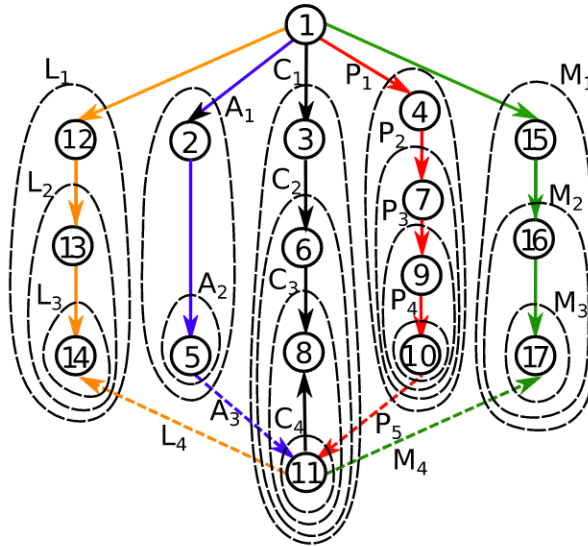
Source – own construction

Each line of the (Q_A) is transformed in a diagonal matrix dQ_A, and used to calculate the matrix of network couplings A_N (Eq. 26).

$$A_{N_{96x102}} = \begin{bmatrix} A_D \cdot dQ_{A_{L1}} \\ A_D \cdot dQ_{A_{L2}} \\ A_D \cdot dQ_{A_{L3}} \\ A_D \cdot dQ_{A_{A1}} \\ A_D \cdot dQ_{A_{A2}} \\ A_D \cdot dQ_{A_{C1}} \\ A_D \cdot dQ_{A_{C2}} \\ A_D \cdot dQ_{A_{C3}} \\ A_D \cdot dQ_{A_{C4}} \\ A_D \cdot dQ_{A_{P1}} \\ A_D \cdot dQ_{A_{P2}} \\ A_D \cdot dQ_{A_{P3}} \\ A_D \cdot dQ_{A_{P4}} \\ A_D \cdot dQ_{A_{M1}} \\ A_D \cdot dQ_{A_{M2}} \\ A_D \cdot dQ_{A_{M3}} \end{bmatrix} \qquad (26)$$

The last two columns of the A_N matrix are the two forces applied to the mechanism, as they are inputs, in order to calculate the magnitude vector (ψ), these two columns are removed from the A_N matrix. The magnitude vector is formed by all of constraints variables, at the same order than A_D, with 100 lines and one column, (ψ_{100x1}).

$$\psi_{100x1} = \begin{bmatrix} L_{4_{Fx}} \\ L_{4_{Fy}} \\ L_{4_{Fz}} \\ L_{4_{My}} \\ L_{4_{Mz}} \\ A_{3_{Fx}} \\ A_{3_{Fz}} \\ \vdots \\ M_{3_{Fy}} \\ M_{3_{Fz}} \\ M_{3_{Mx}} \\ M_{3_{My}} \\ M_{3_{Mz}} \end{bmatrix} \tag{27}$$

As the AN matrix is not square, there is no solution for this system. This result was expected because an overconstrained mechanism may result in more variables than equations.

To overcome this problem, as the mechanism is planar, presenting a kinematic behavior similar to a 4-bar mechanism, it is proposed to analyze the mechanisms in a planar workspace, excluding the joints that do not belong in the Y-Z plane.

5.2.1 Static analysis in a planar workspace

When the mobility analysis was made in Chapter 4.1, some revolute joints were added to the mechanism. Without the revolute joints, the mechanism would not move, unless the joints were repositioned. If they were repositioned, it would not be possible to use as reference the position of the insertion areas of the ligaments.

However, when these revolute joints were added, the only constraint to forces in the z-axis were concentrated in the representation of the ACL. This does not happen in a real human knee, the ACL is the major constraint to forces in the z-axis in the anterior direction, but it is not the only constraint.

As other ligaments are not constraining the movement, the expected result is that ACL will support all force applied in the z-axis.

To continue using the insertion area of the ligaments as reference and keeping the mechanism motion, it is proposed to add a constraint in the prismatic joints of the y-axis in the representation of LCL (L_2) and MCL (M_2), as both of them are active and should

resist the applied force with the ACL. To do so, it is used as reference the experimental data of (KANAMORI *et al.*, 2000), adding an equation of distribution of forces according to the range of flexion, obtained by experiments (Annex B).

The external force (Eq. 28) applied to all the mechanisms is equivalent to a force in the z-axis and a proportional moment about the x-axis, resulting in static mechanisms.

$$F = \begin{bmatrix} F_y \\ F_z \\ M_x \end{bmatrix} \tag{28}$$

During all the static analysis, a force F_z is applied in a position equivalent to -200mm in y-axis (O_t) as shown in Figure 48. The analysis is made varying the amplitude of F_z in each analyzed degree of flexion. Five forces amplitudes are analyzed, 22N, 44N, 66N, 88N and 110N, respectively, the same used by Woo in an experimental study (WOO *et al.*, 1998). During the static analysis, M_x is always equivalent to the applied F_z force and F_y is always equal to zero.

Figure 48 – Mechanism force application.
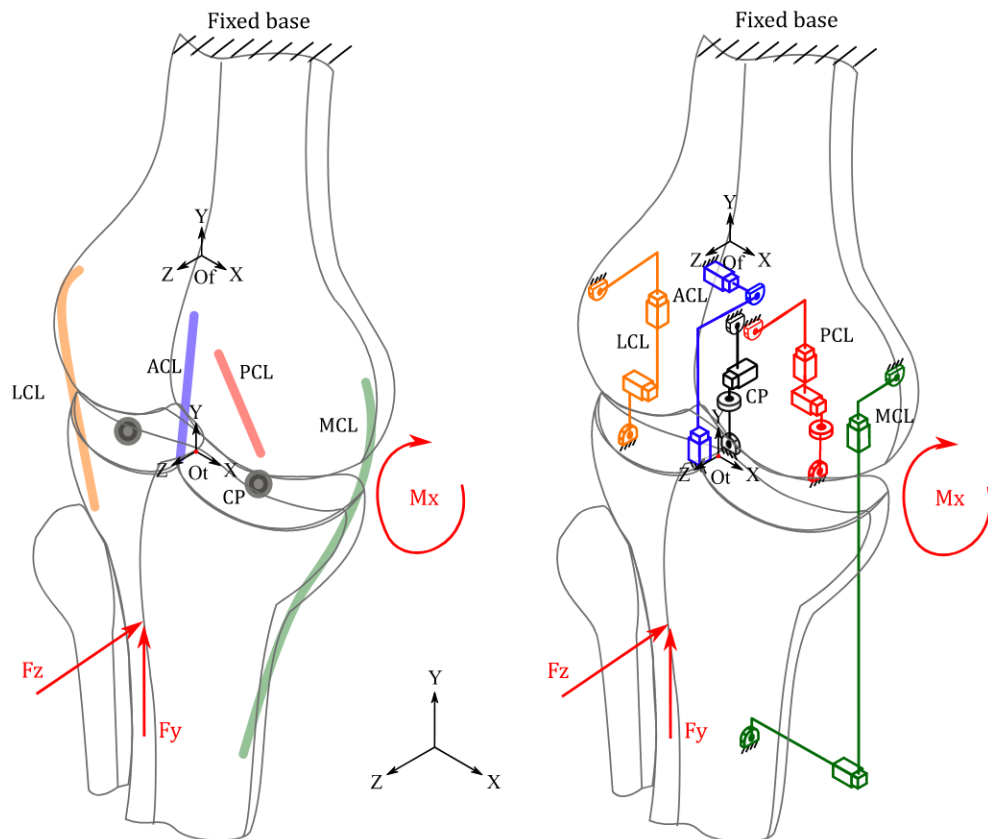
Source – own construction

5.2.1.1 Static analysis - Mechanism 0°to 30°

The position vectors and wrenches are available in Appendix A and B, respectively.

From the mechanism wrenches it is possible to obtain the matrix of actions (A_D) (Eq. 29):

$$[A_D]_{3x31} = \begin{bmatrix} \$^A_{L_{4_{Fy}}} & \$^A_{L_{4_{Fz}}} & \$^A_{A_{3_{Fz}}} & \$^A_{A_{3_{Mx}}} & \$^A_{P_{5_{Fy}}} & \$^A_{P_{5_{Fz}}} & \$^A_{M_{4_{Fy}}} & \$^A_{M_{4_{Fz}}} & \$^A_{L_{1_{Fy}}} & \$^A_{L_{1_{Fz}}} & \$^A_{L_{2_{Fy}}} & \$^A_{L_{2_{Fz}}} & \$^A_{L_{2_{Mx}}} & \cdots \end{bmatrix}$$

$$\begin{array}{cccccccccccc} \$^A_{A_{2_{Fy}}} & \$^A_{A_{2_{Fz}}} & \$^A_{C_{1_{Fy}}} & \$^A_{C_{1_{Fz}}} & \$^A_{C_{2_{Fy}}} & \$^A_{C_{2_{Mx}}} & \$^A_{P_{1_{Fy}}} & \$^A_{P_{1_{Fz}}} & \$^A_{P_{2_{Fz}}} & \$^A_{P_{2_{Mx}}} & \$^A_{M_{1_{Fy}}} & \$^A_{M_{1_{Fz}}} & \$^A_{M_{2_{Fy}}} & \cdots \end{array}$$

$$\begin{array}{ccccc} \$^A_{M_{2_{Fz}}} & \$^A_{M_{2_{Mx}}} & \$^A_{F'_y} & \$^A_{F'_z} & \$^A_{M'_x} \end{array}](29)$$

From the graph presented in Fig. 24 , the joints that are not in the y-z plane are removed and than it is obtained the cutset graph of the mechanism in the plane (Fig. 49)

Figure 49 – Cutset graph and identification of the strings of the planar mechanism 0°to 30°.
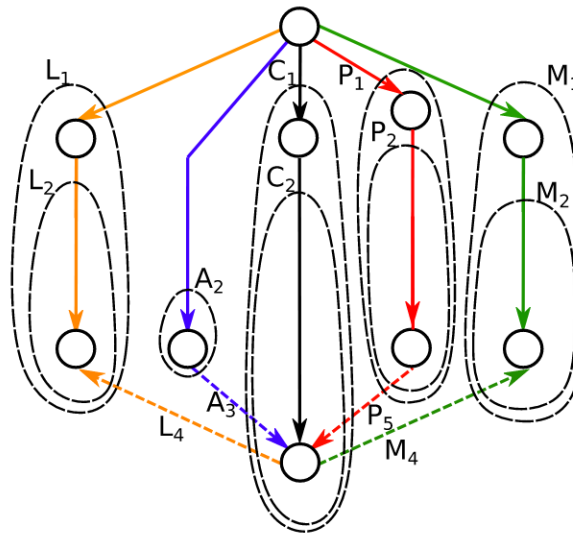
Source – own construction

From the Graph 49, it is obtained the cutset matrix $Q_{A_{0°to30°}}$ presented in Appendix C.

From the cutset matrix, the matrix of network couplings A_N 30 is calculated.

$$
A_{N_{27x31}} = \begin{bmatrix}
A_D \cdot dQ_{A_{L1}} \\
A_D \cdot dQ_{A_{L2}} \\
A_D \cdot dQ_{A_{A2}} \\
A_D \cdot dQ_{A_{C1}} \\
A_D \cdot dQ_{A_{C2}} \\
A_D \cdot dQ_{A_{P1}} \\
A_D \cdot dQ_{A_{P2}} \\
A_D \cdot dQ_{A_{M1}} \\
A_D \cdot dQ_{A_{M2}}
\end{bmatrix}
\tag{30}
$$

The last three columns of the A_N matrix are the applied forces, resulting in a 27x28 matrix, as there are more variables than equations it was proposed to use related experimental data to complete the static analysis.

An experimental result of an anterior drawer test made in eight fresh-frozen human cadaveric knees is the topic of the study made by Karamori *et al.*, (2000). This experiment applied a force of 134N in different angles of flexion, analyzing the *in situ* forces of the knees structures, comparing a perfect human knee to a ACL deficient knee. The data used during this Thesis was the experimental data of a perfect functioning human knee. The study analyzed the ACL, MCL and PSL (Posterolateral Structures), during this Thesis the PSL was considered equivalent to the LCL, as the LCL is a important part of PSL and the focus of the presented static analysis is the ACL, (Annex B, Table 20).

From the experimental data (KANAMORI *et al.*, 2000), it is possible to obtain the force distribution proportion shown on the Equation 31 obtained from Annex B. Each equation is add to the A_N matrix (Eq. 30) in its respective flexion angle.

$$
\begin{cases}
0° \rightarrow 79,85 \cdot A_{3_{Fz}} + 9,7 \cdot \sin(\theta_{L_4})^2 \cdot L_{2_{Fy}} + 9,7 \cdot \cos(\theta_{L_4})^2 \cdot L_{2_{Fz}} + \\
\qquad +10,45 \cdot \sin(\theta_{M_4})^2 \cdot M_{2_{Fy}} + 10,45 \cdot \cos(\theta_{M_4})^2 \cdot M_{2_{Fz}} = 100 \\
15° \rightarrow 83,58 \cdot A_{3_{Fz}} + 5,97 \cdot \sin(\theta_{L_4})^2 \cdot L_{2_{Fy}} + 5,97 \cdot \cos(\theta_{L_4})^2 \cdot L_{2_{Fz}} + \\
\qquad +10,45 \cdot \sin(\theta_{M_4})^2 \cdot M_{2_{Fy}} + 10,45 \cdot \cos(\theta_{M_4})^2 \cdot M_{2_{Fz}} = 100 \\
30° \rightarrow 79,10 \cdot A_{3_{Fz}} + 9,7 \cdot \sin(\theta_{L_4})^2 \cdot L_{2_{Fy}} + 9,7 \cdot \cos(\theta_{L_4})^2 \cdot L_{2_{Fz}} + \\
\qquad +11,19 \cdot \sin(\theta_{M_4})^2 \cdot M_{2_{Fy}} + 11,19 \cdot \cos(\theta_{M_4})^2 \cdot M_{2_{Fz}} = 100
\end{cases}
\tag{31}
$$

Adding the equation 31 the system cam be expressed as Eq. 32.

$$
[A_N]_{28x31} \cdot \{\psi\}_{31x1} = \{\vec{0}\}_{28x1}
\tag{32}
$$

As the last three columns of the A_N matrix (Eq. 30) are the input forces (Eq. 33).

$$
\left[[A_{N_V}]_{28x28} \ \vdots \ [A_{N_F}]_{28x3} \right] \cdot \left[[\{\psi_V\}_{28x1} \ \vdots \ \{\psi_F\}_{3x1}] \right]^T = \{\vec{0}\}_{28x1}
\tag{33}
$$

Isolating the input forces it is possible to calculate the magnitude vector (Eq. 34)

$$\psi V_{28x1} = \begin{bmatrix} L_{4_{Fy}} \\ L_{4_{Fz}} \\ A_{3_{Fz}} \\ A_{3_{Mx}} \\ \vdots \\ M_{2_{Fy}} \\ M_{2_{Fz}} \\ M_{2_{Mx}} \end{bmatrix} \tag{34}$$

5.2.1.2 Static analysis - Mechanism 60°to 90°

The position vectors and wrenches are available in Appendix A and B, respectively.

From the mechanism wrenches it is possible to obtain the matrix of actions (A_D) (Eq. 35):

$$[A_D]_{3x31} = \begin{bmatrix} \$^A_{L_{3_{Fy}}} & \$^A_{L_{3_{Fz}}} & \$^A_{L_{3_{Mx}}} & \$^A_{A_{3_{Fz}}} & \$^A_{A_{3_{Mx}}} & \$^A_{P_{4_{Fy}}} & \$^A_{P_{4_{Fz}}} & \$^A_{M_{3_{Fy}}} & \$^A_{M_{3_{Fz}}} & \$^A_{M_{3_{Mx}}} & \$^A_{L_{1_{Fy}}} & \$^A_{L_{1_{Fz}}} & \$^A_{L_{2_{Fy}}} & \$^A_{L_{2_{Mx}}} \cdots \end{bmatrix}$$

$$\$^A_{A_{2_{Fy}}} \quad \$^A_{A_{2_{Fz}}} \quad \$^A_{C_{1_{Fy}}} \quad \$^A_{C_{1_{Fz}}} \quad \$^A_{C_{2_{Fy}}} \quad \$^A_{C_{2_{Mx}}} \quad \$^A_{P_{1_{Fy}}} \quad \$^A_{P_{1_{Fz}}} \quad \$^A_{P_{2_{Fz}}} \quad \$^A_{P_{2_{Mx}}} \quad \$^A_{M_{1_{Fy}}} \quad \$^A_{M_{1_{Fz}}} \quad \$^A_{M_{2_{Fy}}} \cdots$$

$$\left. \$^A_{M_{2_{Mx}}} \quad \$^A_{F'_y} \quad \$^A_{F'_z} \quad \$^A_{M'_x} \right] \tag{35}$$

From the graph presented in Fig. 34 , the joints that are not in the Y-Z plane are removed and than it is obtained the cutset graph of the mechanism in the plane (Fig. 50)

From the cutset graph, it is obtained the cutset matrix $Q_{A_{60°to90°}}$ presented in Appendix C.

From the cutset matrix, the matrix of network couplings A_N (Eq. 36) is calculated.

$$A_{N_{27x31}} = \begin{bmatrix} A_D \cdot dQ_{A_{L1}} \\ A_D \cdot dQ_{A_{L2}} \\ A_D \cdot dQ_{A_{A2}} \\ A_D \cdot dQ_{A_{C1}} \\ A_D \cdot dQ_{A_{C2}} \\ A_D \cdot dQ_{A_{P1}} \\ A_D \cdot dQ_{A_{P2}} \\ A_D \cdot dQ_{A_{M1}} \\ A_D \cdot dQ_{A_{M2}} \end{bmatrix} \tag{36}$$

From the experimental data (KANAMORI *et al.*, 2000), the Equation 37 obtained

Figure 50 – Cutset graph and identification of the strings of the planar mechanism 60°to 90°.
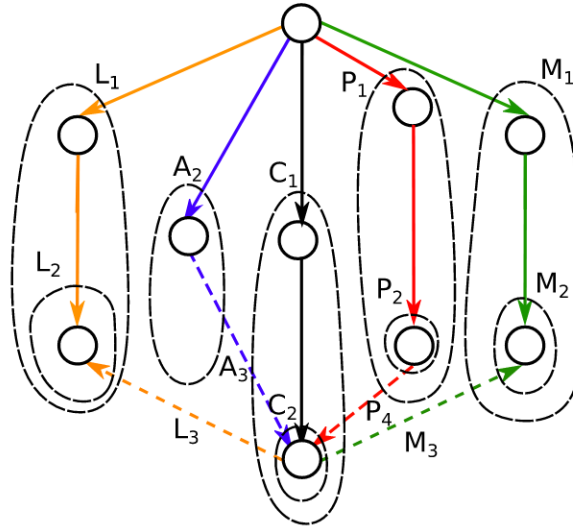
Source – own construction

from Annex B is add to the A_N matrix (36) on the respective flexion angles.

$$
\begin{cases}
60° \to 70,15 \cdot A_{3_{Fz}} + 14,93 \cdot \sin(\theta_{L_4})^2 \cdot L_{3_{Fy}} + 14,93 \cdot \cos(\theta_{L_4})^2 \cdot L_{3_{Fz}} + \\
\quad\quad +14,93 \cdot \sin(\theta_{M_4})^2 \cdot M_{3_{Fy}} + 14,93 \cdot \cos(\theta_{M_4})^2 \cdot M_{3_{Fz}} = 100 \\
\\
90° \to 73,88 \cdot A_{3_{Fz}} + 14,93 \cdot \sin(\theta_{L_4})^2 \cdot L_{3_{Fy}} + 14,93 \cdot \cos(\theta_{L_4})^2 \cdot L_{3_{Fz}} + \\
\quad\quad +11,19 \cdot \sin(\theta_{M_4})^2 \cdot M_{3_{Fy}} + 11,19 \cdot \cos(\theta_{M_4})^2 \cdot M_{3_{Fz}} = 100
\end{cases}
\tag{37}
$$

Adding the equation 37 the system cam be expressed as Eq. 38.

$$
[A_N]_{28x31} \cdot \{\psi\}_{31x1} = \{\vec{0}\}_{28x1}
\tag{38}
$$

As the last three columns of the A_N matrix (Eq. 36) are the input forces (Eq. 39).

$$
\left[[A_{N_V}]_{28x28} \ \vdots \ [A_{N_F}]_{28x3} \right] \cdot \left[\{\psi_V\}_{28x1} \ \vdots \ \{\psi_F\}_{3x1} \right]^{\mathrm{T}} = \{\vec{0}\}_{28x1}
\tag{39}
$$

Isolating the input forces it is possible to calculate the magnitude vector (Eq. 40)

$$\psi_{V_{29x1}} = \begin{bmatrix} L3_{Fy} \\ L3_{Fz} \\ L3_{Mx} \\ A3_{Fz} \\ A3_{Mx} \\ \vdots \\ M2_{Fy} \\ M2_{Mx} \end{bmatrix} \tag{40}$$

5.2.2 Static Analysis Result

From the static analysis it is possible to observe the behavior of the internal forces in the ACL, comparing the mechanisms results to the experimental data (Fig. 51).

Figure 51 – *In situ* forces in ACL - (a) proposed mechanism (b) experimental results (WOO *et al.*, 1998)

(a)   (b)
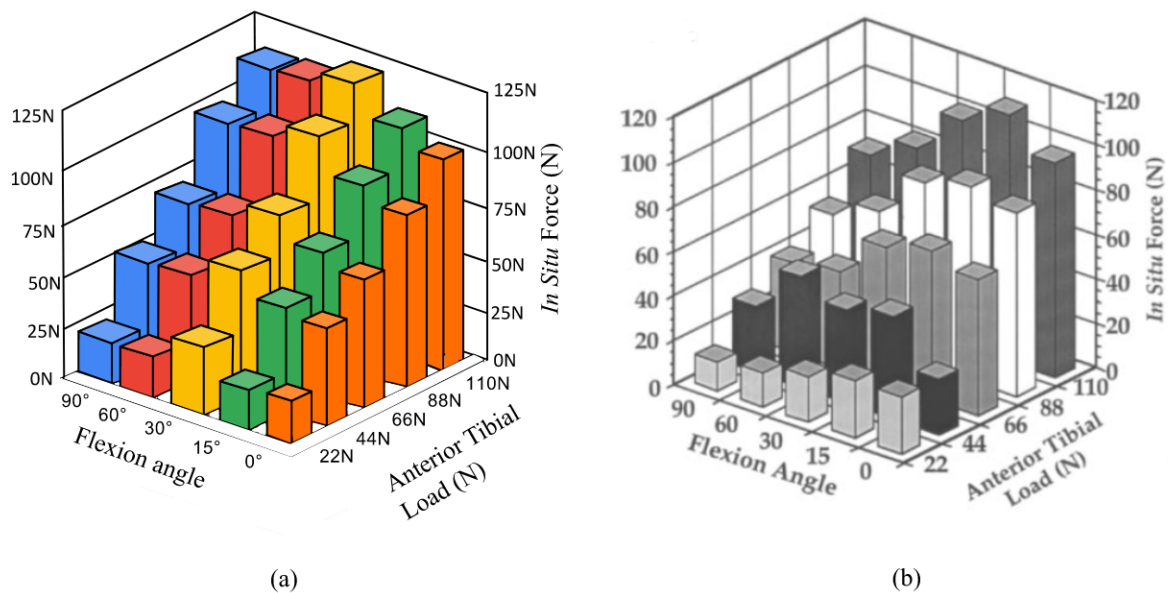
Source – (a) own construction (b) (WOO *et al.*, 1998)

The *in situ* force discrepancy and the percentage error between the experimental results and the proposed mechanism is presented in Figure 52 and 53, respectively.

For the flexion angles of 0°and 15°, the mechanical representation of the ACL presented *in situ* forces similar to the experimental data. For the flexion angle of 30°, the in situ force of the mechanical representation of the ACL rise a little, while the experimental data decrease.

Figure 52 – Force discrepancy between the experimental results and the proposed mechanism results in different flexion angles
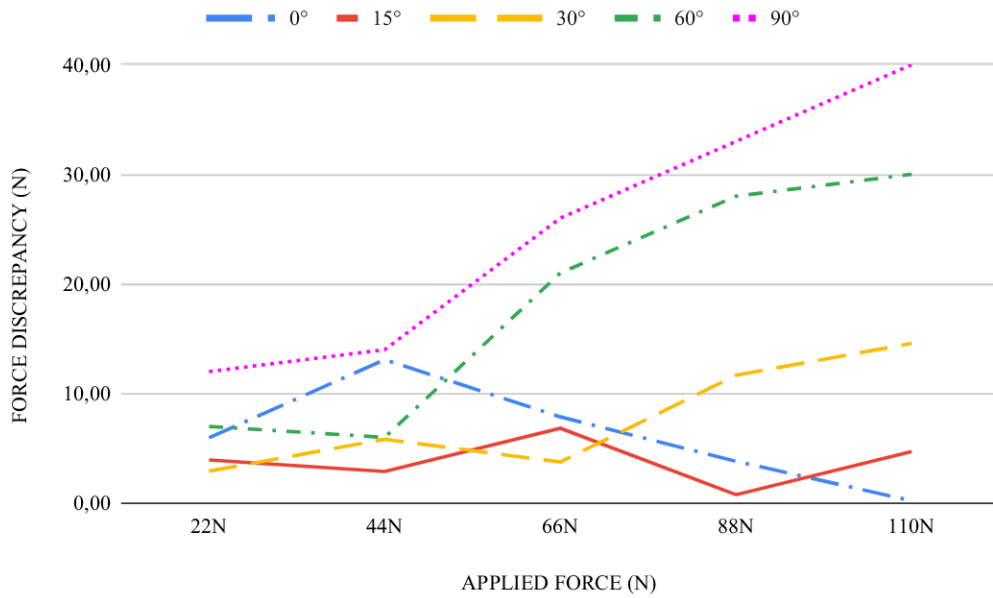
Source – own construction

Figure 53 – Force percentage error between the experimental results and the proposed mechanism results in different flexion angles

Source – own construction

The static analysis for the flexion of 60°and 90°shows that the mechanical representation of the ACL*in situ* forces diverge from the experimental data. A divergent result was already expected because of the mechanism trajectory, but this result is due to the addition of prismatic joints in the representation of MCL and LCL in the mechanism 60°to 90°, making the ACL be the main responsible for the force constraint in the z-axis.

5.3   FINAL CONSIDERATIONS

By analyzing the results, it is possible to observe that, despite being planar mechanisms, the proposed mechanisms achieved a trajectory close to the human knee. This result is emphasized specially at the y-axis, where the trajectory presented a behavior similar to the experimental data.

In the z-axis analysis it is possible to observe that the trajectory begins very close to the experimental data, but starts to diverge from the expected result after 40°of flexion and specially after 90°of flexion. This behavior may occur due the limitations of the model, not being a spatial mechanism, and also due the positioning of the joints.

It is known that a ligament does not have a linear behavior, resulting from the irregular arrangement of its fibers and diverse composition. However, thinking about reducing the computational cost and reaching a result close to the expected, the development of mechanical equivalent structures is widely discussed.

The proposed mechanisms proposed a different perspective of the human knee, proposing and analyzing different kinematic chains presented during its motion.

Due the large number of variables, the spatial mechanism had no viable solution, redirecting the static analysis to a planar workspace. Considering external experimental data, it was possible to analyze the response of the proposed mechanisms for the *in situ* forces of the ACL.

As a result it is possible tho observer a convergent behavior at the first degrees of flexion and a divergent behavior at the latest degrees, due the mechanical considerations made for each proposed mechanism.

6 CONCLUSIONS AND FUTURE WORK

The present Thesis reviewed the knee anatomy and biomechanic behavior, along with different studies of knee models using parallel mechanisms. It was also reviewed the different clinical tests applied to the human knee and the expected behavior of the knees main structures. This review enabled the mechanical analysis, comparing each ligament to equivalent mechanical joints and proposing a new perspective of a knee model.

The present Thesis brings an discussion about the behavior and analysis of the human knee structures. During the analysis, the constraints for each knee structure were discussed, indicating the direction and the equivalent DoF during different clinical tests. The analysis translated the clinical information to an equivalent mechanical analysis.

After the analysis of each knee structure, it was proposed the use of mechanical equivalencies, assembling a different mechanism for each knee range of flexion, using theory of mechanisms.

The graph theory was reviewed and applied for each proposed mechanism. It was also reviewed the mobility analysis and Reshetov's Method, which was applied to each proposed mechanism, validating the mechanism DoF.

A Position Analysis was made for each proposed mechanism, resulting in a planar trajectory which was compared to experimental data. The trajectory of the proposed model is close to the human knee in the y-z plane, being a valid result for a planar mechanism.

The static analysis was made using Davies method in a planar workspace. The result converged to the experimental data for the firsts degrees of flexion, validating the proposed mechanism and the methodology used during the static analysis. As for the higher degrees of flexion, the result diverged from the experimental data, indicating that the considerations made in the mechanical equivalences to analyze the force distribution during an anterior drawer test may not correspond to the knee anatomy in this range of flexion.

These result opens for discussion which mechanical joint may be the best to represent the behavior of human ligaments in a specific circumstance, presenting more accurate results in a static analysis. The more precise the results, the greater the chance that the model will be used to aid positioning ligament insertion area in ligament reconstructions.

This Thesis presented an innovative proposal to analyze the human knee as a different mechanism to each range of flexion, analyzing its trajectory and the static behavior of the equivalent ACL ligament by using Davies Method.

Tough the static analysis of the *in situ* forces of the ACL did not converged throughout the analysis, the proposed Thesis present a positive impact in the development of models of orthesis and external prosthesis, delivering a better understanding of the constraints present in the human knee. This Thesis is a first step, bringing to discussion the use of reconfigurable mechanisms to biomechanical applications.

As future work, it is proposed:

- A new model in a spatial workspace, based on the constraint analysis.

- An optimization of the joints positioning to improve the trajectory, also increasing the results convergence in a static analysis.

- Using the constraints of Table 2 for develop another knee mechanism, preserving the same directions (positive or negative), employing end-course joints.

- A reconfigurable mechanism, changing its kinematic chain during the knee flexion.

REFERENCES

BALL, Robert Stawell. **A Treatise on the Theory of Screws**. [S.l.]: Cambridge university press, 1900.

BELVEDERE, Claudio; ENSINI, Andrea; FELICIANGELI, Alessandro; CENNI, Francesco; D'ANGELI, Valentina; GIANNINI, Sandro; LEARDINI, Alberto. Geometrical changes of knee ligaments and patellar tendon during passive flexion. **Journal of biomechanics**, Elsevier, v. 45, n. 11, p. 1886–1892, 2012.

CAZANGI, Humberto Reder. Aplicação do método de Davies para análise cinemática e estática de mecanismos com múltiplos graus de liberdade. Florianópolis, SC, 2008.

CONCONI, Michele; SANCISI, Nicola; PARENTI-CASTELLI, Vincenzo. The geometrical arrangement of knee constraints that makes natural motion possible: Theoretical and experimental analysis. **Journal of Biomechanical Engineering**, American Society of Mechanical Engineers, v. 141, n. 5, p. 051001, 2019.

CROWNINSHIELD, R.; POPE, M. H.; JOHNSON, R. J. An analytical model of the knee. **Journal of biomechanics**, Elsevier, v. 9, n. 6, p. 397–405, 1976.

DAVIES, TH. Couplings, coupling networks and their graphs. **Mechanism and Machine Theory**, Elsevier, v. 30, n. 7, p. 991–1000, 1995.

ENGIN, Ali Erkan; TUMER, Sami Turgut. Improved dynamic model of the human knee joint and its response to impact loading on the lower leg, 1993.

FEIKES, J D; O'CONNOR, J J; ZAVATSKY, A B. A constraint-based approach to modelling the mobility of the human knee joint. **Journal of Biomechanics**, v. 36, n. 1, p. 125–129, 2003.

FLOYD, R. T. **Manual of structural kinesiology**. 18. ed. [S.l.]: McGraw-Hill, 2011.

GASPARUTTO, Xavier; SANCISI, Nicola; JACQUELIN, Eric; PARENTI-CASTELLI, Vincenzo; DUMAS, Raphael. Validation of a multi-body optimization with knee kinematic models including ligament constraints. **Journal of biomechanics**, Elsevier, v. 48, n. 6, p. 1141–1146, 2015.

GUPTE, Chinmay; BULL, Anthony; THOMAS, Rhidian; AMIS, Andrew. The meniscofemoral ligaments: secondary restraints to the posterior drawer. Analysis of anteroposterior and rotary laxity in the intact and posterior-cruciate-deficient knee. **The Journal of bone and joint surgery. British volume**, v. 85, p. 765–73, Aug. 2003.

HALEWOOD, Camilla. **Total knee replacements: design and pre-clinical testing methods**. Apr. 2016. PhD thesis – Imperial College London, Mechanical Engineering Department, Imperial College London.

HALEWOOD, Camilla; AMIS, Andrew. Clinically relevant biomechanics of the knee capsule and ligaments. **Knee surgery, sports traumatology, arthroscopy : official journal of the ESSKA**, v. 23, Apr. 2015.

HUNT, Kenneth H. Don't Cross-Thread the Screw! **Journal of Robotic Systems**, Wiley Online Library, v. 20, n. 7, p. 317–339, 2003.

KAKARLAPUDI, T K; BICKERSTAFF, D R. Knee instability: isolated and complex. **British Journal of Sports Medicine**, British Association of Sport and Excercise Medicine, v. 34, n. 5, p. 395–400, 2000.

KANAMORI, Akihiro; SAKANE, Masataka; ZEMINSKI, Jennifer; RUDY, Theodore W; WOO, Savio LY. In-situ force in the medial and lateral structures of intact and ACL-deficient knees. **Journal of orthopaedic science**, Elsevier, v. 5, n. 6, p. 567–571, 2000.

KAPANDJI, A.I. **Fisiologia articular: esquemas comentados de mecânica humana - Membro Inferior**. Fifth edition. [S.l.]: GUANABARA, 2000.

KUO, Chin-Hsing; DAI, Jian S.; YAN, Hong-Sen. Reconfiguration principles and strategies for reconfigurable mechanisms. In: 2009 ASME/IFToMM International Conference on Reconfigurable Mechanisms and Robots. [S.l.: s.n.], 2009.

LIPPERT, L. S. **Clinical Kinesiology and Anatomy**. [S.l.]: F.A. Davis, 2006.

LUBOWITZ, James; BERNARDINI, Brad; REID, John. Current Concepts Review: Comprehensive Physical Examination for Instability of the Knee. **The American journal of sports medicine**, v. 36, p. 577–94, Apr. 2008.

MARTINS, Daniel. **Análise cinemática hierárquica de robôs manipuladores**. 2002.

MEJIA RINCON, Leonardo. **Wrench capability of planar manipulators**. 2016.

MENEGHINI, Luan. Proposta de aprimoramento topológico e paramétrico do robô LAILA, 2020.

MORENO CONTRERAS, Gonzalo Guillermo. **A kinestatic model for the three-dimensional static analysis of long combination vehicles**. 2017.

MOZZI, Giulio. **Discorso matematico sopra il rotamento momentaneo dei corpi**. [S.l.]: nella stamperia di Donato Campo, 1763.

NARDINI, Fabrizio; BELVEDERE, Claudio; SANCISI, Nicola; CONCONI, Michele; LEARDINI, Alberto; DURANTE, Stefano; PARENTI-CASTELLI, Vincenzo. An Anatomical-Based Subject-Specific Model of In-Vivo Knee Joint 3D Kinematics From Medical Imaging. **Applied Sciences**, v. 10, n. 6, 2020.

NETTER, F. **Netter Atlas of Human Anatomy**. Sixth edition. [S.l.]: ELSEVIER, 2014.

NEUMANN, D.A. **Kinesiology of the Musculoskeletal System: Foundations for Rehabilitation**. [S.l.]: Mosby/Elsevier, 2010. (Volve learning system).

OTTOBONI, A.; PARENTI-CASTELLI, V.; SANCISI, N.; BELVEDERE, C.; LEARDINI, A. Articular surface approximation in equivalent spatial parallel mechanism models of the human knee joint: an experiment-based assessment. **Proceedings of the Institution of Mechanical Engineers, Part H: Journal of Engineering in Medicine**, SAGE Publications Sage UK: London, England, v. 224, n. 9, p. 1121–1132, 2010.

PARENTI-CASTELLI, Vincenzo; GREGORIO, R Di. Parallel mechanisms applied to the human knee passive motion simulation. In: ADVANCES in robot kinematics. [S.l.]: Springer, 2000. P. 333–344.

PARENTI-CASTELLI, Vincenzo; LEARDINI, Alberto; DI GREGORIO, Raffaele; O'CONNOR, John J. On the modeling of passive motion of the human knee joint by

means of equivalent planar and spatial parallel mechanisms. **Autonomous Robots**, Springer, v. 16, n. 2, p. 219–232, 2004.

PARENTI-CASTELLI, Vincenzo; SANCISI, Nicola. Synthesis of spatial mechanisms to model human joints. In: 21ST century kinematics. [S.l.]: Springer, 2013. P. 49–84.

PONCE SALDIAS, Daniel Alejandro. **Modeling the human knee joint to support preoperative planning, in portuguese: Modelagem da articulação do joelho humano visando apoio ao planejamento pré-operatório**. 2014. PhD thesis – Universidade Federal de Santa Catarina.

RESHETOV, Leonid Nikolaevich. **Self-aligning mechanisms**. [S.l.]: Moscow: MIR, 1979.

ROSSI, R.; DETTONI, F.; BRUZZONE, M.; U., Cottino; G., D'Elicio D.; BONASIA, D. E. Clinical examination of the knee: know your tools for diagnosis of knee injuries. **Sports medicine, arthroscopy, rehabilitation, therapy technology**, v. 3, p. 25, Oct. 2011.

SANCISI, N; ZANNOLI, D; PARENTI-CASTELLI, V; BELVEDERE, C; LEARDINI, A. A one-degree-of-freedom spherical mechanism for human knee joint modelling. **Proceedings of the Institution of Mechanical Engineers, Part H: Journal of Engineering in Medicine**, SAGE Publications Sage UK: London, England, v. 225, n. 8, p. 725–735, 2011.

SANCISI, Nicola; PARENTI-CASTELLI, Vincenzo. A sequentially-defined stiffness model of the knee. **Mechanism and Machine Theory**, v. 46, n. 12, p. 1920–1928, 2011.

SIMAS, Henrique. **Planejamento de trajetórias e evitamento de colisão em tarefas de manipuladores redundantes operando em ambientes confinados**. 2008.

SOBOTTA, J.; PUTZ, R.; PABST, R.; PUTZ, R. **Atlas of human anatomy**. [S.l.]: Urban & Fischer, 2006. (Atlas of human anatomy, v. 2).

STANDRING, Susan *et al.* **Gray's Anatomy: The Anatomical Basis of Clinical Practice**. 41. ed. [S.l.]: Elsevier Limited, 2016. (Gray's Anatomy Series).

TSAI, Lung-Wen. **Mechanism design: enumeration of kinematic structures according to function**. [S.l.]: CRC press, 2001.

TSAI, Lung-Wen. **Robot analysis: the mechanics of serial and parallel manipulators**. [S.l.]: John Wiley & Sons, 1999.

WEIHMANN, Lucas. **Modelagem e otimização de forças e torques aplicados por robôs com redundância cinemática e de atuação em contato com o meio**. 2011.

WILSON, D. R.; FEIKES, J. D.; O'CONNOR, J. J. Ligaments and articular contact guide passive knee flexion. **Journal of biomechanics**, Elsevier, v. 31, n. 12, p. 1127–1136, 1998.

WILSON, DR; O'CONNOR, JJ. A three-dimensional geometric model of the knee for the study of joint forces in gait. **Gait & posture**, Elsevier, v. 5, n. 2, p. 108–115, 1997.

WOO, Savio LY; FOX, Ross J; SAKANE, Masataka; LIVESAY, Glen A; RUDY, Theodore W; FU, Freddie H. Biomechanics of the ACL: measurements of in situ force in the ACL and knee kinematics. **The Knee**, Elsevier, v. 5, n. 4, p. 267–288, 1998.

WU, Ge; CAVANAGH, Peter R. ISB recommendations for standardization in the reporting of kinematic data. **Journal of Biomechanics**, v. 28, n. 10, p. 1257–1261, 1995.

Appendix

APPENDIX A – POSITION VECTORS

This appendix presents the position vectors and the links' vectors of each mechanism in millimeters.

To guide the analysis. the following nomenclatures have been defined:

- j = joint;

- l = link;

- $\$_{0_j}$ = position vector;

- H_l = link length;

- θ = flexion angle;

- di_j = initial position of the joints;

- d_j = displacement of the joint;

- L_j = final length or position of the joint;

- θ_j = position angle of revolute joints;

- μ = angle of the vector that connects C_1 to A_2 in the plane Y-Z.

A.1   POSITION VECTORS - MECHANISM $0° - 30°$

The origin of the platform representing the tibia. and the platform representing the femur in millimeters [mm]:

$$O_t = \begin{bmatrix} 0.00 \\ 0.00 \\ 0.00 \end{bmatrix} \quad O_{f_i} = \begin{bmatrix} 4.00 \\ 20.35 \\ 2.32 \end{bmatrix}$$

The position vector of each link of the mechanism 0°-30°:

$$H_1 = \begin{bmatrix} 0.00 \\ 0.00 \\ 27.50 \end{bmatrix} \quad H_2 = \begin{bmatrix} 0.00 \\ 45.30 \\ 0.00 \end{bmatrix} \quad H_3 = \begin{bmatrix} 0.90 \\ 0.00 \\ 0.00 \end{bmatrix} \quad H_4 = \begin{bmatrix} -10.10 \\ 12.50 \\ -5.20 \end{bmatrix} \quad H_5 = \begin{bmatrix} 0.00 \\ 16.10 \\ -14.40 \end{bmatrix}$$

$$H_6 = \begin{bmatrix} 1.15 \\ 30.10 \\ 0.00 \end{bmatrix} \quad H_7 = \begin{bmatrix} 0.00 \\ 0.00 \\ 0.00 \end{bmatrix} \quad H_8 = \begin{bmatrix} 0.00 \\ 0.00 \\ 0.00 \end{bmatrix} \quad H_9 = \begin{bmatrix} 0.00 \\ 0.00 \\ 23.10 \end{bmatrix} \quad H_{10} = \begin{bmatrix} 0.00 \\ 32.00 \\ 0.00 \end{bmatrix}$$

$$
\mathrm{H}_{11} = \begin{bmatrix} -1.30 \\ 0.00 \\ 0.00 \end{bmatrix} \quad
\mathrm{H}_{12} = \begin{bmatrix} 0.00 \\ 0.00 \\ 0.00 \end{bmatrix} \quad
\mathrm{H}_{13} = \begin{bmatrix} 0.00 \\ 0.00 \\ 0.00 \end{bmatrix} \quad
\mathrm{H}_{14} = \begin{bmatrix} 0.00 \\ 117.90 \\ 0.00 \end{bmatrix} \quad
\mathrm{H}_{15} = \begin{bmatrix} 41.80 \\ 0.00 \\ 0.00 \end{bmatrix}
$$

Initial position of prismatic joints:

$$
\mathrm{di}_{A1} = \begin{bmatrix} 0.00 \\ 0.00 \\ 0.00 \end{bmatrix} \quad
\mathrm{di}_{A3} = \begin{bmatrix} 0.00 \\ 5.00 \\ 0.00 \end{bmatrix} \quad
\mathrm{di}_{P2} = \begin{bmatrix} 0.00 \\ 5.00 \\ 0.00 \end{bmatrix} \quad
\mathrm{di}_{P3} = \begin{bmatrix} 0.00 \\ 0.00 \\ 0.00 \end{bmatrix} \quad
\mathrm{di}_{L2} = \begin{bmatrix} 0.00 \\ 5.00 \\ 0.00 \end{bmatrix}
$$

$$
\mathrm{di}_{L3} = \begin{bmatrix} 0.00 \\ 0.00 \\ 0.00 \end{bmatrix} \quad
\mathrm{di}_{M2} = \begin{bmatrix} 0.00 \\ 5.00 \\ 0.00 \end{bmatrix} \quad
\mathrm{di}_{M3} = \begin{bmatrix} 0.00 \\ 0.00 \\ 0.00 \end{bmatrix} \quad
\mathrm{di}_{C2} = \begin{bmatrix} 0.00 \\ 0.00 \\ 0.00 \end{bmatrix}
$$

Joints position vectors:

$$
\$_{0_{A3}} = \begin{bmatrix} 4.90 \\ -5.75 \\ 15.12 \end{bmatrix}
$$

$$
\mathrm{d}_{A3} = \begin{bmatrix} 0.00 \\ 7.75 - 7.75 \cdot \sin(\mu - \theta) \\ 0.00 \end{bmatrix} \quad
\mathrm{L}_{A3} = \begin{bmatrix} 0.00 \\ 12.75 - 7.75 \cdot \sin(\mu - \theta) \\ 0.00 \end{bmatrix}
$$

$$
\$_{0_{A2}} = \begin{bmatrix} 4.90 \\ 23.10 - 7.75 \cdot \sin(\mu - \theta) \\ 0.72 \end{bmatrix}
$$

$$
\$_{0_{A1}} = \begin{bmatrix} -5.20 \\ 23.10 - 7.75 \cdot \sin(\mu - \theta) - 5.2 \cdot \sin(\theta) + 12.50 \cdot \cos(\theta) \\ 0.72 - 12.50 \cdot \sin(\theta) - 5.20 \cdot \cos(\theta) \end{bmatrix}
$$

$$
\$_{0_{C4}} = \begin{bmatrix} 1.35 \\ -7.00 \\ -0.13 \end{bmatrix} \quad
\$_{0_{C3}} = \begin{bmatrix} 1.35 \\ -7.00 \\ -0.13 \end{bmatrix} \quad
\$_{0_{C2}} = \begin{bmatrix} 1.35 \\ -7.00 \\ 0.77 \end{bmatrix}
$$

$$
\mathrm{d}_{L3} = \begin{bmatrix} 0.00 \\ 0.00 \\ 0.05 - 7.75 \cdot \cos(\mu - \theta) \end{bmatrix} \quad
\mathrm{L}_{C2} = \begin{bmatrix} 0.00 \\ 0.00 \\ 0.05 - 7.75 \cdot \cos(\mu - \theta) \end{bmatrix}
$$

$$
\$_{0_{C1}} = \begin{bmatrix} 2.50 \\ 23.10 \\ 0.82 - 7.75 \cdot \cos(\mu - \theta) \end{bmatrix}
$$

$$\$0_{L4} = \begin{bmatrix} -33.10 \\ -27.65 \\ -21.98 \end{bmatrix} \quad \$0_{L3} = \begin{bmatrix} -32.20 \\ -27.65 \\ 21.98 \end{bmatrix}$$

$$\$0_{L2} = \begin{bmatrix} -32.20 \\ -27.65 + 45.3 \cdot \cos(\theta_{L4} - \pi/2) \\ -21.98 + 45.3 \cdot \sin(\theta_{L4} - \pi/2) \end{bmatrix}$$

$$\$0_{L1} = \begin{bmatrix} -32.20 \\ 23.10 + 4.75 \cdot \sin(\theta) - 0.45 \cdot \cos(\theta) \\ 0.82 - 7.75 \cdot \cos(\mu - \theta) + 0.45 \cdot \sin(\theta) + 4.75 \cdot \cos(\theta) \end{bmatrix}$$

$$\$0_{P5} = \begin{bmatrix} 7.50 \\ -17.75 \\ -23.48 \end{bmatrix} \quad \$0_{P4} = \begin{bmatrix} 7.50 \\ -17.75 \\ -23.48 \end{bmatrix} \quad \$0_{P3} = \begin{bmatrix} 6.20 \\ -17.75 \\ -23.48 \end{bmatrix}$$

$$\$0_{P2} = \begin{bmatrix} 6.20 \\ -17.75 + 32 \cdot \cos(\theta_{P5} - \pi/2) \\ -23.48 + 32 \cdot \sin(\theta_{P5} - \pi/2) \end{bmatrix}$$

$$\$0_{P1} = \begin{bmatrix} 6.20 \\ 23.10 - 1.15 \cdot \sin(\theta) - 3.85 \cdot \cos(\theta) \\ 0.82 - 7.75 \cdot \cos(\mu - \theta) + 3.85 \cdot \sin(\theta) - 1.15 \cdot \cos(\theta) \end{bmatrix}$$

$$\$0_{M4} = \begin{bmatrix} 9.80 \\ -96.75 \\ 4.42 \end{bmatrix} \quad \$0_{M3} = \begin{bmatrix} 51.60 \\ -96.75 \\ 4.42 \end{bmatrix}$$

$$\$0_{M2} = \begin{bmatrix} 51.60 \\ -96.75 + 117.90 \cdot \cos(\theta_{M4} - \pi/2) \\ 4.42 + 117.90 \cdot \sin(\theta_{M4} - \pi/2) \end{bmatrix}$$

$$\$0_{M1} = \begin{bmatrix} 51.60 \\ 23.10 + 4.25 \cdot \sin(\theta) + 3.05 \cdot \cos(\theta) \\ 0.82 - 7.75 \cdot \cos(\mu - \theta) - 3.05 \cdot \sin(\theta) + 4.25 \cdot \cos(\theta) \end{bmatrix}$$

A.2 POSITION VECTORS - MECHANISM $30° - 40°$

The only change from the mechanism $0° - 30°$ to the mechanism $30° - 40°$ is that the serial chain representing the PCL ligament have 4 joints instead of 5. The vector of each link of the mechanism $0° - 30°$:

$$H_1 = \begin{bmatrix} 0.00 \\ 0.00 \\ 27.50 \end{bmatrix} \quad H_2 = \begin{bmatrix} 0.00 \\ 45.30 \\ 0.00 \end{bmatrix} \quad H_3 = \begin{bmatrix} 0.90 \\ 0.00 \\ 0.00 \end{bmatrix} \quad H_4 = \begin{bmatrix} -10.10 \\ 12.50 \\ -5.20 \end{bmatrix} \quad H_5 = \begin{bmatrix} 0.00 \\ 16.10 \\ -14.40 \end{bmatrix}$$

$$H_6 = \begin{bmatrix} 1.15 \\ 30.10 \\ 0.00 \end{bmatrix} \quad H_7 = \begin{bmatrix} 0.00 \\ 0.00 \\ 0.00 \end{bmatrix} \quad H_8 = \begin{bmatrix} 0.00 \\ 0.00 \\ 0.00 \end{bmatrix} \quad H_9 = \begin{bmatrix} 0.00 \\ 0.00 \\ 23.10 \end{bmatrix} \quad H_{10} = \begin{bmatrix} 0.00 \\ 32.00 \\ 0.00 \end{bmatrix}$$

$$H_{11} = \begin{bmatrix} -1.30 \\ 0.00 \\ 0.00 \end{bmatrix} \quad H_{12} = \begin{bmatrix} 0.00 \\ 0.00 \\ 0.00 \end{bmatrix} \quad H_{13} = \begin{bmatrix} 0.00 \\ 117.90 \\ 0.00 \end{bmatrix} \quad H_{14} = \begin{bmatrix} 41.80 \\ 0.00 \\ 0.00 \end{bmatrix}$$

Initial position of prismatic joints:

$$di_{A1} = \begin{bmatrix} 0.00 \\ 0.00 \\ 0.00 \end{bmatrix} \quad di_{A3} = \begin{bmatrix} 0.00 \\ 5.00 \\ 0.00 \end{bmatrix} \quad di_{P2} = \begin{bmatrix} 0.00 \\ 5.00 \\ 0.00 \end{bmatrix} \quad di_{P3} = \begin{bmatrix} 0.00 \\ 0.00 \\ 0.00 \end{bmatrix} \quad di_{L2} = \begin{bmatrix} 0.00 \\ 5.00 \\ 0.00 \end{bmatrix}$$

$$di_{L3} = \begin{bmatrix} 0.00 \\ 0.00 \\ 0.00 \end{bmatrix} \quad di_{M2} = \begin{bmatrix} 0.00 \\ 5.00 \\ 0.00 \end{bmatrix} \quad di_{M3} = \begin{bmatrix} 0.00 \\ 0.00 \\ 0.00 \end{bmatrix} \quad di_{C2} = \begin{bmatrix} 0.00 \\ 0.00 \\ 0.00 \end{bmatrix}$$

Joints position vectors:

$$\$_{0A3} = \begin{bmatrix} 4.90 \\ -5.75 \\ 15.12 \end{bmatrix}$$

$$d_{A3} = \begin{bmatrix} 0.00 \\ 7.75 - 7.75 \cdot \sin(\mu - \theta) \\ 0.00 \end{bmatrix} \quad L_{A3} = \begin{bmatrix} 0.00 \\ 12.75 - 7.75 \cdot \sin(\mu - \theta) \\ 0.00 \end{bmatrix}$$

$$\$_{0A2} = \begin{bmatrix} 4.90 \\ 23.10 - 7.75 \cdot \sin(\mu - \theta) \\ 0.72 \end{bmatrix}$$

$$\$_{0A1} = \begin{bmatrix} -5.20 \\ 23.10 - 7.75 \cdot \sin(\mu - \theta) - 5.2 \cdot \sin(\theta) + 12.50 \cdot \cos(\theta) \\ 0.72 - 12.50 \cdot \sin(\theta) - 5.20 \cdot \cos(\theta) \end{bmatrix}$$

$$\$_{0C4} = \begin{bmatrix} 1.35 \\ -7.00 \\ -0.13 \end{bmatrix} \quad \$_{0C3} = \begin{bmatrix} 1.35 \\ -7.00 \\ -0.13 \end{bmatrix} \quad \$_{0C2} = \begin{bmatrix} 1.35 \\ -7.00 \\ 0.77 \end{bmatrix}$$

$$
d_{L3} = \begin{bmatrix} 0.00 \\ 0.00 \\ 0.05 - 7.75 \cdot \cos(\mu - \theta) \end{bmatrix} \quad L_{C2} = \begin{bmatrix} 0.00 \\ 0.00 \\ 0.05 - 7.75 \cdot \cos(\mu - \theta) \end{bmatrix}
$$

$$
\$_{0_{C1}} = \begin{bmatrix} 2.50 \\ 23.10 \\ 0.82 - 7.75 \cdot \cos(\mu - \theta) \end{bmatrix}
$$

$$
\$_{0_{L4}} = \begin{bmatrix} -33.10 \\ -27.65 \\ -21.98 \end{bmatrix} \quad \$_{0_{L3}} = \begin{bmatrix} -32.20 \\ -27.65 \\ 21.98 \end{bmatrix}
$$

$$
\$_{0_{L2}} = \begin{bmatrix} -32.20 \\ -27.65 + 45.3 \cdot \cos(\theta_{L4} - \pi/2) \\ -21.98 + 45.3 \cdot \sin(\theta_{L4} - \pi/2) \end{bmatrix}
$$

$$
\$_{0_{L1}} = \begin{bmatrix} -32.20 \\ 23.10 + 4.75 \cdot \sin(\theta) - 0.45 \cdot \cos(\theta) \\ 0.82 - 7.75 \cdot \cos(\mu - \theta) + 0.45 \cdot \sin(\theta) + 4.75 \cdot \cos(\theta) \end{bmatrix}
$$

$$
\$_{0_{P4}} = \begin{bmatrix} 7.50 \\ -17.75 \\ -23.48 \end{bmatrix} \quad \$_{0_{P3}} = \begin{bmatrix} 6.20 \\ -17.75 \\ -23.48 \end{bmatrix}
$$

$$
\$_{0_{P2}} = \begin{bmatrix} 6.20 \\ -17.75 + 32 \cdot \cos(\theta_{P5} - \pi/2) \\ -23.48 + 32 \cdot \sin(\theta_{P5} - \pi/2) \end{bmatrix}
$$

$$
\$_{0_{P1}} = \begin{bmatrix} 6.20 \\ 23.10 - 1.15 \cdot \sin(\theta) - 3.85 \cdot \cos(\theta) \\ 0.82 - 7.75 \cdot \cos(\mu - \theta) + 3.85 \cdot \sin(\theta) - 1.15 \cdot \cos(\theta) \end{bmatrix}
$$

$$
\$_{0_{M4}} = \begin{bmatrix} 9.80 \\ -96.75 \\ 4.42 \end{bmatrix} \quad \$_{0_{M3}} = \begin{bmatrix} 51.60 \\ -96.75 \\ 4.42 \end{bmatrix}
$$

$$
\$_{0_{M2}} = \begin{bmatrix} 51.60 \\ -96.75 + 117.90 \cdot \cos(\theta_{M4} - \pi/2) \\ 4.42 + 117.90 \cdot \sin(\theta_{M4} - \pi/2) \end{bmatrix}
$$

$$
\$_{0_{M1}} = \begin{bmatrix} 51.60 \\ 23.10 + 4.25 \cdot \sin(\theta) + 3.05 \cdot \cos(\theta) \\ 0.82 - 7.75 \cdot \cos(\mu - \theta) - 3.05 \cdot \sin(\theta) + 4.25 \cdot \cos(\theta) \end{bmatrix}
$$

A.3 POSITION VECTORS - MECHANISM $40° - 60°$

The vector of each link of the mechanism $40°$-$60°$:

$$H_1 = \begin{bmatrix} 0.00 \\ 0.00 \\ 27.50 \end{bmatrix} \quad H_2 = \begin{bmatrix} 0.00 \\ 45.30 \\ 0.00 \end{bmatrix} \quad H_3 = \begin{bmatrix} 0.90 \\ 0.00 \\ 0.00 \end{bmatrix} \quad H_4 = \begin{bmatrix} -10.10 \\ 12.50 \\ -5.20 \end{bmatrix} \quad H_5 = \begin{bmatrix} 0.00 \\ 16.10 \\ -14.40 \end{bmatrix}$$

$$H_6 = \begin{bmatrix} 1.15 \\ 30.10 \\ 0.00 \end{bmatrix} \quad H_7 = \begin{bmatrix} 0.00 \\ 0.00 \\ 0.00 \end{bmatrix} \quad H_8 = \begin{bmatrix} 0.00 \\ 0.00 \\ 0.00 \end{bmatrix} \quad H_9 = \begin{bmatrix} 0.00 \\ 0.00 \\ 23.10 \end{bmatrix} \quad H_{10} = \begin{bmatrix} 0.00 \\ 32.00 \\ 0.00 \end{bmatrix}$$

$$H_{11} = \begin{bmatrix} -1.30 \\ 0.00 \\ 0.00 \end{bmatrix} \quad H_{12} = \begin{bmatrix} 0.00 \\ 0.00 \\ 0.00 \end{bmatrix} \quad H_{13} = \begin{bmatrix} 0.00 \\ 117.90 \\ 0.00 \end{bmatrix} \quad H_{14} = \begin{bmatrix} 41.80 \\ 0.00 \\ 0.00 \end{bmatrix}$$

Initial position of prismatic joints:

$$di_{A1} = \begin{bmatrix} 0.00 \\ 0.00 \\ 0.00 \end{bmatrix} \quad di_{A3} = \begin{bmatrix} 0.00 \\ 5.00 \\ 0.00 \end{bmatrix} \quad di_{P2} = \begin{bmatrix} 0.00 \\ 5.00 \\ 0.00 \end{bmatrix} \quad di_{P3} = \begin{bmatrix} 0.00 \\ 0.00 \\ 0.00 \end{bmatrix} \quad di_{L2} = \begin{bmatrix} 0.00 \\ 5.00 \\ 0.00 \end{bmatrix}$$

$$di_{L3} = \begin{bmatrix} 0.00 \\ 0.00 \\ 0.00 \end{bmatrix} \quad di_{M2} = \begin{bmatrix} 0.00 \\ 5.00 \\ 0.00 \end{bmatrix} \quad di_{M3} = \begin{bmatrix} 0.00 \\ 0.00 \\ 0.00 \end{bmatrix} \quad di_{C2} = \begin{bmatrix} 0.00 \\ 0.00 \\ 0.00 \end{bmatrix}$$

Joints position vectors:

$$\$_{0A3} = \begin{bmatrix} 4.90 \\ -5.75 \\ 15.12 \end{bmatrix}$$

$$d_{A3} = \begin{bmatrix} 0.00 \\ 7.75 - 7.75 \cdot \sin(\mu - \theta) \\ 0.00 \end{bmatrix} \quad L_{A3} = \begin{bmatrix} 0.00 \\ 12.75 - 7.75 \cdot \sin(\mu - \theta) \\ 0.00 \end{bmatrix}$$

$$\$_{0A2} = \begin{bmatrix} 4.90 \\ 23.10 - 7.75 \cdot \sin(\mu - \theta) \\ 0.72 \end{bmatrix}$$

$$\$_{0_{A1}} = \begin{bmatrix} -5.20 \\ 23.10 - 7.75 \cdot \sin(\mu - \theta) - 5.2 \cdot \sin(\theta) + 12.50 \cdot \cos(\theta) \\ 0.72 - 12.50 \cdot \sin(\theta) - 5.20 \cdot \cos(\theta) \end{bmatrix}$$

$$\$_{0_{C4}} = \begin{bmatrix} 1.35 \\ -7.00 \\ -0.13 \end{bmatrix} \quad \$_{0_{C3}} = \begin{bmatrix} 1.35 \\ -7.00 \\ -0.13 \end{bmatrix} \quad \$_{0_{C2}} = \begin{bmatrix} 1.35 \\ -7.00 \\ 0.77 \end{bmatrix}$$

$$L_{C2} = \begin{bmatrix} 0.00 \\ 0.00 \\ 0.05 - 7.75 \cdot \cos(\mu - \theta) \end{bmatrix} \quad \$_{0_{C1}} = \begin{bmatrix} 2.50 \\ 23.10 \\ 0.82 - 7.75 \cdot \cos(\mu - \theta) \end{bmatrix}$$

$$\$_{0_{L1}} = \begin{bmatrix} -32.2 \\ 23.10 + 4.75 \cdot \sin(\theta) - 0.45 \cdot \cos(theta) \\ 0.82 - 7.75 \cdot \cos(\mu - \theta) + 0.45 \cdot \sin(\theta) + 4.75 \cdot \cos(\theta) \end{bmatrix}$$

$$\begin{cases} \theta_{L1_{40-60}} = \theta_{L1_{30-40}} + \theta - 40° \\ \theta_{L4_{40-60}} = \theta_{L4_{30-40}}(40°) \\ (H_1 + dL_2) \cdot \sin(\theta_{L1_{30-40}}) + (H_2 + dL_3) \cdot \sin(\theta_{L4_{30-40}}) = 54.73 \\ (H_1 + dL_2) \cdot \cos(\theta_{L1_{30-40}}) + (H_2 + dL_3) \cdot \cos(\theta_{L4_{30-40}}) = 18.78 \end{cases}$$

$$R_{x_{L4_{40-60}}} = \begin{bmatrix} 1 & 0 & 0 \\ 0 & \cos(\frac{\pi}{2} - \theta_{L4_{40-60}}) & \sin(\frac{\pi}{2} - \theta_{L4_{40-60}}) \\ 0 & -\sin(\frac{\pi}{2} - \theta_{L4_{40-60}}) & \cos(\frac{\pi}{2} - \theta_{L4_{40-60}}) \end{bmatrix}$$

$$\$_{0_{L4}} = \begin{bmatrix} -33.10 \\ -27.65 \\ -21.98 \end{bmatrix}$$

$$\$_{0_{L3}} = \$_{0_{L4}} + R_{x_{L4_{40-60}}} \cdot H_3$$

$$\$_{0_{L2}} = \$_{0_{L3}} + R_{x_{L4_{40-60}}} \cdot (H_2 + dL_3)$$

$$\$_{0_{P4}} = \begin{bmatrix} 7.50 \\ -17.75 \\ -23.48 \end{bmatrix}$$

$$\$_{0_{P3}} = \begin{bmatrix} 6.20 \\ -17.75 \\ -23.48 \end{bmatrix} \quad \$_{0_{P2}} = \begin{bmatrix} 6.20 \\ -17.75 + 32 \cdot \cos(\pi/2 - \theta_{P4_{40-60}}) \\ -23.48 - 32 \cdot \sin(\pi/2 - \theta_{P4_{40-60}}) \end{bmatrix}$$

$$\$0_{P1} = \begin{bmatrix} 6.20 \\ -1.15 \cdot \sin(\theta) - 3.85 \cdot \cos(\theta) + 23.10 \\ 3.85 \cdot \sin(\theta) - 1.15 \cdot \cos(\theta) + 0.82 - 7.75 \cdot \cos(\mu - \theta) \end{bmatrix}$$

$$\$0_{M1} = \begin{bmatrix} -32.2 \\ 23.10 + 4.25 \cdot \sin(\theta) + 3.05 \cdot \cos(theta) \\ 0.82 - 7.75 \cdot \cos(\mu - \theta) - 3.05 \cdot \sin(\theta) + 4.25 \cdot \cos(\theta) \end{bmatrix}$$

$$\begin{cases} \theta_{M1_{40-60}} = \theta_{M1_{30-40}} + \theta - 40° \\ \theta_{M4_{40-60}} = \theta_{M4_{30-40}}(40°) \\ (H_1 2 + dM_2) \cdot \sin(\theta_{M1_{30-40}}) + (H_1 3 + dM_3) \cdot \sin(\theta_{M4_{30-40}}) = 125.14 \\ (H_1 2 + dM_2) \cdot \cos(\theta_{M1_{30-40}}) + (H_1 3 + dM_3) \cdot \cos(\theta_{M4_{30-40}}) = -10.90 \end{cases}$$

$$R_{x_{M4_{40-60}}} = \begin{bmatrix} 1 & 0 & 0 \\ 0 & \cos(\pi/2 - \theta_{M4_{40-60}}) & \sin(\pi/2 - \theta_{M4_{40-60}}) \\ 0 & -\sin(\pi/2 - \theta_{M4_{40-60}}) & \cos(\pi/2 - \theta_{M4_{40-60}}) \end{bmatrix}$$

$$\$0_{M4} = \begin{bmatrix} 9.80 \\ -96.75 \\ 4.42 \end{bmatrix}$$

$$\$0_{M3} = \$0_{M4} + R_{x_{M4_{40-60}}} \cdot H_{14}$$

$$\$0_{M2} = \$0_{M3} + R_{x_{M4_{40-60}}} \cdot (H_{13} + dM_3)$$

A.4   POSITION VECTORS - MECHANISM $60° - 90°$

The vector of each link of the mechanism $60°$-$90°$:

$$H_1 = \begin{bmatrix} 0.00 \\ 0.00 \\ 27.50 \end{bmatrix} \quad H_2 = \begin{bmatrix} 0.00 \\ 45.30 \\ 0.00 \end{bmatrix} \quad H_3 = \begin{bmatrix} 0.90 \\ 0.00 \\ 0.00 \end{bmatrix} \quad H_4 = \begin{bmatrix} -10.10 \\ 12.50 \\ -5.20 \end{bmatrix} \quad H_5 = \begin{bmatrix} 0.00 \\ 16.10 \\ -14.40 \end{bmatrix}$$

$$H_6 = \begin{bmatrix} 0.00 \\ 0.00 \\ 0.00 \end{bmatrix} \quad H_7 = \begin{bmatrix} 1.15 \\ 30.10 \\ 0.00 \end{bmatrix} \quad H_8 = \begin{bmatrix} 0.00 \\ 0.00 \\ 0.00 \end{bmatrix} \quad H_9 = \begin{bmatrix} 0.00 \\ 0.00 \\ 0.00 \end{bmatrix} \quad H_{10} = \begin{bmatrix} 0.00 \\ 0.00 \\ 23.10 \end{bmatrix}$$

$$H_{11} = \begin{bmatrix} 0.00 \\ 32.00 \\ 0.00 \end{bmatrix} \quad H_{12} = \begin{bmatrix} -1.30 \\ 0.00 \\ 0.00 \end{bmatrix} \quad H_{13} = \begin{bmatrix} 0.00 \\ 0.00 \\ 0.00 \end{bmatrix} \quad H_{14} = \begin{bmatrix} 0.00 \\ 117.90 \\ 0.00 \end{bmatrix} \quad H_{15} = \begin{bmatrix} 41.80 \\ 0.00 \\ 0.00 \end{bmatrix}$$

Initial position of prismatic joints:

$$
\mathrm{di_{A1}} = \begin{bmatrix} 0.00 \\ 0.00 \\ 0.00 \end{bmatrix} \quad
\mathrm{di_{A3}} = \begin{bmatrix} 0.00 \\ 5.00 \\ 0.00 \end{bmatrix} \quad
\mathrm{di_{P2}} = \begin{bmatrix} 0.00 \\ 5.00 \\ 0.00 \end{bmatrix} \quad
\mathrm{di_{P3}} = \begin{bmatrix} 0.00 \\ 0.00 \\ 0.00 \end{bmatrix} \quad
\mathrm{di_{L2}} = \begin{bmatrix} 0.00 \\ 5.00 \\ 0.00 \end{bmatrix}
$$

$$
\mathrm{di_{L3}} = \begin{bmatrix} 0.00 \\ 0.00 \\ 0.00 \end{bmatrix} \quad
\mathrm{di_{M2}} = \begin{bmatrix} 0.00 \\ 5.00 \\ 0.00 \end{bmatrix} \quad
\mathrm{di_{M3}} = \begin{bmatrix} 0.00 \\ 0.00 \\ 0.00 \end{bmatrix} \quad
\mathrm{di_{C2}} = \begin{bmatrix} 0.00 \\ 0.00 \\ 0.00 \end{bmatrix}
$$

Joints position vectors:

$$
\$_{0_{A4}} = \begin{bmatrix} 4.90 \\ -5.75 \\ 15.12 \end{bmatrix} \quad
\$_{0_{A3}} = \begin{bmatrix} 4.90 \\ -5.75 \\ 15.12 \end{bmatrix}
$$

$$
\mathrm{d_{A3}} = \begin{bmatrix} 0.00 \\ 7.75 - 7.75 \cdot \sin(\mu - \theta) \\ 0.00 \end{bmatrix} \quad
\mathrm{L_{A3}} = \begin{bmatrix} 0.00 \\ 12.75 - 7.75 \cdot \sin(\mu - \theta) \\ 0.00 \end{bmatrix}
$$

$$
\$_{0_{A2}} = \begin{bmatrix} 4.90 \\ 23.10 - 7.75 \cdot \sin(\mu - \theta) \\ 0.72 \end{bmatrix}
$$

$$
\$_{0_{A1}} = \begin{bmatrix} -5.20 \\ 23.10 - 7.75 \cdot \sin(\mu - \theta) - 5.2 \cdot \sin(\theta) + 12.50 \cdot \cos(\theta) \\ 0.72 - 12.50 \cdot \sin(\theta) - 5.20 \cdot \cos(\theta) \end{bmatrix}
$$

$$
\$_{0_{C4}} = \begin{bmatrix} 1.35 \\ -7.00 \\ -0.13 \end{bmatrix} \quad
\$_{0_{C3}} = \begin{bmatrix} 1.35 \\ -7.00 \\ -0.13 \end{bmatrix} \quad
\$_{0_{C2}} = \begin{bmatrix} 1.35 \\ -7.00 \\ 0.77 \end{bmatrix}
$$

$$
\mathrm{L_{C2}} = \begin{bmatrix} 0.00 \\ 0.00 \\ 0.05 - 7.75 \cdot \cos(\mu - \theta) \end{bmatrix} \quad
\$_{0_{C1}} = \begin{bmatrix} 2.50 \\ 23.10 \\ 0.82 - 7.75 \cdot \cos(\mu - \theta) \end{bmatrix}
$$

$$
\$_{0_{L1}} = \begin{bmatrix} -32.2 \\ 23.10 + 4.75 \cdot \sin(\theta) - 0.45 \cdot \cos(\mathrm{theta}) \\ 0.82 - 7.75 \cdot \cos(\mu - \theta) + 0.45 \cdot \sin(\theta) + 4.75 \cdot \cos(\theta) \end{bmatrix}
$$

$$
\begin{cases}
\theta_{L1_{60-90}} = \theta_{L1_{30-40}} + \theta - 40^\circ \\
\theta_{L4_{60-90}} = \theta_{L4_{30-40}}(40^\circ) \\
(H_1 + dL_2) \cdot \sin(\theta_{L1_{30-40}}) + (H_2 + dL_3) \cdot \sin(\theta_{L4_{30-40}}) = 54.73 \\
(H_1 + dL_2) \cdot \cos(\theta_{L1_{30-40}}) + (H_2 + dL_3) \cdot \cos(\theta_{L4_{30-40}}) = 18.78
\end{cases}
$$

$$R_{X_{L4_{60-90}}} = \begin{bmatrix} 1 & 0 & 0 \\ 0 & \cos(\frac{\pi}{2} - \theta_{L4_{60-90}}) & \sin(\frac{\pi}{2} - \theta_{L4_{60-90}}) \\ 0 & -\sin(\frac{\pi}{2} - \theta_{L4_{60-90}}) & \cos(\frac{\pi}{2} - \theta_{L4_{40-60}}) \end{bmatrix}$$

$$\$_{0_{L4}} = \begin{bmatrix} -33.10 \\ -27.65 \\ -21.98 \end{bmatrix}$$

$$\$_{0_{L3}} = \$_{0_{L4}} + R_{X_{L4_{40-60}}} \cdot H_3$$

$$\$_{0_{L2}} = \$_{0_{L3}} + R_{X_{L4_{40-60}}} \cdot (H_2 + dL_3)$$

$$\$_{0_{P4}} = \begin{bmatrix} 7.50 \\ -17.75 \\ -23.48 \end{bmatrix}$$

$$\$_{0_{P3}} = \begin{bmatrix} 6.20 \\ -17.75 \\ -23.48 \end{bmatrix} \quad \$_{0_{P2}} = \begin{bmatrix} 6.20 \\ -17.75 + 32 \cdot \cos(\pi/2 - \theta_{P4_{60-90}}) \\ -23.48 - 32 \cdot \sin(\pi/2 - \theta_{P4_{60-90}}) \end{bmatrix}$$

$$\$_{0_{P1}} = \begin{bmatrix} 6.20 \\ -1.15 \cdot \sin(\theta) - 3.85 \cdot \cos(\theta) + 23.10 \\ 3.85 \cdot \sin(\theta) - 1.15 \cdot \cos(\theta) + 0.82 - 7.75 \cdot \cos(\mu - \theta) \end{bmatrix}$$

$$\$_{0_{M1}} = \begin{bmatrix} -32.2 \\ 23.10 + 4.25 \cdot \sin(\theta) + 3.05 \cdot \cos(theta) \\ 0.82 - 7.75 \cdot \cos(\mu - \theta) - 3.05 \cdot \sin(\theta) + 4.25 \cdot \cos(\theta) \end{bmatrix}$$

$$\begin{cases} \theta_{M1_{60-90}} = \theta_{M1_{30-40}} + \theta - 40° \\ \theta_{M4_{60-90}} = \theta_{M4_{30-40}}(40°) \\ (H_13 + dM_2) \cdot \sin(\theta_{M1_{30-40}}) + (H_14 + dM_3) \cdot \sin(\theta_{M4_{30-40}}) = 125.14 \\ (H_13 + dM_2) \cdot \cos(\theta_{M1_{30-40}}) + (H_14 + dM_3) \cdot \cos(\theta_{M4_{30-40}}) = -10.90 \end{cases}$$

$$R_{X_{M4_{6090}}} = \begin{bmatrix} 1 & 0 & 0 \\ 0 & \cos(\pi/2 - \theta_{M4_{60-90}}) & \sin(\pi/2 - \theta_{M4_{60-90}}) \\ 0 & -\sin(\pi/2 - \theta_{M4_{60-90}}) & \cos(\pi/2 - \theta_{M4_{60-90}}) \end{bmatrix}$$

$$\$_{0_{M4}} = \begin{bmatrix} 9.80 \\ -96.75 \\ 4.42 \end{bmatrix}$$

$$\$_{0_{M3}} = \$_{0_{M4}} + R_{x_{M4_{60-90}}} \cdot H_{15}$$

$$\$_{0_{M2}} = \$_{0_{M3}} + R_{x_{M4_{60-90}}} \cdot (H_{14} + dM_3)$$

A.5 POSITION VECTORS - MECHANISM $90° - 120°$

The Mechanism $90° - 120°$, has the same position vectors than the Mechanism $60° - 90°$, except by some joints that were add or excluded.

The joint C_4 that exist on the mechanism $60° - 90°$ does not exist in the mechanism $90° - 120°$, as C_3 is positioned at the same spot than C_4, the insertion area is still the same.

The joints L_5, A_5, P_5 and M_5, are added at the same spot than L_4, A_4, P_4 and M_4, respectively. This joints are all revolute joints about the z-axis, they do not change the trajectory of the mechanism.

A.6 POSITION VECTORS - MECHANISM $120° - 140°$

The Mechanism $120° - 140°$, has the same position vectors than the Mechanism $90° - 120°$, except by some joints that were add or excluded.

The joints representing the MCL and the LCL ligaments are excluded from this mechanism, as the revolute joint about the y-axis of the representation of the ACL ligament.

APPENDIX B – WRENCHES

The unit vectors (eq. 41) represent the orientation of each constraint for a spatial workspace ($\lambda = 6$).

$$\$_x = \begin{bmatrix} 1 \\ 0 \\ 0 \end{bmatrix} \quad \$_y = \begin{bmatrix} 0 \\ 1 \\ 0 \end{bmatrix} \quad \$_z = \begin{bmatrix} 0 \\ 0 \\ 1 \end{bmatrix} \tag{41}$$

The unit vectors (eq. 42) represent the orientation of each constraint for a planar workspace Y-Z ($\lambda = 3$).

$$\$_y p = \begin{bmatrix} 1 \\ 0 \end{bmatrix} \quad \$_z p = \begin{bmatrix} 0 \\ 1 \end{bmatrix} \tag{42}$$

The wrenches representing axial forces are formed by the cross product of the position vector and the unit vector and the wrenches representing moments are the correspondent unit vector itself.

B.1   WRENCHES OF THE MECHANISM 0°-30°IN A SPATIAL WORKSPACE

$$\$^A_{L_{4_{Fx}}} = \begin{bmatrix} \$_{0_{L_4}} \times \$_x \\ \$_x \end{bmatrix} \quad \$^A_{L_{4_{Fy}}} = \begin{bmatrix} \$_{0_{L_4}} \times \$_y \\ \$_y \end{bmatrix} \quad \$^A_{L_{4_{Fz}}} = \begin{bmatrix} \$_{0_{L_4}} \times \$_z \\ \$_z \end{bmatrix}$$

$$\$^A_{L_{4_{My}}} = \begin{bmatrix} \$_y \\ 0 \\ 0 \\ 0 \end{bmatrix} \quad \$^A_{L_{4_{Mz}}} = \begin{bmatrix} \$_z \\ 0 \\ 0 \\ 0 \end{bmatrix}$$

$$\$^A_{A_{3_{Fy}}} = \begin{bmatrix} \$_{0_{A_3}} \times \$_y \\ \$_y \end{bmatrix} \quad \$^A_{A_{3_{Fz}}} = \begin{bmatrix} \$_{0_{A_3}} \times \$_z \\ \$_z \end{bmatrix} \quad \$^A_{A_{3_{Mx}}} = \begin{bmatrix} \$_x \\ 0 \\ 0 \\ 0 \end{bmatrix}$$

$$\$^A_{A_{3_{My}}} = \begin{bmatrix} \$_y \\ 0 \\ 0 \\ 0 \end{bmatrix} \quad \$^A_{A_{3_{Mz}}} = \begin{bmatrix} \$_z \\ 0 \\ 0 \\ 0 \end{bmatrix}$$

$$\$^A_{P_{5_{Fx}}} = \begin{bmatrix} \$_{0_{P_5}} \times \$_x \\ \$_x \end{bmatrix} \quad \$^A_{P_{5_{Fy}}} = \begin{bmatrix} \$_{0_{P_5}} \times \$_y \\ \$_y \end{bmatrix} \quad \$^A_{P_{5_{Fz}}} = \begin{bmatrix} \$_{0_{P_5}} \times \$_z \\ \$_z \end{bmatrix}$$

$$\$^A_{P_{5_{My}}} = \begin{bmatrix} \$_y \\ 0 \\ 0 \\ 0 \end{bmatrix} \quad \$^A_{P_{5_{Mz}}} = \begin{bmatrix} \$_z \\ 0 \\ 0 \\ 0 \end{bmatrix}$$

$$\$^A_{M_{4_{Fx}}} = \begin{bmatrix} \$0_{M_4} \times \$_x \\ \$_x \end{bmatrix} \quad \$^A_{M_{4_{Fy}}} = \begin{bmatrix} \$0_{M_4} \times \$_y \\ \$_y \end{bmatrix} \quad \$^A_{M_{4_{Fz}}} = \begin{bmatrix} \$0_{M_4} \times \$_z \\ \$_z \end{bmatrix}$$

$$\$^A_{M_{4_{My}}} = \begin{bmatrix} \$_y \\ 0 \\ 0 \\ 0 \end{bmatrix} \quad \$^A_{M_{4_{Mz}}} = \begin{bmatrix} \$_z \\ 0 \\ 0 \\ 0 \end{bmatrix}$$

$$\$^A_{L_{1_{Fx}}} = \begin{bmatrix} \$0_{L_1} \times \$_x \\ \$_x \end{bmatrix} \quad \$^A_{L_{1_{Fy}}} = \begin{bmatrix} \$0_{L_1} \times \$_y \\ \$_y \end{bmatrix} \quad \$^A_{L_{1_{Fz}}} = \begin{bmatrix} \$0_{L_1} \times \$_z \\ \$_z \end{bmatrix}$$

$$\$^A_{L_{1_{My}}} = \begin{bmatrix} \$_y \\ 0 \\ 0 \\ 0 \end{bmatrix} \quad \$^A_{L_{1_{Mz}}} = \begin{bmatrix} \$_z \\ 0 \\ 0 \\ 0 \end{bmatrix}$$

$$\$^A_{L_{2_{Fx}}} = \begin{bmatrix} \$0_{L_2} \times \$_x \\ \$_x \end{bmatrix} \quad \$^A_{L_{2_{Fz}}} = \begin{bmatrix} \$0_{L_2} \times \$_z \\ \$_z \end{bmatrix}$$

$$\$^A_{L_{2_{Mx}}} = \begin{bmatrix} \$_x \\ 0 \\ 0 \\ 0 \end{bmatrix} \quad \$^A_{L_{2_{My}}} = \begin{bmatrix} \$_y \\ 0 \\ 0 \\ 0 \end{bmatrix} \quad \$^A_{L_{2_{Mz}}} = \begin{bmatrix} \$_z \\ 0 \\ 0 \\ 0 \end{bmatrix}$$

$$\$^A_{L_{3_{Fy}}} = \begin{bmatrix} \$0_{L_3} \times \$_y \\ \$_y \end{bmatrix} \quad \$^A_{L_{3_{Fz}}} = \begin{bmatrix} \$0_{L_3} \times \$_z \\ \$_z \end{bmatrix}$$

$$\$^A_{L_{3_{Mx}}} = \begin{bmatrix} \$_x \\ 0 \\ 0 \\ 0 \end{bmatrix} \quad \$^A_{L_{3_{My}}} = \begin{bmatrix} \$_y \\ 0 \\ 0 \\ 0 \end{bmatrix} \quad \$^A_{L_{3_{Mz}}} = \begin{bmatrix} \$_z \\ 0 \\ 0 \\ 0 \end{bmatrix}$$

$$\$^A_{A_{1_{Fy}}} = \begin{bmatrix} \$0_{A_1} \times \$_y \\ \$_y \end{bmatrix} \quad \$^A_{A_{1_{Fz}}} = \begin{bmatrix} \$0_{A_1} \times \$_z \\ \$_z \end{bmatrix}$$

$$\$^A_{A_{1_{Mx}}} = \begin{bmatrix} \$_x \\ 0 \\ 0 \\ 0 \end{bmatrix} \quad \$^A_{A_{1_{My}}} = \begin{bmatrix} \$_y \\ 0 \\ 0 \\ 0 \end{bmatrix} \quad \$^A_{A_{1_{Mz}}} = \begin{bmatrix} \$_z \\ 0 \\ 0 \\ 0 \end{bmatrix}$$

$$\$^{A}_{A_{2_{Fx}}} = \begin{bmatrix} \$0_{A_2} \times \$_x \\ \$_x \end{bmatrix} \quad \$^{A}_{A_{2_{Fy}}} = \begin{bmatrix} \$0_{A_2} \times \$_y \\ \$_y \end{bmatrix} \quad \$^{A}_{A_{2_{Fz}}} = \begin{bmatrix} \$0_{A_2} \times \$_z \\ \$_z \end{bmatrix}$$

$$\$^{A}_{A_{2_{My}}} = \begin{bmatrix} \$_y \\ 0 \\ 0 \\ 0 \end{bmatrix} \quad \$^{A}_{A_{2_{Mz}}} = \begin{bmatrix} \$_z \\ 0 \\ 0 \\ 0 \end{bmatrix}$$

$$\$^{A}_{C_{1_{Fx}}} = \begin{bmatrix} \$0_{C_1} \times \$_x \\ \$_x \end{bmatrix} \quad \$^{A}_{C_{1_{Fy}}} = \begin{bmatrix} \$0_{C_1} \times \$_y \\ \$_y \end{bmatrix} \quad \$^{A}_{C_{1_{Fz}}} = \begin{bmatrix} \$0_{C_1} \times \$_z \\ \$_z \end{bmatrix}$$

$$\$^{A}_{C_{1_{My}}} = \begin{bmatrix} \$_y \\ 0 \\ 0 \\ 0 \end{bmatrix} \quad \$^{A}_{C_{1_{Mz}}} = \begin{bmatrix} \$_z \\ 0 \\ 0 \\ 0 \end{bmatrix}$$

$$\$^{A}_{C_{2_{Fx}}} = \begin{bmatrix} \$0_{C_2} \times \$_x \\ \$_x \end{bmatrix} \quad \$^{A}_{C_{2_{Fy}}} = \begin{bmatrix} \$0_{C_2} \times \$_y \\ \$_y \end{bmatrix}$$

$$\$^{A}_{C_{2_{Mx}}} = \begin{bmatrix} \$_x \\ 0 \\ 0 \\ 0 \end{bmatrix} \quad \$^{A}_{C_{2_{My}}} = \begin{bmatrix} \$_y \\ 0 \\ 0 \\ 0 \end{bmatrix} \quad \$^{A}_{C_{2_{Mz}}} = \begin{bmatrix} \$_z \\ 0 \\ 0 \\ 0 \end{bmatrix}$$

$$\$^{A}_{P_{1_{Fx}}} = \begin{bmatrix} \$0_{P_1} \times \$_x \\ \$_x \end{bmatrix} \quad \$^{A}_{P_{1_{Fy}}} = \begin{bmatrix} \$0_{P_1} \times \$_y \\ \$_y \end{bmatrix} \quad \$^{A}_{P_{1_{Fz}}} = \begin{bmatrix} \$0_{P_1} \times \$_z \\ \$_z \end{bmatrix}$$

$$\$^{A}_{P_{1_{My}}} = \begin{bmatrix} \$_y \\ 0 \\ 0 \\ 0 \end{bmatrix} \quad \$^{A}_{P_{1_{Mz}}} = \begin{bmatrix} \$_z \\ 0 \\ 0 \\ 0 \end{bmatrix}$$

$$\$^{A}_{P_{2_{Fx}}} = \begin{bmatrix} \$0_{P_2} \times \$_x \\ \$_x \end{bmatrix} \quad \$^{A}_{P_{2_{Fz}}} = \begin{bmatrix} \$0_{P_2} \times \$_z \\ \$_z \end{bmatrix}$$

$$\$^{A}_{P_{2_{Mx}}} = \begin{bmatrix} \$_x \\ 0 \\ 0 \\ 0 \end{bmatrix} \quad \$^{A}_{P_{2_{My}}} = \begin{bmatrix} \$_y \\ 0 \\ 0 \\ 0 \end{bmatrix} \quad \$^{A}_{P_{2_{Mz}}} = \begin{bmatrix} \$_z \\ 0 \\ 0 \\ 0 \end{bmatrix}$$

$$\$^{A}_{P_{3_{Fy}}} = \begin{bmatrix} \$0_{P_3} \times \$_y \\ \$_y \end{bmatrix} \quad \$^{A}_{P_{3_{Fz}}} = \begin{bmatrix} \$0_{P_3} \times \$_z \\ \$_z \end{bmatrix}$$

$$\$_{P_{3_{Mx}}}^{A} = \begin{bmatrix} \$_x \\ 0 \\ 0 \\ 0 \end{bmatrix} \quad \$_{P_{3_{My}}}^{A} = \begin{bmatrix} \$_y \\ 0 \\ 0 \\ 0 \end{bmatrix} \quad \$_{P_{3_{Mz}}}^{A} = \begin{bmatrix} \$_z \\ 0 \\ 0 \\ 0 \end{bmatrix}$$

$$\$_{P_{4_{Fx}}}^{A} = \begin{bmatrix} \$0_{P_4} \times \$_x \\ \$_x \end{bmatrix} \quad \$_{P_{4_{Fy}}}^{A} = \begin{bmatrix} \$0_{P_4} \times \$_y \\ \$_y \end{bmatrix} \quad \$_{P_{4_{Fz}}}^{A} = \begin{bmatrix} \$0_{P_4} \times \$_z \\ \$_z \end{bmatrix}$$

$$\$_{P_{4_{Mx}}}^{A} = \begin{bmatrix} \$_x \\ 0 \\ 0 \\ 0 \end{bmatrix} \quad \$_{P_{4_{Mz}}}^{A} = \begin{bmatrix} \$_z \\ 0 \\ 0 \\ 0 \end{bmatrix}$$

$$\$_{M_{1_{Fx}}}^{A} = \begin{bmatrix} \$0_{M_1} \times \$_x \\ \$_x \end{bmatrix} \quad \$_{M_{1_{Fy}}}^{A} = \begin{bmatrix} \$0_{M_1} \times \$_y \\ \$_y \end{bmatrix} \quad \$_{M_{1_{Fz}}}^{A} = \begin{bmatrix} \$0_{M_1} \times \$_z \\ \$_z \end{bmatrix}$$

$$\$_{M_{1_{My}}}^{A} = \begin{bmatrix} \$_y \\ 0 \\ 0 \\ 0 \end{bmatrix} \quad \$_{M_{1_{Mz}}}^{A} = \begin{bmatrix} \$_z \\ 0 \\ 0 \\ 0 \end{bmatrix}$$

$$\$_{M_{2_{Fx}}}^{A} = \begin{bmatrix} \$0_{M_2} \times \$_x \\ \$_x \end{bmatrix} \quad \$_{M_{2_{Fz}}}^{A} = \begin{bmatrix} \$0_{M_2} \times \$_z \\ \$_z \end{bmatrix}$$

$$\$_{M_{2_{Mx}}}^{A} = \begin{bmatrix} \$_x \\ 0 \\ 0 \\ 0 \end{bmatrix} \quad \$_{M_{2_{My}}}^{A} = \begin{bmatrix} \$_y \\ 0 \\ 0 \\ 0 \end{bmatrix} \quad \$_{M_{2_{Mz}}}^{A} = \begin{bmatrix} \$_z \\ 0 \\ 0 \\ 0 \end{bmatrix}$$

$$\$_{M_{3_{Fy}}}^{A} = \begin{bmatrix} \$0_{M_3} \times \$_y \\ \$_y \end{bmatrix} \quad \$_{M_{3_{Fz}}}^{A} = \begin{bmatrix} \$0_{M_3} \times \$_z \\ \$_z \end{bmatrix}$$

$$\$_{M_{3_{Mx}}}^{A} = \begin{bmatrix} \$_x \\ 0 \\ 0 \\ 0 \end{bmatrix} \quad \$_{M_{3_{My}}}^{A} = \begin{bmatrix} \$_y \\ 0 \\ 0 \\ 0 \end{bmatrix} \quad \$_{M_{3_{Mz}}}^{A} = \begin{bmatrix} \$_z \\ 0 \\ 0 \\ 0 \end{bmatrix}$$

$$\$_{F'_y}^{A} = \begin{bmatrix} \$0_F \times \$_y \\ \$_y \end{bmatrix} \quad \$_{F'_z}^{A} = \begin{bmatrix} \$0_F \times \$_z \\ \$_z \end{bmatrix} \quad \$_{M'_x}^{A} = \begin{bmatrix} \$_x \\ 0 \\ 0 \\ 0 \end{bmatrix}$$

B.2   WRENCHES OF THE MECHANISM 0°-30°IN A PLANAR WORKSPACE

$$\$^{A}_{L_{4Fy}} = \begin{bmatrix} (\$0_{L_4} \times \$_y)(1) \\ \$_y p \end{bmatrix} \quad \$^{A}_{L_{4Fz}} = \begin{bmatrix} (\$0_{L_4} \times \$_z)(1) \\ \$_z p \end{bmatrix} \quad \$^{A}_{A_{3Fz}} = \begin{bmatrix} (\$0_{A_3} \times \$_z)(1) \\ \$_z p \end{bmatrix}$$

$$\$^{A}_{P_{5Fy}} \begin{bmatrix} (\$0_{P_5} \times \$_y p)(1) \\ \$_y p \end{bmatrix} \quad \$^{A}_{P_{5Fz}} = \begin{bmatrix} (\$0_{P_5} \times \$_z p)(1) \\ \$_z p \end{bmatrix} \quad \$^{A}_{M_{4Fy}} = \begin{bmatrix} (\$0_{M_4} \times \$_y p)(1) \\ \$_y p \end{bmatrix}$$

$$\$^{A}_{A_{3Mx}} = \begin{bmatrix} 1 \\ 0 \\ 0 \end{bmatrix} \quad \$^{A}_{M_{4Fz}} = \begin{bmatrix} (\$0_{M_4} \times \$_z p)(1) \\ \$_z p \end{bmatrix}$$

$$\$^{A}_{L_{1Fy}} = \begin{bmatrix} (\$0_{L_1} \times \$_y)(1) \\ \$_y p \end{bmatrix} \quad \$^{A}_{L_{1Fz}} = \begin{bmatrix} (\$0_{L_1} \times \$_z)(1) \\ \$_z p \end{bmatrix} \quad \$^{A}_{L_{2Fy}} = \begin{bmatrix} (\$0_{L_2} \times \$_y)(1) \\ \$_y p \end{bmatrix}$$

$$\$^{A}_{L_{2Fz}} = \begin{bmatrix} (\$0_{L_2} \times \$_z)(1) \\ \$_z p \end{bmatrix} \quad \$^{A}_{L_{2Mx}} = \begin{bmatrix} 1 \\ 0 \\ 0 \end{bmatrix}$$

$$\$^{A}_{A_{2Fy}} = \begin{bmatrix} (\$0_{A_2} \times \$_y)(1) \\ \$_y p \end{bmatrix} \quad \$^{A}_{A_{2Fz}} = \begin{bmatrix} (\$0_{A_2} \times \$_z)(1) \\ \$_z p \end{bmatrix} \quad \$^{A}_{C_{1Fy}} = \begin{bmatrix} (\$0_{C_1} \times \$_y)(1) \\ \$_y p \end{bmatrix}$$

$$\$^{A}_{C_{1Fz}} = \begin{bmatrix} (\$0_{C_1} \times \$_z)(1) \\ \$_z p \end{bmatrix} \quad \$^{A}_{C_{2Fy}} = \begin{bmatrix} (\$0_{C_2} \times \$_y)(1) \\ \$_y p \end{bmatrix} \quad \$^{A}_{C_{2Mx}} = \begin{bmatrix} 1 \\ 0 \\ 0 \end{bmatrix}$$

$$\$^{A}_{P_{1Fy}} = \begin{bmatrix} (\$0_{P_1} \times \$_y)(1) \\ \$_y p \end{bmatrix} \quad \$^{A}_{P_{1Fz}} = \begin{bmatrix} (\$0_{P_1} \times \$_z)(1) \\ \$_z p \end{bmatrix}$$

$$\$^{A}_{P_{2Fz}} = \begin{bmatrix} (\$0_{P_2} \times \$_z)(1) \\ \$_z p \end{bmatrix} \quad \$^{A}_{P_{2Mx}} = \begin{bmatrix} 1 \\ 0 \\ 0 \end{bmatrix} \quad \$^{A}_{M_{1Fy}} = \begin{bmatrix} (\$0_{M_1} \times \$_y)(1) \\ \$_y p \end{bmatrix}$$

$$\$^{A}_{M_{1Fz}} = \begin{bmatrix} (\$0_{M_1} \times \$_z)(1) \\ \$_z p \end{bmatrix} \quad \$^{A}_{M_{2Fy}} = \begin{bmatrix} (\$0_{M_2} \times \$_y)(1) \\ \$_y p \end{bmatrix} \quad \$^{A}_{M_{2Fz}} = \begin{bmatrix} (\$0_{M_2} \times \$_z)(1) \\ \$_z p \end{bmatrix}$$

$$\$^{A}_{M_{2Mx}} = \begin{bmatrix} 1 \\ 0 \\ 0 \end{bmatrix} \quad \$^{A}_{F'_y} = \begin{bmatrix} (\$0_F \times \$_y)(1) \\ \$_y p \end{bmatrix} \quad \$^{A}_{F'_z} = \begin{bmatrix} (\$0_F \times \$_z)(1) \\ \$_z p \end{bmatrix} \quad \$^{A}_{M'_x} = \begin{bmatrix} 1 \\ 0 \\ 0 \end{bmatrix}$$

B.3 WRENCHES OF THE MECHANISM 60°-90°IN A PLANAR WORKSPACE

$$\$^A_{L3_{Fy}} = \begin{bmatrix} (\$_{0_{L3}} \times \$_y)(1) \\ \$_y p \end{bmatrix} \quad \$^A_{L3_{Fz}} = \begin{bmatrix} (\$_{0_{L3}} \times \$_z)(1) \\ \$_z p \end{bmatrix} \quad \$^A_{L3_{Mx}} = \begin{bmatrix} 1 \\ 0 \\ 0 \end{bmatrix}$$

$$\$^A_{A3_{Fz}} = \begin{bmatrix} (\$_{0_{A3}} \times \$_z)(1) \\ \$_z p \end{bmatrix} \quad \$^A_{A3_{Mx}} = \begin{bmatrix} 1 \\ 0 \\ 0 \end{bmatrix}$$

$$\$^A_{P4_{Fy}} \begin{bmatrix} (\$_{0_{P4}} \times \$_y p)(1) \\ \$_y p \end{bmatrix} \quad \$^A_{P4_{Fz}} = \begin{bmatrix} (\$_{0_{P4}} \times \$_z p)(1) \\ \$_z p \end{bmatrix}$$

$$\$^A_{M3_{Fy}} = \begin{bmatrix} (\$_{0_{M3}} \times \$_y p)(1) \\ \$_y p \end{bmatrix} \quad \$^A_{M3_{Fz}} = \begin{bmatrix} (\$_{0_{M3}} \times \$_z p)(1) \\ \$_z p \end{bmatrix} \quad \$^A_{M3_{Mx}} = \begin{bmatrix} 1 \\ 0 \\ 0 \end{bmatrix}$$

$$\$^A_{L1_{Fy}} = \begin{bmatrix} (\$_{0_{L1}} \times \$_y)(1) \\ \$_y p \end{bmatrix} \quad \$^A_{L1_{Fz}} = \begin{bmatrix} (\$_{0_{L1}} \times \$_z)(1) \\ \$_z p \end{bmatrix}$$

$$\$^A_{L2_{Fy}} = \begin{bmatrix} (\$_{0_{L2}} \times \$_y)(1) \\ \$_y p \end{bmatrix} \quad \$^A_{L2_{Mx}} = \begin{bmatrix} 1 \\ 0 \\ 0 \end{bmatrix}$$

$$\$^A_{A2_{Fy}} = \begin{bmatrix} (\$_{0_{A2}} \times \$_y)(1) \\ \$_y p \end{bmatrix} \quad \$^A_{A2_{Fz}} = \begin{bmatrix} (\$_{0_{A2}} \times \$_z)(1) \\ \$_z p \end{bmatrix}$$

$$\$^A_{C1_{Fy}} = \begin{bmatrix} (\$_{0_{C1}} \times \$_y)(1) \\ \$_y p \end{bmatrix} \quad \$^A_{C1_{Fz}} = \begin{bmatrix} (\$_{0_{C1}} \times \$_z)(1) \\ \$_z p \end{bmatrix}$$

$$\$^A_{C2_{Fy}} = \begin{bmatrix} (\$_{0_{C2}} \times \$_y)(1) \\ \$_y p \end{bmatrix} \quad \$^A_{C2_{Mx}} = \begin{bmatrix} 1 \\ 0 \\ 0 \end{bmatrix}$$

$$\$^A_{P1_{Fy}} = \begin{bmatrix} (\$_{0_{P1}} \times \$_y)(1) \\ \$_y p \end{bmatrix} \quad \$^A_{P1_{Fz}} = \begin{bmatrix} (\$_{0_{P1}} \times \$_z)(1) \\ \$_z p \end{bmatrix}$$

$$\$^A_{P2_{Fz}} = \begin{bmatrix} (\$_{0_{P2}} \times \$_z)(1) \\ \$_z p \end{bmatrix} \quad \$^A_{P2_{Mx}} = \begin{bmatrix} 1 \\ 0 \\ 0 \end{bmatrix}$$

$$\$^A_{M1_{Fy}} = \begin{bmatrix} (\$_{0_{M1}} \times \$_y)(1) \\ \$_y p \end{bmatrix} \quad \$^A_{M1_{Fz}} = \begin{bmatrix} (\$_{0_{M1}} \times \$_z)(1) \\ \$_z p \end{bmatrix}$$

$$\$^{A}_{M_{2Fy}} = \begin{bmatrix} (\$_{0_{M_2}} \times \$_y)(1) \\ \$_y p \end{bmatrix} \quad \$^{A}_{M_{2Mx}} = \begin{bmatrix} 1 \\ 0 \\ 0 \end{bmatrix}$$

$$\$^{A}_{F'_y} = \begin{bmatrix} (\$_{0_F} \times \$_y)(1) \\ \$_y p \end{bmatrix} \quad \$^{A}_{F'_z} = \begin{bmatrix} (\$_{0_F} \times \$_z)(1) \\ \$_z p \end{bmatrix} \quad \$^{A}_{M'_x} = \begin{bmatrix} 1 \\ 0 \\ 0 \end{bmatrix}$$

APPENDIX C – CUTSET MATRIX

C.1 MECHANISM 0°-30°IN A PLANAR WORKSPACE

For the mechanism 0°-30°in a spatial workspace ($\lambda = 6$), the cutset matrix is presented (eq. 44).

$$[Q]_{16x102} = \left[Q_{L_4} Q_{A_3} Q_{P_5} Q_{M_4} Q_{L_1} Q_{L_2} Q_{L_3} Q_{A_1} Q_{A_2} Q_{C_1} Q_{C_2} Q_{C_3} Q_{C_4} \cdots \right.$$

$$\left. \cdots Q_{P_1} Q_{P_2} Q_{P_3} Q_{P_4} Q_{M_1} Q_{M_2} Q_{M_3} Q_F \right] (43)$$

Where:

$$[Q_{L_4}] = \begin{array}{c} \\ L1 \\ L2 \\ L3 \\ A1 \\ A2 \\ C1 \\ C2 \\ C3 \\ C4 \\ P1 \\ P2 \\ P3 \\ P4 \\ M1 \\ M2 \\ M3 \end{array} \begin{array}{ccccc} \bar{L4}_{Fx} & \bar{L4}_{Fy} & \bar{L4}_{Fz} & \bar{L4}_{My} & \bar{L4}_{Mz} \\ \left(\begin{array}{ccccc} 1 & 1 & 1 & 1 & 1 \\ 1 & 1 & 1 & 1 & 1 \\ 1 & 1 & 1 & 1 & 1 \\ 0 & 0 & 0 & 0 & 0 \\ 0 & 0 & 0 & 0 & 0 \\ -1 & -1 & -1 & -1 & -1 \\ -1 & -1 & -1 & -1 & -1 \\ -1 & -1 & -1 & -1 & -1 \\ -1 & -1 & -1 & -1 & -1 \\ 0 & 0 & 0 & 0 & 0 \\ 0 & 0 & 0 & 0 & 0 \\ 0 & 0 & 0 & 0 & 0 \\ 0 & 0 & 0 & 0 & 0 \\ 0 & 0 & 0 & 0 & 0 \\ 0 & 0 & 0 & 0 & 0 \\ 0 & 0 & 0 & 0 & 0 \end{array} \right) \end{array}$$

$$
[Q_{A_3}] = \quad
\begin{array}{c|ccccc}
 & A\bar{3}_{Fx} & A\bar{3}_{Fz} & A\bar{3}_{Mx} & A\bar{3}_{My} & A\bar{3}_{Mz} \\
\hline
L1 & 0 & 0 & 0 & 0 & 0 \\
L2 & 0 & 0 & 0 & 0 & 0 \\
L3 & 0 & 0 & 0 & 0 & 0 \\
A1 & -1 & -1 & -1 & -1 & -1 \\
A2 & -1 & -1 & -1 & -1 & -1 \\
C1 & 1 & 1 & 1 & 1 & 1 \\
C2 & 1 & 1 & 1 & 1 & 1 \\
C3 & 1 & 1 & 1 & 1 & 1 \\
C4 & 1 & 1 & 1 & 1 & 1 \\
P1 & 0 & 0 & 0 & 0 & 0 \\
P2 & 0 & 0 & 0 & 0 & 0 \\
P3 & 0 & 0 & 0 & 0 & 0 \\
P4 & 0 & 0 & 0 & 0 & 0 \\
M1 & 0 & 0 & 0 & 0 & 0 \\
M2 & 0 & 0 & 0 & 0 & 0 \\
M3 & 0 & 0 & 0 & 0 & 0 \\
\end{array}
$$

$$
[Q_{P_5}] = \quad
\begin{array}{c|ccccc}
 & P\bar{5}_{Fx} & P\bar{5}_{Fy} & P\bar{5}_{Fz} & P\bar{5}_{My} & P\bar{5}_{Mz} \\
\hline
L1 & 0 & 0 & 0 & 0 & 0 \\
L2 & 0 & 0 & 0 & 0 & 0 \\
L3 & 0 & 0 & 0 & 0 & 0 \\
A1 & 0 & 0 & 0 & 0 & 0 \\
A2 & 0 & 0 & 0 & 0 & 0 \\
C1 & 1 & 1 & 1 & 1 & 1 \\
C2 & 1 & 1 & 1 & 1 & 1 \\
C3 & 1 & 1 & 1 & 1 & 1 \\
C4 & 1 & 1 & 1 & 1 & 1 \\
P1 & -1 & -1 & -1 & -1 & -1 \\
P2 & -1 & -1 & -1 & -1 & -1 \\
P3 & -1 & -1 & -1 & -1 & -1 \\
P4 & -1 & -1 & -1 & -1 & -1 \\
M1 & 0 & 0 & 0 & 0 & 0 \\
M2 & 0 & 0 & 0 & 0 & 0 \\
M3 & 0 & 0 & 0 & 0 & 0 \\
\end{array}
$$

$$[Q_{M_4}] = \begin{array}{c} \\ L1 \\ L2 \\ L3 \\ A1 \\ A2 \\ C1 \\ C2 \\ C3 \\ C4 \\ P1 \\ P2 \\ P3 \\ P4 \\ M1 \\ M2 \\ M3 \end{array} \begin{array}{ccccc} \overline{M4}_{Fx} & \overline{M4}_{Fy} & \overline{M4}_{Fz} & \overline{M4}_{My} & \overline{M4}_{Mz} \\ 0 & 0 & 0 & 0 & 0 \\ 0 & 0 & 0 & 0 & 0 \\ 0 & 0 & 0 & 0 & 0 \\ 0 & 0 & 0 & 0 & 0 \\ 0 & 0 & 0 & 0 & 0 \\ -1 & -1 & -1 & -1 & -1 \\ -1 & -1 & -1 & -1 & -1 \\ -1 & -1 & -1 & -1 & -1 \\ -1 & -1 & -1 & -1 & -1 \\ 0 & 0 & 0 & 0 & 0 \\ 0 & 0 & 0 & 0 & 0 \\ 0 & 0 & 0 & 0 & 0 \\ 0 & 0 & 0 & 0 & 0 \\ 1 & 1 & 1 & 1 & 1 \\ 1 & 1 & 1 & 1 & 1 \\ 1 & 1 & 1 & 1 & 1 \end{array}$$

$$[Q_{L_1}] = \begin{array}{c} \\ L1 \\ L2 \\ L3 \\ A1 \\ A2 \\ C1 \\ C2 \\ C3 \\ C4 \\ P1 \\ P2 \\ P3 \\ P4 \\ M1 \\ M2 \\ M3 \end{array} \begin{array}{ccccc} \overline{L1}_{Fx} & \overline{L1}_{Fy} & \overline{L1}_{Fz} & \overline{L1}_{My} & \overline{L1}_{Mz} \\ 1 & 1 & 1 & 1 & 1 \\ 0 & 0 & 0 & 0 & 0 \\ 0 & 0 & 0 & 0 & 0 \\ 0 & 0 & 0 & 0 & 0 \\ 0 & 0 & 0 & 0 & 0 \\ 0 & 0 & 0 & 0 & 0 \\ 0 & 0 & 0 & 0 & 0 \\ 0 & 0 & 0 & 0 & 0 \\ 0 & 0 & 0 & 0 & 0 \\ 0 & 0 & 0 & 0 & 0 \\ 0 & 0 & 0 & 0 & 0 \\ 0 & 0 & 0 & 0 & 0 \\ 0 & 0 & 0 & 0 & 0 \\ 0 & 0 & 0 & 0 & 0 \\ 0 & 0 & 0 & 0 & 0 \\ 0 & 0 & 0 & 0 & 0 \end{array}$$

$$[Q_{L_2}] = \begin{array}{c} \\ L1 \\ L2 \\ L3 \\ A1 \\ A2 \\ C1 \\ C2 \\ C3 \\ C4 \\ P1 \\ P2 \\ P3 \\ P4 \\ M1 \\ M2 \\ M3 \end{array} \begin{array}{ccccc} \overline{L2}_{Fx} & \overline{L2}_{Fz} & \overline{L2}_{Mx} & \overline{L2}_{My} & \overline{L2}_{Mz} \\ \left(\begin{array}{ccccc} 0 & 0 & 0 & 0 & 0 \\ 1 & 1 & 1 & 1 & 1 \\ 0 & 0 & 0 & 0 & 0 \\ 0 & 0 & 0 & 0 & 0 \\ 0 & 0 & 0 & 0 & 0 \\ 0 & 0 & 0 & 0 & 0 \\ 0 & 0 & 0 & 0 & 0 \\ 0 & 0 & 0 & 0 & 0 \\ 0 & 0 & 0 & 0 & 0 \\ 0 & 0 & 0 & 0 & 0 \\ 0 & 0 & 0 & 0 & 0 \\ 0 & 0 & 0 & 0 & 0 \\ 0 & 0 & 0 & 0 & 0 \\ 0 & 0 & 0 & 0 & 0 \\ 0 & 0 & 0 & 0 & 0 \\ 0 & 0 & 0 & 0 & 0 \end{array} \right) \end{array}$$

$$[Q_{L_3}] = \begin{array}{c} \\ L1 \\ L2 \\ L3 \\ A1 \\ A2 \\ C1 \\ C2 \\ C3 \\ C4 \\ P1 \\ P2 \\ P3 \\ P4 \\ M1 \\ M2 \\ M3 \end{array} \begin{array}{ccccc} \overline{L3}_{Fy} & \overline{L3}_{Fz} & \overline{L3}_{Mx} & \overline{L3}_{My} & \overline{L3}_{Mz} \\ \left(\begin{array}{ccccc} 0 & 0 & 0 & 0 & 0 \\ 0 & 0 & 0 & 0 & 0 \\ 1 & 1 & 1 & 1 & 1 \\ 0 & 0 & 0 & 0 & 0 \\ 0 & 0 & 0 & 0 & 0 \\ 0 & 0 & 0 & 0 & 0 \\ 0 & 0 & 0 & 0 & 0 \\ 0 & 0 & 0 & 0 & 0 \\ 0 & 0 & 0 & 0 & 0 \\ 0 & 0 & 0 & 0 & 0 \\ 0 & 0 & 0 & 0 & 0 \\ 0 & 0 & 0 & 0 & 0 \\ 0 & 0 & 0 & 0 & 0 \\ 0 & 0 & 0 & 0 & 0 \\ 0 & 0 & 0 & 0 & 0 \\ 0 & 0 & 0 & 0 & 0 \end{array} \right) \end{array}$$

$$
[Q_{C_1}] =
\begin{array}{c}
\\
L1 \\ L2 \\ L3 \\ A1 \\ A2 \\ C1 \\ C2 \\ C3 \\ C4 \\ P1 \\ P2 \\ P3 \\ P4 \\ M1 \\ M2 \\ M3
\end{array}
\begin{array}{ccccc}
C1_{Fx}^- & C1_{Fy}^- & C1_{Fz}^- & C1_{My}^- & C1_{Mz}^- \\
\left(\begin{array}{ccccc}
0 & 0 & 0 & 0 & 0 \\
0 & 0 & 0 & 0 & 0 \\
0 & 0 & 0 & 0 & 0 \\
0 & 0 & 0 & 0 & 0 \\
0 & 0 & 0 & 0 & 0 \\
1 & 1 & 1 & 1 & 1 \\
0 & 0 & 0 & 0 & 0 \\
0 & 0 & 0 & 0 & 0 \\
0 & 0 & 0 & 0 & 0 \\
0 & 0 & 0 & 0 & 0 \\
0 & 0 & 0 & 0 & 0 \\
0 & 0 & 0 & 0 & 0 \\
0 & 0 & 0 & 0 & 0 \\
0 & 0 & 0 & 0 & 0 \\
0 & 0 & 0 & 0 & 0 \\
0 & 0 & 0 & 0 & 0
\end{array} \right)
\end{array}
$$

$$
[Q_{C_2}] =
\begin{array}{c}
\\
L1 \\ L2 \\ L3 \\ A1 \\ A2 \\ C1 \\ C2 \\ C3 \\ C4 \\ P1 \\ P2 \\ P3 \\ P4 \\ M1 \\ M2 \\ M3
\end{array}
\begin{array}{ccccc}
C2_{Fx}^- & C2_{Fy}^- & C2_{Mx}^- & C2_{My}^- & C2_{Mz}^- \\
\left(\begin{array}{ccccc}
0 & 0 & 0 & 0 & 0 \\
0 & 0 & 0 & 0 & 0 \\
0 & 0 & 0 & 0 & 0 \\
0 & 0 & 0 & 0 & 0 \\
0 & 0 & 0 & 0 & 0 \\
0 & 0 & 0 & 0 & 0 \\
1 & 1 & 1 & 1 & 1 \\
0 & 0 & 0 & 0 & 0 \\
0 & 0 & 0 & 0 & 0 \\
0 & 0 & 0 & 0 & 0 \\
0 & 0 & 0 & 0 & 0 \\
0 & 0 & 0 & 0 & 0 \\
0 & 0 & 0 & 0 & 0 \\
0 & 0 & 0 & 0 & 0 \\
0 & 0 & 0 & 0 & 0 \\
0 & 0 & 0 & 0 & 0
\end{array} \right)
\end{array}
$$

$$[Q_{C_3}] =$$

	$C3^-_{Fx}$	$C3^-_{Fy}$	$C3^-_{Fz}$	$C3^-_{Mx}$	$C3^-_{Mz}$
L1	0	0	0	0	0
L2	0	0	0	0	0
L3	0	0	0	0	0
A1	0	0	0	0	0
A2	0	0	0	0	0
C1	0	0	0	0	0
C2	0	0	0	0	0
C3	1	1	1	1	1
C4	0	0	0	0	0
P1	0	0	0	0	0
P2	0	0	0	0	0
P3	0	0	0	0	0
P4	0	0	0	0	0
M1	0	0	0	0	0
M2	0	0	0	0	0
M3	0	0	0	0	0

$$[Q_{C_4}] =$$

	$C4^-_{Fx}$	$C4^-_{Fy}$	$C4^-_{Fz}$	$C4^-_{Mx}$	$C4^-_{My}$
L1	0	0	0	0	0
L2	0	0	0	0	0
L3	0	0	0	0	0
A1	0	0	0	0	0
A2	0	0	0	0	0
C1	0	0	0	0	0
C2	0	0	0	0	0
C3	0	0	0	0	0
C4	1	1	1	1	1
P1	0	0	0	0	0
P2	0	0	0	0	0
P3	0	0	0	0	0
P4	0	0	0	0	0
M1	0	0	0	0	0
M2	0	0	0	0	0
M3	0	0	0	0	0

$$[Q_{P_1}] = \begin{array}{c} \\ L1 \\ L2 \\ L3 \\ A1 \\ A2 \\ C1 \\ C2 \\ C3 \\ C4 \\ P1 \\ P2 \\ P3 \\ P4 \\ M1 \\ M2 \\ M3 \end{array} \begin{pmatrix} \bar{P1}_{Fx} & \bar{P1}_{Fy} & \bar{P1}_{Fz} & \bar{P1}_{My} & \bar{P1}_{Mz} \\ 0 & 0 & 0 & 0 & 0 \\ 0 & 0 & 0 & 0 & 0 \\ 0 & 0 & 0 & 0 & 0 \\ 0 & 0 & 0 & 0 & 0 \\ 0 & 0 & 0 & 0 & 0 \\ 0 & 0 & 0 & 0 & 0 \\ 0 & 0 & 0 & 0 & 0 \\ 0 & 0 & 0 & 0 & 0 \\ 0 & 0 & 0 & 0 & 0 \\ 1 & 1 & 1 & 1 & 1 \\ 0 & 0 & 0 & 0 & 0 \\ 0 & 0 & 0 & 0 & 0 \\ 0 & 0 & 0 & 0 & 0 \\ 0 & 0 & 0 & 0 & 0 \\ 0 & 0 & 0 & 0 & 0 \\ 0 & 0 & 0 & 0 & 0 \end{pmatrix}$$

$$[Q_{P_2}] = \begin{array}{c} \\ L1 \\ L2 \\ L3 \\ A1 \\ A2 \\ C1 \\ C2 \\ C3 \\ C4 \\ P1 \\ P2 \\ P3 \\ P4 \\ M1 \\ M2 \\ M3 \end{array} \begin{pmatrix} \bar{P2}_{Fx} & \bar{P2}_{Fz} & \bar{P2}_{Mx} & \bar{P2}_{My} & \bar{P2}_{Mz} \\ 0 & 0 & 0 & 0 & 0 \\ 0 & 0 & 0 & 0 & 0 \\ 0 & 0 & 0 & 0 & 0 \\ 0 & 0 & 0 & 0 & 0 \\ 0 & 0 & 0 & 0 & 0 \\ 0 & 0 & 0 & 0 & 0 \\ 0 & 0 & 0 & 0 & 0 \\ 0 & 0 & 0 & 0 & 0 \\ 0 & 0 & 0 & 0 & 0 \\ 0 & 0 & 0 & 0 & 0 \\ 1 & 1 & 1 & 1 & 1 \\ 0 & 0 & 0 & 0 & 0 \\ 0 & 0 & 0 & 0 & 0 \\ 0 & 0 & 0 & 0 & 0 \\ 0 & 0 & 0 & 0 & 0 \\ 0 & 0 & 0 & 0 & 0 \end{pmatrix}$$

$$[Q_{P_3}] = \begin{array}{c} \\ L1 \\ L2 \\ L3 \\ A1 \\ A2 \\ C1 \\ C2 \\ C3 \\ C4 \\ P1 \\ P2 \\ P3 \\ P4 \\ M1 \\ M2 \\ M3 \end{array} \begin{array}{ccccc} P3_{Fy}^- & P3_{Fz}^- & P3_{Mx}^- & P3_{My}^- & P3_{Mz}^- \\ 0 & 0 & 0 & 0 & 0 \\ 0 & 0 & 0 & 0 & 0 \\ 0 & 0 & 0 & 0 & 0 \\ 0 & 0 & 0 & 0 & 0 \\ 0 & 0 & 0 & 0 & 0 \\ 0 & 0 & 0 & 0 & 0 \\ 0 & 0 & 0 & 0 & 0 \\ 0 & 0 & 0 & 0 & 0 \\ 0 & 0 & 0 & 0 & 0 \\ 0 & 0 & 0 & 0 & 0 \\ 0 & 0 & 0 & 0 & 0 \\ 1 & 1 & 1 & 1 & 1 \\ 0 & 0 & 0 & 0 & 0 \\ 0 & 0 & 0 & 0 & 0 \\ 0 & 0 & 0 & 0 & 0 \\ 0 & 0 & 0 & 0 & 0 \end{array}$$

$$[Q_{P_4}] = \begin{array}{c} \\ L1 \\ L2 \\ L3 \\ A1 \\ A2 \\ C1 \\ C2 \\ C3 \\ C4 \\ P1 \\ P2 \\ P3 \\ P4 \\ M1 \\ M2 \\ M3 \end{array} \begin{array}{ccccc} P4_{Fx}^- & P4_{Fy}^- & P4_{Fz}^- & P4_{Mx}^- & P4_{Mz}^- \\ 0 & 0 & 0 & 0 & 0 \\ 0 & 0 & 0 & 0 & 0 \\ 0 & 0 & 0 & 0 & 0 \\ 0 & 0 & 0 & 0 & 0 \\ 0 & 0 & 0 & 0 & 0 \\ 0 & 0 & 0 & 0 & 0 \\ 0 & 0 & 0 & 0 & 0 \\ 0 & 0 & 0 & 0 & 0 \\ 0 & 0 & 0 & 0 & 0 \\ 0 & 0 & 0 & 0 & 0 \\ 0 & 0 & 0 & 0 & 0 \\ 0 & 0 & 0 & 0 & 0 \\ 1 & 1 & 1 & 1 & 1 \\ 0 & 0 & 0 & 0 & 0 \\ 0 & 0 & 0 & 0 & 0 \\ 0 & 0 & 0 & 0 & 0 \end{array}$$

$$
[Q_{M_1}] =
\begin{array}{c}
\\
L1 \\ L2 \\ L3 \\ A1 \\ A2 \\ C1 \\ C2 \\ C3 \\ C4 \\ P1 \\ P2 \\ P3 \\ P4 \\ M1 \\ M2 \\ M3
\end{array}
\begin{array}{ccccc}
\overline{M1}_{Fx} & \overline{M1}_{Fy} & \overline{M1}_{Fz} & \overline{M1}_{My} & \overline{M1}_{Mz} \\
0 & 0 & 0 & 0 & 0 \\
0 & 0 & 0 & 0 & 0 \\
0 & 0 & 0 & 0 & 0 \\
0 & 0 & 0 & 0 & 0 \\
0 & 0 & 0 & 0 & 0 \\
0 & 0 & 0 & 0 & 0 \\
0 & 0 & 0 & 0 & 0 \\
0 & 0 & 0 & 0 & 0 \\
0 & 0 & 0 & 0 & 0 \\
0 & 0 & 0 & 0 & 0 \\
0 & 0 & 0 & 0 & 0 \\
0 & 0 & 0 & 0 & 0 \\
0 & 0 & 0 & 0 & 0 \\
1 & 1 & 1 & 1 & 1 \\
0 & 0 & 0 & 0 & 0 \\
0 & 0 & 0 & 0 & 0
\end{array}
$$

$$
[Q_{M_2}] =
\begin{array}{c}
\\
L1 \\ L2 \\ L3 \\ A1 \\ A2 \\ C1 \\ C2 \\ C3 \\ C4 \\ P1 \\ P2 \\ P3 \\ P4 \\ M1 \\ M2 \\ M3
\end{array}
\begin{array}{ccccc}
\overline{M2}_{Fx} & \overline{M2}_{Fz} & \overline{M2}_{Mx} & \overline{M2}_{My} & \overline{M2}_{Mz} \\
0 & 0 & 0 & 0 & 0 \\
0 & 0 & 0 & 0 & 0 \\
0 & 0 & 0 & 0 & 0 \\
0 & 0 & 0 & 0 & 0 \\
0 & 0 & 0 & 0 & 0 \\
0 & 0 & 0 & 0 & 0 \\
0 & 0 & 0 & 0 & 0 \\
0 & 0 & 0 & 0 & 0 \\
0 & 0 & 0 & 0 & 0 \\
0 & 0 & 0 & 0 & 0 \\
0 & 0 & 0 & 0 & 0 \\
0 & 0 & 0 & 0 & 0 \\
0 & 0 & 0 & 0 & 0 \\
0 & 0 & 0 & 0 & 0 \\
1 & 1 & 1 & 1 & 1 \\
0 & 0 & 0 & 0 & 0
\end{array}
$$

$$[Q_{M_3}] = \begin{array}{c} \\ L1 \\ L2 \\ L3 \\ A1 \\ A2 \\ C1 \\ C2 \\ C3 \\ C4 \\ P1 \\ P2 \\ P3 \\ P4 \\ M1 \\ M2 \\ M3 \end{array} \begin{array}{ccccc} \bar{M3}_{Fy} & \bar{M3}_{Fz} & \bar{M3}_{Mx} & \bar{M3}_{My} & \bar{M3}_{Mz} \\ 0 & 0 & 0 & 0 & 0 \\ 0 & 0 & 0 & 0 & 0 \\ 0 & 0 & 0 & 0 & 0 \\ 0 & 0 & 0 & 0 & 0 \\ 0 & 0 & 0 & 0 & 0 \\ 0 & 0 & 0 & 0 & 0 \\ 0 & 0 & 0 & 0 & 0 \\ 0 & 0 & 0 & 0 & 0 \\ 0 & 0 & 0 & 0 & 0 \\ 0 & 0 & 0 & 0 & 0 \\ 0 & 0 & 0 & 0 & 0 \\ 0 & 0 & 0 & 0 & 0 \\ 0 & 0 & 0 & 0 & 0 \\ 0 & 0 & 0 & 0 & 0 \\ 0 & 0 & 0 & 0 & 0 \\ 1 & 1 & 1 & 1 & 1 \end{array}$$

$$[Q_F] = \begin{array}{c} \\ L1 \\ L2 \\ L3 \\ A1 \\ A2 \\ C1 \\ C2 \\ C3 \\ C4 \\ P1 \\ P2 \\ P3 \\ P4 \\ M1 \\ M2 \\ M3 \end{array} \begin{array}{cc} \bar{F}'_z & \bar{M}'_x \\ 0 & 0 \\ 0 & 0 \\ 0 & 0 \\ 0 & 0 \\ 0 & 0 \\ 1 & 1 \\ 1 & 1 \\ 1 & 1 \\ 1 & 1 \\ 0 & 0 \\ 0 & 0 \\ 0 & 0 \\ 0 & 0 \\ 0 & 0 \\ 0 & 0 \\ 0 & 0 \end{array}$$

C.2 MECHANISM 0°-30°IN A PLANAR WORKSPACE

For the mechanism 0°-30°in a planar workspace, the cutset matrix is presented (eq. 44).

$$[Q]_{9\text{x}31} = \left[Q_{L_4} Q_{A_3} Q_{P_5} Q_{M_4} Q_{L_1} Q_{L_2} Q_{A_2} Q_{C_1} Q_{C_2} Q_{P_1} Q_{P_2} Q_{M_1} Q_{M_2} Q_F \right] \qquad (44)$$

Where:

$$[Q_{L_4}] = \begin{array}{c} \\ L1 \\ L2 \\ A2 \\ C1 \\ C2 \\ P1 \\ P2 \\ M1 \\ M2 \end{array} \begin{array}{cc} \bar{L4}_{Fy} & \bar{L4}_{Fz} \\ 1 & 1 \\ 1 & 1 \\ 0 & 0 \\ -1 & -1 \\ -1 & -1 \\ 0 & 0 \\ 0 & 0 \\ 0 & 0 \\ 0 & 0 \end{array} \qquad [Q_{A_3}] = \begin{array}{c} \\ L1 \\ L2 \\ A2 \\ C1 \\ C2 \\ P1 \\ P2 \\ M1 \\ M2 \end{array} \begin{array}{cc} \bar{A3}_{Fz} & \bar{A3}_{Mx} \\ 0 & 0 \\ 0 & 0 \\ -1 & -1 \\ 1 & 1 \\ 1 & 1 \\ 0 & 0 \\ 0 & 0 \\ 0 & 0 \\ 0 & 0 \end{array}$$

$$[Q_{P_5}] = \begin{array}{c} \\ L1 \\ L2 \\ A2 \\ C1 \\ C2 \\ P1 \\ P2 \\ M1 \\ M2 \end{array} \begin{array}{cc} \bar{P5}_{Fy} & \bar{P5}_{Fz} \\ 0 & 0 \\ 0 & 0 \\ 0 & 0 \\ 1 & 1 \\ 1 & 1 \\ -1 & -1 \\ -1 & -1 \\ 0 & 0 \\ 0 & 0 \end{array} \qquad [Q_{M_4}] = \begin{array}{c} \\ L1 \\ L2 \\ A2 \\ C1 \\ C2 \\ P1 \\ P2 \\ M1 \\ M2 \end{array} \begin{array}{cc} \bar{M4}_{Fy} & \bar{M4}_{Fz} \\ 0 & 0 \\ 0 & 0 \\ 0 & 0 \\ -1 & -1 \\ -1 & -1 \\ 0 & 0 \\ 0 & 0 \\ 1 & 1 \\ 1 & 1 \end{array}$$

$$[Q_{L_1}] = \begin{array}{c} \\ L1 \\ L2 \\ A2 \\ C1 \\ C2 \\ P1 \\ P2 \\ M1 \\ M2 \end{array} \begin{array}{cc} \bar{L1}_{Fy} & \bar{L1}_{Fz} \\ 1 & 1 \\ 0 & 0 \\ 0 & 0 \\ 0 & 0 \\ 0 & 0 \\ 0 & 0 \\ 0 & 0 \\ 0 & 0 \\ 0 & 0 \end{array} \qquad [Q_{L_2}] = \begin{array}{c} \\ L1 \\ L2 \\ A2 \\ C1 \\ C2 \\ P1 \\ P2 \\ M1 \\ M2 \end{array} \begin{array}{ccc} \bar{L2}_{Fy} & \bar{L2}_{Fz} & \bar{L2}_{Mx} \\ 0 & 0 & 0 \\ 1 & 1 & 1 \\ 0 & 0 & 0 \\ 0 & 0 & 0 \\ 0 & 0 & 0 \\ 0 & 0 & 0 \\ 0 & 0 & 0 \\ 0 & 0 & 0 \\ 0 & 0 & 0 \end{array}$$

$$
[Q_{A_2}] = \begin{array}{c} \\ L1 \\ L2 \\ A2 \\ C1 \\ C2 \\ P1 \\ P2 \\ M1 \\ M2 \end{array}
\begin{array}{cc} A2_{F_y}^- & A2_{F_z}^- \\ \left(\begin{array}{cc} 0 & 0 \\ 0 & 0 \\ 1 & 1 \\ 0 & 0 \\ 0 & 0 \\ 0 & 0 \\ 0 & 0 \\ 0 & 0 \\ 0 & 0 \end{array} \right) \end{array}
\qquad
[Q_{C_1}] = \begin{array}{c} \\ L1 \\ L2 \\ A2 \\ C1 \\ C2 \\ P1 \\ P2 \\ M1 \\ M2 \end{array}
\begin{array}{cc} C1_{F_y}^- & C1_{F_z}^- \\ \left(\begin{array}{cc} 0 & 0 \\ 0 & 0 \\ 0 & 0 \\ 1 & 1 \\ 0 & 0 \\ 0 & 0 \\ 0 & 0 \\ 0 & 0 \\ 0 & 0 \end{array} \right) \end{array}
$$

$$
[Q_{C_2}] = \begin{array}{c} \\ L1 \\ L2 \\ A2 \\ C1 \\ C2 \\ P1 \\ P2 \\ M1 \\ M2 \end{array}
\begin{array}{cc} C2_{F_y}^- & C2_{M_x}^- \\ \left(\begin{array}{cc} 0 & 0 \\ 0 & 0 \\ 0 & 0 \\ 0 & 0 \\ 1 & 1 \\ 0 & 0 \\ 0 & 0 \\ 0 & 0 \\ 0 & 0 \end{array} \right) \end{array}
\qquad
[Q_{P_1}] = \begin{array}{c} \\ L1 \\ L2 \\ A2 \\ C1 \\ C2 \\ P1 \\ P2 \\ M1 \\ M2 \end{array}
\begin{array}{cc} P1_{F_y}^- & P1_{F_z}^- \\ \left(\begin{array}{cc} 0 & 0 \\ 0 & 0 \\ 0 & 0 \\ 0 & 0 \\ 0 & 0 \\ 1 & 1 \\ 0 & 0 \\ 0 & 0 \\ 0 & 0 \end{array} \right) \end{array}
$$

$$
[Q_{P_2}] = \begin{array}{c} \\ L1 \\ L2 \\ A2 \\ C1 \\ C2 \\ P1 \\ P2 \\ M1 \\ M2 \end{array}
\begin{array}{cc} P2_{F_z}^- & P2_{M_x}^- \\ \left(\begin{array}{cc} 0 & 0 \\ 0 & 0 \\ 0 & 0 \\ 0 & 0 \\ 0 & 0 \\ 0 & 0 \\ 1 & 1 \\ 0 & 0 \\ 0 & 0 \end{array} \right) \end{array}
\qquad
[Q_{M_1}] = \begin{array}{c} \\ L1 \\ L2 \\ A2 \\ C1 \\ C2 \\ P1 \\ P2 \\ M1 \\ M2 \end{array}
\begin{array}{cc} M1_{F_y}^- & M1_{F_z}^- \\ \left(\begin{array}{cc} 0 & 0 \\ 0 & 0 \\ 0 & 0 \\ 0 & 0 \\ 0 & 0 \\ 0 & 0 \\ 0 & 0 \\ 1 & 1 \\ 0 & 0 \end{array} \right) \end{array}
$$

$$[Q_{M_2}] = \begin{array}{c} \\ L1 \\ L2 \\ A2 \\ C1 \\ C2 \\ P1 \\ P2 \\ M1 \\ M2 \end{array} \begin{array}{ccc} \overline{M2}_{Fy} & \overline{M2}_{Fz} & \overline{M2}_{Mx} \\ \left(\begin{array}{ccc} 0 & 0 & 0 \\ 0 & 0 & 0 \\ 0 & 0 & 0 \\ 0 & 0 & 0 \\ 0 & 0 & 0 \\ 0 & 0 & 0 \\ 0 & 0 & 0 \\ 0 & 0 & 0 \\ 1 & 1 & 1 \end{array} \right) \end{array} \qquad [Q_F] = \begin{array}{c} \\ L1 \\ L2 \\ A2 \\ C1 \\ C2 \\ P1 \\ P1 \\ M1 \\ M2 \end{array} \begin{array}{ccc} \overline{F}'_y & \overline{F}'_z & \overline{M}'_x \\ \left(\begin{array}{ccc} 0 & 0 & 0 \\ 0 & 0 & 0 \\ 0 & 0 & 0 \\ 1 & 1 & 1 \\ 1 & 1 & 1 \\ 0 & 0 & 0 \\ 0 & 0 & 0 \\ 0 & 0 & 0 \\ 0 & 0 & 0 \end{array} \right) \end{array}$$

C.3   MECHANISM 60°-90°IN A PLANAR WORKSPACE

For the mechanism 60°-90°in a planar workspace, the cutset matrix is presented (eq. 45).

$$[Q]_{9x31} = \left[Q_{L_3} Q_{A_3} Q_{P_4} Q_{M_3} Q_{L_1} Q_{L_2} Q_{A_2} Q_{C_1} Q_{C_2} Q_{P_1} Q_{P_2} Q_{M_1} Q_{M_2} Q_F \right] \qquad (45)$$

Where:

$$[Q_{L_3}] = \begin{array}{c} \\ L1 \\ L2 \\ A2 \\ C1 \\ C2 \\ P1 \\ P2 \\ M1 \\ M2 \end{array} \begin{array}{ccc} \overline{L3}_{Fy} & \overline{L3}_{Fz} & \overline{L3}_{Mx} \\ \left(\begin{array}{ccc} 1 & 1 & 1 \\ 1 & 1 & 1 \\ 0 & 0 & 0 \\ -1 & -1 & -1 \\ -1 & -1 & -1 \\ 0 & 0 & 0 \\ 0 & 0 & 0 \\ 0 & 0 & 0 \\ 0 & 0 & 0 \end{array} \right) \end{array} \qquad [Q_{A_3}] = \begin{array}{c} \\ L1 \\ L2 \\ A2 \\ C1 \\ C2 \\ P1 \\ P2 \\ M1 \\ M2 \end{array} \begin{array}{cc} \overline{A3}_{Fz} & \overline{A3}_{Mx} \\ \left(\begin{array}{cc} 0 & 0 \\ 0 & 0 \\ -1 & -1 \\ 1 & 1 \\ 1 & 1 \\ 0 & 0 \\ 0 & 0 \\ 0 & 0 \\ 0 & 0 \end{array} \right) \end{array}$$

$$
[Q_{P_4}] = \begin{array}{c} \\ L1 \\ L2 \\ A2 \\ C1 \\ C2 \\ P1 \\ P2 \\ M1 \\ M2 \end{array} \begin{array}{cc} P\bar{4}_{Fy} & P\bar{4}_{Fz} \\ \left(\begin{array}{cc} 0 & 0 \\ 0 & 0 \\ 0 & 0 \\ 1 & 1 \\ 1 & 1 \\ -1 & -1 \\ -1 & -1 \\ 0 & 0 \\ 0 & 0 \end{array}\right) \end{array}
\qquad
[Q_{M_3}] = \begin{array}{c} \\ L1 \\ L2 \\ A2 \\ C1 \\ C2 \\ P1 \\ P2 \\ M1 \\ M2 \end{array} \begin{array}{ccc} M\bar{3}_{Fy} & M\bar{3}_{Fz} & M\bar{3}_{Mx} \\ \left(\begin{array}{ccc} 0 & 0 & 0 \\ 0 & 0 & 0 \\ 0 & 0 & 0 \\ -1 & -1 & -1 \\ -1 & -1 & -1 \\ 0 & 0 & 0 \\ 0 & 0 & 0 \\ 1 & 1 & 1 \\ 1 & 1 & 1 \end{array}\right) \end{array}
$$

$$
[Q_{L_1}] = \begin{array}{c} \\ L1 \\ L2 \\ A2 \\ C1 \\ C2 \\ P1 \\ P2 \\ M1 \\ M2 \end{array} \begin{array}{cc} L\bar{1}_{Fy} & L\bar{1}_{Fz} \\ \left(\begin{array}{cc} 1 & 1 \\ 0 & 0 \\ 0 & 0 \\ 0 & 0 \\ 0 & 0 \\ 0 & 0 \\ 0 & 0 \\ 0 & 0 \\ 0 & 0 \end{array}\right) \end{array}
\qquad
[Q_{L_2}] = \begin{array}{c} \\ L1 \\ L2 \\ A2 \\ C1 \\ C2 \\ P1 \\ P2 \\ M1 \\ M2 \end{array} \begin{array}{cc} L\bar{2}_{Fy} & L\bar{2}_{Mx} \\ \left(\begin{array}{cc} 0 & 0 \\ 1 & 1 \\ 0 & 0 \\ 0 & 0 \\ 0 & 0 \\ 0 & 0 \\ 0 & 0 \\ 0 & 0 \\ 0 & 0 \end{array}\right) \end{array}
$$

$$
[Q_{A_2}] = \begin{array}{c} \\ L1 \\ L2 \\ A2 \\ C1 \\ C2 \\ P1 \\ P2 \\ M1 \\ M2 \end{array} \begin{array}{cc} A\bar{2}_{Fy} & A\bar{2}_{Fz} \\ \left(\begin{array}{cc} 0 & 0 \\ 0 & 0 \\ 1 & 1 \\ 0 & 0 \\ 0 & 0 \\ 0 & 0 \\ 0 & 0 \\ 0 & 0 \\ 0 & 0 \end{array}\right) \end{array}
\qquad
[Q_{C_1}] = \begin{array}{c} \\ L1 \\ L2 \\ A2 \\ C1 \\ C2 \\ P1 \\ P2 \\ M1 \\ M2 \end{array} \begin{array}{cc} C\bar{1}_{Fy} & C\bar{1}_{Fz} \\ \left(\begin{array}{cc} 0 & 0 \\ 0 & 0 \\ 0 & 0 \\ 1 & 1 \\ 0 & 0 \\ 0 & 0 \\ 0 & 0 \\ 0 & 0 \\ 0 & 0 \end{array}\right) \end{array}
$$

$$
[Q_{C_2}] = \begin{array}{c} \\ L1 \\ L2 \\ A2 \\ C1 \\ C2 \\ P1 \\ P2 \\ M1 \\ M2 \end{array}
\begin{array}{cc} \bar{C2}_{Fy} & \bar{C2}_{Mx} \\ \begin{pmatrix} 0 & 0 \\ 0 & 0 \\ 0 & 0 \\ 0 & 0 \\ 1 & 1 \\ 0 & 0 \\ 0 & 0 \\ 0 & 0 \\ 0 & 0 \end{pmatrix} \end{array}
\qquad
[Q_{P_1}] = \begin{array}{c} \\ L1 \\ L2 \\ A2 \\ C1 \\ C2 \\ P1 \\ P2 \\ M1 \\ M2 \end{array}
\begin{array}{cc} \bar{P1}_{Fy} & \bar{P1}_{Fz} \\ \begin{pmatrix} 0 & 0 \\ 0 & 0 \\ 0 & 0 \\ 0 & 0 \\ 0 & 0 \\ 1 & 1 \\ 0 & 0 \\ 0 & 0 \\ 0 & 0 \end{pmatrix} \end{array}
$$

$$
[Q_{P_2}] = \begin{array}{c} \\ L1 \\ L2 \\ A2 \\ C1 \\ C2 \\ P1 \\ P2 \\ M1 \\ M2 \end{array}
\begin{array}{cc} \bar{P2}_{Fz} & \bar{P2}_{Mx} \\ \begin{pmatrix} 0 & 0 \\ 0 & 0 \\ 0 & 0 \\ 0 & 0 \\ 0 & 0 \\ 0 & 0 \\ 1 & 1 \\ 0 & 0 \\ 0 & 0 \end{pmatrix} \end{array}
\qquad
[Q_{M_1}] = \begin{array}{c} \\ L1 \\ L2 \\ A2 \\ C1 \\ C2 \\ P1 \\ P2 \\ M1 \\ M2 \end{array}
\begin{array}{cc} \bar{M1}_{Fy} & \bar{M1}_{Fz} \\ \begin{pmatrix} 0 & 0 \\ 0 & 0 \\ 0 & 0 \\ 0 & 0 \\ 0 & 0 \\ 0 & 0 \\ 0 & 0 \\ 1 & 1 \\ 0 & 0 \end{pmatrix} \end{array}
$$

$$
[Q_{M_2}] = \begin{array}{c} \\ L1 \\ L2 \\ A2 \\ C1 \\ C2 \\ P1 \\ P2 \\ M1 \\ M2 \end{array}
\begin{array}{cc} \bar{M2}_{Fy} & \bar{M2}_{Mx} \\ \begin{pmatrix} 0 & 0 \\ 0 & 0 \\ 0 & 0 \\ 0 & 0 \\ 0 & 0 \\ 0 & 0 \\ 0 & 0 \\ 0 & 0 \\ 1 & 1 \end{pmatrix} \end{array}
\qquad
[Q_{F}] = \begin{array}{c} \\ L1 \\ L2 \\ A2 \\ C1 \\ C2 \\ P1 \\ P1 \\ M1 \\ M2 \end{array}
\begin{array}{ccc} \bar{F}'_{y} & \bar{F}'_{z} & \bar{M}'_{x} \\ \begin{pmatrix} 0 & 0 & 0 \\ 0 & 0 & 0 \\ 0 & 0 & 0 \\ 1 & 1 & 1 \\ 1 & 1 & 1 \\ 0 & 0 & 0 \\ 0 & 0 & 0 \\ 0 & 0 & 0 \\ 0 & 0 & 0 \end{pmatrix} \end{array}
$$

Annex

ANNEX A – EXPERIMENTAL DATA - LIGAMENTS INSERTION AREA

Experimental data obtained by Ottoboni et al. (2010) and by Parenti-Castelli and Sancisi (2013), presented in the study made by Gasparutto et al. (2015) (Table 19, (OTTOBONI *et al.*, 2010; PARENTI-CASTELLI; SANCISI, Nicola, 2013; GASPARUTTO *et al.*, 2015)).

Table 19 – Experimental data of Ligaments insertion areas and contact between femur and tibia

Segment	Anatomical part	Coordinate [mm]		
		X	Y	Z
Femur	ACL insertion	-6.8	7.5	9.2
	PCL insertion	-2.7	-1.1	-2.2
	LCL insertion	3.2	2.3	36.2
	MCL insertion	2.7	5.8	-47.6
	Medial condyle centre	0.2	3.4	-23.2
	Lateral condyle centre	-3.3	2.1	26.2
Tibia	ACL insertion	12.8	-26.1	-0.9
	PCL insertion	-25.8	-38.1	-3.5
	LCL insertion	-24.3	-48	37.1
	MCL insertion	2.1	-117.1	-5.8
	Medial tibial plateau	-2.1	-28.6	-19.1
	Lateral tibial plateau	-2.8	-26.1	24.4

(GASPARUTTO *et al.*, 2015)

The coordinate system used by Gasparutto *et al.,* 2015, is different from the one used in this thesis (eq. 46).

$$
\text{Coordinate} \quad \text{system} \longrightarrow
\begin{cases}
\text{Thesis} \quad \text{X} = -\text{Z} \quad (\text{GASPARUTTO}\,et\,al., 2015) \\
\text{Thesis} \quad \text{Y} = \text{Y} \quad (\text{GASPARUTTO}\,et\,al., 2015) \\
\text{Thesis} \quad \text{Z} = \text{X} \quad (\text{GASPARUTTO}\,et\,al., 2015)
\end{cases}
\tag{46}
$$

ANNEX B – EXPERIMENTAL DATA - FORCE DISTRIBUTION

In situ forces obtained as experimental results (KANAMORI *et al.*, 2000)

Table 20 – Experimental data of *in situ* forces of knee anatomical parts, during a anterior drawer test applying a force of 134N.

Anatomical part	Degree	of	Flexion		
	0°	15°	30°	60°	90°
ACL	107	112	106	94	99
MCL	13	8	13	20	20
PSL	14	14	15	20	15

ACL - Anterior Collateral Ligament; MCL - Medial Collateral Ligament, PSL - Posterolateral Structures (KANAMORI *et al.*, 2000).